AD737203

NAVAL SHIP RESEARCH AND DEVELOPMENT CENTER
Washington.D.C. 20007

METHODS FOR COMPUTING FLUID LOADING AND THE VIBRATORY

RESPONSE OF FLUID-LOADED FINITE RECTANGULAR PLATES
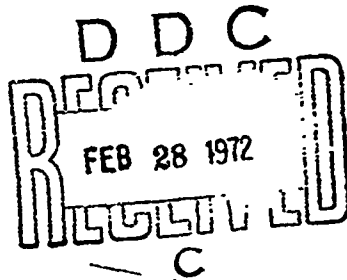
SUBJECT TO TURBULENCE EXCITATION--OPTION 3

by

Ralph C. Leibowitz

Approved for public release; distribution unlimited.

SHIP ACOUSTICS DEPARTMENT

RESEARCH AND DEVELOPMENT REPORT

D D C

FEB 28 1972

C

September 1971   Report 2976C

(87

The Naval Ship Research and Development Center is a U. S. Navy center for laboratory effort directed at achieving improved sea and air vehicles. It was formed in March 1967 by merging the David Taylor Model Basin at Carderock, Maryland with the Marine Engineering Laboratory at Annapolis, Maryland. The Mine Defense Laboratory (now Naval Ship R & D Laboratory) Panama City, Florida became part of the Center in November 1967.

Naval Ship Research and Development Center

Bethesda, Md. 20034

MAJOR NSRDC ORGANIZATIONAL COMPONENTS

＊REPORT ORIGINATOR

NSRDC
COMMANDER 00
TECHNICAL DIRECTOR 01

NSRDL
PANAMA CITY
COMMANDING OFFICER P100
TECHNICAL DIRECTOR P101

OFFICER-IN-CHARGE CARDEROCK 05

OFFICER-IN-CHARGE ANNAPOLIS 04

SYSTEMS DEVELOPMENT DEPARTMENT 11

OCEAN TECHNOLOGY DEPARTMENT P710

SHIP PERFORMANCE DEPARTMENT 15

AVIATION AND SURFACE EFFECTS DEPARTMENT 16

MINE COUNTERMEASURES DEPARTMENT (SHIPS) P720

STRUCTURES DEPARTMENT 17

COMPUTATION AND MATHEMATICS DEPARTMENT 18

MINE COUNTERMEASURES DEPARTMENT (AIR) P730

＊SHIP ACOUSTICS DEPARTMENT 19

PROPULSION AND AUXILIARY SYSTEMS DEPARTMENT 27

INSHORE WARFARE AND TORPEDO DEFENSE DEPARTMENT P740

MATERIALS DEPARTMENT 28

CENTRAL INSTRUMENTATION DEPARTMENT 29

NDW-NSRDC 3960/43 (3-70)

DOCUMENT CONTROL DATA - R & D

Security classification of title, body of abstract and indexing annotation must be entered when the overall report is classified)

1 ORIGINATING ACTIVITY (Corporate author)	2a. REPORT SECURITY CLASSIFICATION
Naval Ship Research & Development Center Bethesda, Maryland 20034	UNCLASSIFIED
	2b. GROUP

3 REPORT TITLE

METHODS FOR COMPUTING FLUID LOADING AND THE VIBRATORY RESPONSE OF FLUID-LOADED FINITE RECTANGULAR PLATES SUBJECT TO TURBULENCE EXCITATION--OPTION 3

4 DESCRIPTIVE NOTES (Type of report and inclusive dates)

5 AUTHOR(S) (First name, middle initial, last name)

Ralph C. Leibowitz

6 REPORT DATE	7a. TOTAL NO OF PAGES	7b. NO. OF REFS
September 1971	185 187	46
8a. CONTRACT OR GRANT NO	9a. ORIGINATOR'S REPORT NUMBER(S)	
b. PROJECT NO	2976C	
c.	9b. OTHER REPORT NO(S) (Any other numbers that may be assigned this report)	
d.		

10 DISTRIBUTION STATEMENT

Approved for public release; distribution unlimited.

11 SUPPLEMENTARY NOTES	12. SPONSORING MILITARY ACTIVITY
	Naval Ship Systems Command

13 ABSTRACT

Various methods are presented for computing heavy or light fluid loading (i.e., added mass) of thin finite rectangular plates. Based on the results, preferred methods of computation are recommended. These methods and a corresponding computer program, Option 3, are of particular value in extending previously formulated digital computer programs for obtaining the vibroacoustic response to turbulence excitation of a plate. Computer results are given for a particular case which includes the effect of fluid loading on the vibratory response of a plate subject to turbulence excitation.

DD FORM 1473 (PAGE 1)
1 NOV 65

S/N 0101-807-6801

14 KEY WORDS	LINK A		LINK B		LINK C	
	ROLE	WT	ROLE	WT	ROLE	WT
Fluid Loading of Flat Rectangular Plates						
Mathematical Analysis						
Turbulence Induced Vibration and Radiation of Plates 1. Simply Supported and Clamped Boundaries 2. Water and Air Fluid Media						
Digital Computer Programs						
Digital Computer Computations						
Continuum Approach						
Recommendations						

DD _{1 NOV 65}^{FORM} **1473** (BACK)

(PAGE 2)

DEPARTMENT OF THE NAVY

NAVAL SHIP RESEARCH AND DEVELOPMENT CENTER

WASHINGTON, D. C.   20007

METHODS FOR COMPUTING FLUID LOADING AND THE VIBRATORY

RESPONSE OF FLUID-LOADED FINITE RECTANGULAR PLATES

SUBJECT TO TURBULENCE EXCITATION--OPTION 3

by

Ralph C. Leibowitz

September 1971

Report 2976C

TABLE OF CONTENTS

Page

LIST OF FIGURES

Page

LIST OF TABLES

iii

ABSTRACT

Various methods are presented for computing heavy or
light fluid loading (i.e., added mass) of thin finite
rectangular plates. Based on the results, preferred methods
of computation are recommended. These methods and a
corresponding computer program--Option 3--are of particular
value in extending previously formulated digital computer
programs for obtaining the vibroacoustic response to turbu-
lence excitation of a plate. Computer results are given for
a particular case which includes the effect of fluid load-
ing on the vibratory response of a plate subject to turbu-
lence excitation.

ADMINISTRATIVE INFORMATION

INTRODUCTION

Reference 1 documents four available computer programs for determin-
ing the vibratory response and the associated acoustic radiation of a
finite rectangular plate to fully developed turbulence.* Several compu-
tational frameworks are provided which can be modified and extended through
additional research to furnish more accurate and realistic programs to meet
naval needs. The chief objective of the original study was to furnish a
base for future development.

Extension of these computations are treated in Reference 2 (Option 1)
and 3 (Option 2). Reference 2 includes a correction in the computer pro-
grams for the effects on vibroacoustic response of the boundary layer
thickness and pressure pickup dimensions. Reference 3 includes in the pro-
grams the vibration modes and natural frequencies of thin rectangular
plates with clamped and rotational supports and cylindrical curvature.

The overall program now includes the response of simple and clamped
plates in air and in water. However, the fluid loading on the plate has

---

*References are listed on page 172.

1

hitherto been determined for the case of an infinite plate.[*] Hence there is a need to incorporate into the program the results of recent investigations of the loading effects of a heavy or light fluid on a thin finite rectangular plate. This modification is required to improve the accuracy of the computations and to extend the applicability of the program.

Accordingly, the present report presents a modification (Option 3) *of an updated version of one of the original programs--that of Maestrello--* to include the effects of fluid loading for finite plates.[**] The modified program is based on results obtained by the use of various analytical methods. The following titles identify the methods treated and their location in the report; notations relevant to each method are also included in the Appendixes.

Appendix A - The Feit-Junger Method

Appendix B - The Davies Method

Appendix C - The Leibowitz Method I

Appendix D - The Leibowitz Method II

Appendix E - The Bolt Beranek and Newman Method

Appendix F - The Greenspon Method

Appendix G - The Leibowitz Method III

For the convenience of the reader, the Appendixes include an adequate amount of the mathematical development underlying these methods. An understanding of the development will assist the reader to appreciate the merits, shortcomings, subtleties, and complexities of a particular method and to apply the various methods. Certain figures are adapted from the basic references.

---

[*] See the Dyer representation, includable in all programs, for added mass in Appendix A of Reference 1.

[**] In Appendix H, the original Maestrello program is updated. This updated version is then modified to include fluid loading (Option 3). Other programs presented in Reference 1 may be modified in a similar manner.

TABLE 1
Summary of Key Features of Analytical Study

BASIC REFERENCES	PROGRAM DESIGNATION	LOCATION IN REPORT	THEORETICAL APPROACH	MAJOR ASSUMPTIONS AND LIMITATIONS	PLATE BOUNDARY CONDITIONS	
4	FEIT-PINCZk METHOD	APPENDIX A	GENERALIZED FORCE-MODAL TRANSFORM METHOD	1. Analysis performed for even modes. 2. Modal coupling ignored in final solution. 3. Solution obtained for $k_x L_x = n\lambda$, $k_y L_y = 0$; $x^2 \cdot k_y^2 > k^2$. $x < x_c$. Final expression assumed to hold for finite plate.	SIMPLY SUPPORTED PLATE	
7	DAVIES METHOD	APPENDIX B	NORMAL MODE METHOD	1. Applied force causes no additional modal coupling i.e., typical correlation lengths of the forcing field are much less than the panel dimensions (modes coupled by external field are treated in appendix to Reference 7). 2. Neither panel vibration nor the acoustic field affect the applied external force acting on the panel.	SIMPLY SUPPORTED PLATE INSERTED IN INFINITE RIGID BAFFLE	
4,7	LEIBOWITZ METHOD I	APPENDIX C	COMBINATION OF METHODS OF APPENDICES A AND B	Similar to those of Appendices A and B.	SIMPLY SUPPORTED PLATE INSERTED IN INFINITE RIGID BAFFLE	
8,9	Leibowitz Method II	APPENDIX D	Fourier Transform - Normal Mode Method	1. No intermodal coupling, i.e., the response of one mode is nearly independent of the response of others. 2. The modal force f_m can be split into two parts $f_m = f_m^{blocked} + f_m^{rad}$ where f_m^{rad} can be used to find the fluid loading.	SIMPLY SUPPORTED PLATE INSERTED IN INFINITE RIGID BAFFLE	
10, 11, 12	BOLT BERANEK AND NEWMAN METHOD	APPENDIX E	NO METHOD OF ANALYSIS PRESENTED	1. Mass loading reduces modal resonance frequencies from their values in vacuo, in proportion to the square root of total mass. 2. Results are considered precisely correct only for waves on a large flat plate.	SIMPLY SUPPORTED PLATE (OR SHELL)	Total
13,14	GREENSPON METHOD	APPENDIX F	AVERAGING OF FINITE ELEMENT MODAL RESPONSE	1. Assumed that the average modal pressure on a finite element area can be computed by considering the entire plate to act as a rectangular piston with a deflection equal to the average modal displacement over the plate. 2. Virtual mass is approximated by average values for each mode independent of the forcing frequency. 3. Mode shapes of the vibrating plate (in air or water) for simply supported and clamped plates are assumed to be represented by a product of beam functions.	SIMPLY SUPPORTED AND CLAMPED PLATES	
13, 14	LEIBOWITZ METHOD III	APPENDIX G	INCORPORATION OF LOW FREQUENCY APPROXIMATION INTO ANALYSIS OF APPENDIX F	1. A low frequency approximation for the mass reactance of piston is made.	SIMPLY SUPPORTED AND CLAMPED PLATES	

3

CONDITIONS	RESULTS	REMARKS OR MISCELLANEOUS
...ED PLATE		1. In large $k_a L_x$, $k_a L_y$ limit the results are directly applicable to even-odd and odd-odd modal configurations. See Appendix D. 2. Results obtained for determinate system (using generalized force) but applicable to indeterminate system subject to random forces. 3. Basic equations developed permit solution including modal coupling. 4. Results applicable for $k_a L_x$, $k_a L_y$ not approaching infinity since p,q summation is small when $k_a L_x$, $k_a L_y$ is sufficiently large; see reference 7.
...ED PLATE ...FINITE	1. FOR ALL MODES IS K SPACE FOR WHICH $|k_1| > k_o$ (ACOUSTICALLY SLOW MODES) 2. FOR (m,n) AS X-TYPE EDGE MODE AND (s,r) AS EDGE MODE 3. FOR (m,n) AS X-TYPE EDGE MODE AND (s,r) A CORNER MODE 4. FOR (m,n) AS X-TYPE EDGE MODE AND (s,r) AS ACOUSTICALLY FAST MODE 5. FOR (m,n) AND (s,r) CORNER MODES	1. The first result is the dominant one for all modes. It is very approximately applicable at low frequencies, $k_o L_x$ and $k_o L_y < \pi$, corresponding to modes of corner mode radiation character. It is also applicable at high frequencies (but below k_c) where $k_o L_x$ and $k_o L_y \gg \pi$, for which the radiation and coupling characteristics of the modes are not the same for all modes as in the low frequency case. 2. For large inertial coupling between modes it is necessary that two mode numbers be the same so that the modes vibrate in the same shape in one direction. This is symbolized by the Kronecker delta function.
...ED PLATE ...FINITE	SAME RESULTS AS DAVIES (see Equations C13, C16, C19, C22, C25). Note: Davies symbol $q = p$ and $r = q$ here; mn stay the same; mode numbers are odd for even modes. $L_1 = 2L_x$, $L_3 = 2L_y$.	1. The work of Appendices A and B are harmonized to extend the solution of the Feit-Junger basic vibroacoustic equation to yield results identical to those obtained by Davies for uncoupled and coupled modes. Feit's origin is taken at the center of the plate and Davies origin is taken at the corner of the plate. Modes numbered m=1,3... and with respect to Davies origin represent the even modes with respect to Feit's origin.
...ED PLATE ...FINITE	$$m_{mn} = \frac{\rho}{\sqrt{k_{mn}^2 - k_o^2}}$$ $$= \frac{\rho}{k_{mn}} \quad \text{for } k_{mn}^2 \gg k_o^2$$	1. Due to the lack of modal coupling results for the virtual mass are limited to the mn mode. The results do however agree with equivalent results in Appendices A, B, and C. 2. Normal mode representation includes as a special case the even-even mode representation of Appendix A. Since both representations yield the same results for m_{mn} it is reasonable to extend the applicability of the results for Appendix A to even-odd and odd-odd modes.
...ED PLATE	Total $M_{added} = \frac{A\rho_f}{k_h}$; $M_o = A\rho_s h$ $M_{mn} = M_o + M_{added} = A\rho_s h(1 + \frac{\rho_f}{\rho_s k_h h})$ $\omega_{mn} = \omega_{mn}(1 + \frac{\rho_f}{\rho_s k_h h})^{-\frac{1}{2}}$; $k_h > k_f$	1. Results are also approximately correct for cylindrical shells of interest in References 11 and 12. 2. Results are used in Reference 12 as an approximation for modes having fairly large mode numbers ($k_h a = k_p a$ large where a is the shell radius.) As $k_h a$ becomes large the modal vibration more nearly approximates bending vibrations on a flat plate for which tangential contributions to kinetic energy are unimportant compared with the radial. 3. Results are inapplicable for surface modes having $k_p = k_h < k_f$ since the virtual mass tends to vanish for these modes.
...TED AND ...ES	$M_a = \left[\frac{\rho_o b}{2m_p} f(\frac{a}{b}) \frac{A_{ij}^2}{B_{ij}}\right] m_p$ $\omega_{mn} = (\omega_{mn})_{water on one side} \frac{(\omega_{mn})_{vacuum}}{\sqrt{1 + \frac{\rho_o b}{2m_p} f(\frac{a}{b}) \frac{A_{ij}^2}{B_{ij}}}}$	1. A_{ij} and B_{ij} depend on the beam functions used to represent the mode shapes and therefore depend on the boundary conditions of the plate. The values of A_{ij} and B_{ij} for several of the lower modes of plates which are clamped or simply supported on all edges are given in Table 4.
...TED AND ...ES	$M_a = \frac{0.48\rho_o(ab)^{\frac{1}{2}}}{m_p} \frac{A_{ij}^2}{B_{ij}} m_p$ $\omega_{mn} = (\omega_{mn})_{water on one side} \frac{(\omega_{mn})_{vacuum}}{\sqrt{1 + \frac{0.48\rho_o(ab)^{\frac{1}{2}}}{m_p} \frac{A_{ij}^2}{B_{ij}}}}$	1. For low frequencies the present procedure does not require that $f(\frac{a}{b})$ be explicitly determined from a curve.

3-A

TABLE 2

Input Data for Computing Normalized Modal Mean Square Displacement $\overline{Y^2(\omega)}/\overline{p^2}$ for Simply Supported Aluminum Plate in Water

TABLE 2a

Computed Natural Frequencies and Total Damping Ratio for Simply Supported Plate in Air

Mode Number (n,n)	f(Hz) Warburton	$\omega_{mn}(\frac{rad}{sec})$ Warburton	$\zeta_{mn} \times \frac{15}{f_{mn}}$	Mode Number (n,n)	f(Hz) Warburton	$\omega_{mn}(\frac{rad}{sec})$ Warburton	$\zeta_{mn} \times \frac{15}{f_{mn}}$
1,1	88.82	558.10	0.16888	7,1	223.43	1403.85	0.06713
1,2	346.88	2179.54	0.04324	7,2	481.49	3025.29	0.03115
1,3	776.98	4881.94	0.01930	7,3	911.59	5727.69	0.01645
1,4	1379.13	8665.30	0.01087	7,4	1513.73	9511.05	0.00990
1,5	2153.31	13529.62	0.00696	7,5	2287.91	14375.37	0.00655
1,6	3099.53	19474.89	0.00485	8,1	265.49	1668.15	0.05649
2,1	97.24	610.96	0.15425	8,2	523.55	3289.59	0.02865
2,2	355.30	2232.40	0.04221	8,3	953.65	5991.99	0.01572
2,3	785.40	4934.80	0.01909	8,4	1555.79	9775.35	0.00954
2,4	1387.54	8718.16	0.01081	8,5	2329.98	14639.67	0.00644
2,5	2161.72	13582.48	0.00695	9,1	313.17	1967.68	0.04789
3,1	111.26	699.06	0.13481	9,2	571.23	3589.13	0.02625
3,2	369.32	2320.50	0.04061	9,3	1001.33	6291.52	0.01493
3,3	799.42	5022.90	0.01876	9,4	1603.47	10074.88	0.00935
3,4	1401.56	8806.26	0.01070	9,5	2377.65	14939.20	0.00631
3,5	2175.74	13670.58	0.00690	10,1	366.45	2302.46	0.04093
4,1	130.89	822.40	0.11460	10,2	624.51	3923.90	0.02401
4,2	388.95	2443.84	0.03856	10,3	1054.61	6626.30	0.01422
4,3	819.05	5146.24	0.01831	10,4	1656.75	10409.66	0.00905
4,4	1421.19	8929.60	0.01055	10,5	2430.93	15273.93	0.00616
4,5	2195.36	13793.92	0.00684				
5,1	156.13	980.98	0.09607				
5,2	414.19	2602.42	0.03621				
5,3	844.29	5304.22	0.01776				
5,4	1446.43	9088.17	0.01037				
5,5	2220.61	13952.49	0.00681				
6,1	186.98	1174.80	0.08022				
6,2	445.03	2796.23	0.03370				
6,3	875.13	5498.63	0.01714				
6,4	1477.28	9281.99	0.01015				
6,5	2251.46	14146.31	0.00666				

a = 3.0 ft

b = 0.541666 ft

h = 0.04 in.

E = 10 x 10^6 lb/in.^{2}

σ = 0.33

weight density (ρ_w) of plate aluminum = 0.1075 lb/in.^{3} = 185.8 lb/ft^3

g = 32.2 ft/sec^2 = 384.6 in./sec^2

κ = 9.64 x 10^{-4} ft

c_ℓ = 17,000 ft/sec

TABLE 2b

Input Data for Computing $\dfrac{\overline{Y^2(\omega)}}{\overline{p}^2}$ for Simply Supported Aluminum Plate in Water--

Frequency Computation by Method I; $q = 0$

Mode Number (m,n)	$w_p (lb/ft^2)$ Aluminum	$w_{mn} (lb/ft^2)$ (Water)	$w'=(w_p+w_{mn})$ (lb/ft^2)	$(w')^2 (lb/ft^2)^2$	f_{mn} (Hz)	ω_{mn} (rad/sec)	$\bar{\delta}_{mn}$ (1/sec)	$\bar{\zeta}_{mn}$
1,3	0.6	7.3652	7.9652	63.44	215.57	1356.33	3.55	0.00623
1,4		5.5283	6.1283	37.56	333.34	2093.49	4.61	0.0044
1,5		4.4243	5.0243	25.24	578.21	3631.21	5.63	0.0031
1,6		3.6876	4.2876	18.32	918.20	5766.33	6.59	0.0021
2,3		7.3257	7.9257	62.42	218.87	1374.42	3.57	0.0053
2,4		5.5115	6.1115	37.35	437.53	2747.73	4.62	0.0033
2,5		4.4155	5.0156	25.16	752.16	4727.60	5.64	0.0023
3,3		7.2612	7.8612	61.30	219.23	1376.82	3.60	0.00622
3,4		5.4839	6.0839	37.01	441.15	2770.43	4.65	0.00335
3,5		4.4014	5.0014	25.01	756.17	4743.78	5.65	0.00237
4,3		7.1737	7.7737	60.43	224.40	1409.26	3.64	0.00616
4,4		5.4459	6.0459	36.55	446.01	2800.96	4.68	0.00334
4,5		4.3817	4.9817	24.82	762.58	4789.01	5.67	0.00236
5,2		10.0680	10.6380	114.23	99.17	622.84	2.65	0.00950
5,3		7.0656	7.6656	58.76	231.52	1453.93	3.69	0.00507
5,4		5.3982	5.9982	35.98	454.05	2851.44	4.71	0.00330
5,5		4.3567	4.9567	24.57	771.35	4844.34	5.70	0.00235
6,2		9.7321	10.3321	106.75	109.38	620.64	2.74	0.00985
6,3		6.9400	7.5400	56.85	240.63	1511.20	3.75	0.00496
6,4		5.3415	5.9415	31.83	464.30	2915.85	4.76	0.00326
6,5		4.3263	4.9263	24.27	782.62	4914.86	5.74	0.00233
7,2		9.3565	9.9565	93.25	119.44	750.44	2.93	0.00781
7,3		6.7399	7.3999	54.76	251.77	1581.15	3.82	0.00483
7,4		5.2762	5.8762	34.54	476.80	2994.34	4.81	0.00321
7,5		4.2922	4.8922	23.93	796.28	5000.62	5.78	0.00231
8,2		8.9728	9.5728	91.64	132.45	831.84	2.95	0.00709
8,3		6.6482	7.2482	54.54	264.98	1664.12	3.90	0.00462
8,4		5.2050	5.8050	33.70	491.57	3087.11	4.87	0.00315
8,5		4.2533	4.8533	28.55	812.40	5101.90	5.82	0.00228
9,2		8.5903	9.1903	84.46	147.49	926.25	3.08	0.00665
9,3		6.4831	7.0831	50.24	280.32	1760.44	3.99	0.00453
9,4		5.1271	5.7271	32.80	508.65	3194.37	4.94	0.00309
9,5		4.2104	4.8104	23.14	831.01	5218.75	5.88	0.00225
10,2		8.2158	8.8158	77.72	164.63	1033.90	3.21	0.00620
10,3		6.3221	6.9221	47.92	297.84	1870.43	4.06	0.00436
10,4		5.0440	5.6440	31.85	528.08	3316.34	5.01	0.00302
10,5	0.6	4.1640	4.7640	22.70	852.12	5351.32	5.93	0.00221

$\dfrac{1}{\dfrac{\overline{Y^2(\omega)}}{\overline{p}^2}}$

Computations not performed for these mode numbers

a = 3.0 ft	$(w')^2 (lb/ft^2)^2$ (see Column E)
b = 0.541666 ft	$\gamma = 0.33$
h = 0.04 in.	$E = 10 \times 10^6 \ lb/in.^2$
$r = \dfrac{h}{2\sqrt{3}} = 9.64 \times 10^{-4}$ ft	$(\rho_w)_{aluminum} = 0.1075 \ lb/in.^3 = 185.8 \ lb/ft^3$
$c_l = 17,000$ ft/sec	$g = 384.6 \ in./sec^2$
$x = x' = 1.5$ ft	$\overline{p}^2 = 1.0 \ (lb/ft^2)^2$
$y = y' = 0.270833$ ft	$z' = 0.033$ ft

$w_u = 0.323 \ lb/ft^2$

$(\rho_w) = 64.2 \ lb/ft^3 = 0.037 \ lb/in.^3$ water

$\eta = 2.0$

i	$\bar{A}_i$	$\bar{\kappa}_i$
1	1.6	0.47
2	7.2	3.0
3	12.0	14.0

U_c (ft/sec)	τ(sec)
8	2.25×10^{-3}
16	
32	
64	2.25×10^{-3}

Note: $\bar{\delta}_{mn} = a_{mn}\left(\dfrac{w_p}{w'}\right) \cdot (15\tau)\left(\dfrac{0.6}{0.6 + w_{mn}}\right) = \dfrac{28.27}{w'}$

$\bar{\zeta}_{mn} = \dfrac{2\bar{\delta}_{mn}}{\omega_{mn}}$

Note: In computing f_{mn} or ω_{mn} (see Program C' in Section 3 of Appendix H) the program input in in $lb/in.^3$ units for $(\rho_w)_{aluminum}$. In computing $\bar{\zeta}_{mn}$ or $\bar{\omega}_{mn}$ (see Program B' in Section 3 of Appendix H) the program input is in lb/ft^3 units for both $(\rho_w)_{aluminum}$ and $(\rho_w)_{water}$.

TABLE 2c
Computation of Normalized Modal Mean Square Displacement
$$\overline{Y^2(\omega)}/\overline{p^2} \text{ for Simply Supported Aluminum Plate in Water}$$

q = 0 (only)   ALUMINUM PLATE

U_c (ft/sec)	Mode Number (m,n)	$\dfrac{\overline{Y^2(\omega)}}{\overline{p^2}}$ [*]	$\dfrac{\overline{Y^2(\omega)}}{\overline{p^2}}$ [**]	$\dfrac{\overline{Y^2(\omega)}}{\overline{p^2}}$ [***]
8	1,3	3.1×10^{-8}	3.1×10^{-5}	3.3×10^{-10}
	1,4	4.4×10^{-9}	4.5×10^{-10}	4.8×10^{-11}
	1,5	5.0×10^{-10}	5.0×10^{-11}	5.5×10^{-12}
	1,6	6.5×10^{-11}	6.6×10^{-12}	7.3×10^{-13}
	2,3	1.9×10^{-8}	1.9×10^{-9}	2.0×10^{-10}
	2,4	8.9×10^{-10}	9.0×10^{-11}	9.8×10^{-12}
	2,5	1.0×10^{-10}	1.0×10^{-11}	1.1×10^{-12}
	3,3	1.6×10^{-8}	1.6×10^{-9}	1.7×10^{-10}
	3,4	7.2×10^{-10}	7.3×10^{-11}	7.9×10^{-12}
	3,5	7.5×10^{-11}	7.6×10^{-12}	8.5×10^{-13}
	4,3	1.3×10^{-8}	1.3×10^{-9}	1.3×10^{-10}
	4,4	6.4×10^{-10}	6.4×10^{-11}	7.9×10^{-12}
	4,5	6.2×10^{-11}	6.3×10^{-12}	7.0×10^{-13}
	5,2	2.5×10^{-7}	2.5×10^{-8}	2.6×10^{-9}
	5,3	9.9×10^{-9}	1.0×10^{-9}	1.1×10^{-10}
	5,4	5.7×10^{-10}	5.7×10^{-11}	6.2×10^{-12}
	5,5	5.2×10^{-11}	5.3×10^{-12}	6.0×10^{-13}
16	1,3	3.4×10^{-8}	3.4×10^{-9}	3.6×10^{-10}
	1,4	5.7×10^{-9}	5.7×10^{-10}	6.0×10^{-11}
	1,5	7.1×10^{-10}	7.1×10^{-11}	7.6×10^{-12}
	1,6	8.7×10^{-11}	8.8×10^{-12}	9.6×10^{-13}
	2,3	2.1×10^{-8}	2.1×10^{-9}	2.2×10^{-10}
	2,4	1.2×10^{-9}	1.2×10^{-10}	1.3×10^{-11}
	2,5	1.3×10^{-10}	1.3×10^{-11}	1.4×10^{-12}
	3,3	1.6×10^{-8}	1.6×10^{-9}	1.7×10^{-10}
	3,4	8.7×10^{-10}	8.7×10^{-11}	9.4×10^{-12}
	3,5	9.1×10^{-11}	9.2×10^{-12}	1.0×10^{-12}
	4,3	1.4×10^{-8}	1.4×10^{-9}	1.5×10^{-10}
	4,4	8.4×10^{-10}	8.5×10^{-11}	8.9×10^{-12}
	4,5	7.0×10^{-11}	7.0×10^{-12}	7.8×10^{-13}
	5,2	2.5×10^{-7}	2.5×10^{-8}	2.6×10^{-9}
	5,3	1.0×10^{-8}	1.0×10^{-9}	1.1×10^{-10}
	5,4	5.9×10^{-10}	5.9×10^{-11}	6.4×10^{-12}
	5,5	6.5×10^{-12}	6.5×10^{-12}	7.2×10^{-13}
32	1,3	3.8×10^{-8}	3.8×10^{-9}	4.0×10^{-10}
	1,4	7.1×10^{-9}	7.1×10^{-10}	7.3×10^{-11}

Note: The extensive results for the response obtained by Mr. Lucio Maestrello and Mrs. Christine Brown at Langley Research Center, NASA, using the author's program, are tabulated in Table 2c.

6

Table 2c (Continued)

ALUMINUM PLATE (Continued)

q = 0 (only)

U_c (ft/sec)	Mode Number (p,n)	$\dfrac{\overline{Y^2(\_)}}{\overline{p^2}}$ [*]	$\dfrac{\overline{Y^2(\_)}}{\overline{p^2}}$ [**]	$\dfrac{\overline{Y^2(\_)}}{\overline{p^2}}$ [***]
	1,5	1.0×10^{-9}	1.0×10^{-10}	1.1×10^{-11}
	1,6	1.8×10^{-10}	1.8×10^{-11}	1.8×10^{-12}
.	2,3	2.5×10^{-8}	2.5×10^{-9}	2.6×10^{-10}
	2,4	1.9×10^{-9}	1.9×10^{-10}	1.9×10^{-11}
	2,5	1.6×10^{-10}	1.6×10^{-11}	1.7×10^{-12}
	3,3	1.2×10^{-8}	1.2×10^{-9}	1.3×10^{-10}
	3,4	8.3×10^{-10}	8.4×10^{-11}	9.1×10^{-12}
	3,5	1.1×10^{-10}	1.1×10^{-11}	1.2×10^{-12}
	4,3	8.4×10^{-9}	8.5×10^{-10}	9.4×10^{-11}
	4,4	1.5×10^{-9}	1.5×10^{-10}	1.5×10^{-11}
	4,5	1.0×10^{-10}	1.0×10^{-11}	1.1×10^{-12}
	5,2	2.7×10^{-7}	2.7×10^{-8}	2.7×10^{-9}
	5,3	7.8×10^{-9}	7.8×10^{-10}	8.5×10^{-11}
	5,4	8.0×10^{-10}	8.0×10^{-11}	8.4×10^{-12}
	5,5	4.0×10^{-11}	4.1×10^{-12}	5.0×10^{-13}
64	1,3	5.3×10^{-8}	5.3×10^{-9}	5.2×10^{-10}
	1,4	5.1×10^{-9}	5.2×10^{-10}	5.6×10^{-11}
	1,5	1.1×10^{-9}	1.1×10^{-10}	1.2×10^{-11}
	1,6	2.6×10^{-10}	2.6×10^{-11}	2.7×10^{-12}
	2,3	5.5×10^{-9}	5.6×10^{-10}	7.0×10^{-11}
	2,4	3.9×10^{-9}	3.9×10^{-10}	3.8×10^{-11}
	2,5	2.2×10^{-10}	2.2×10^{-11}	2.3×10^{-12}
	3,3	1.2×10^{-8}	1.2×10^{-9}	1.3×10^{-10}
	3,4	3.5×10^{-10}	3.6×10^{-11}	4.0×10^{-12}
	3,5	2.6×10^{-10}	2.6×10^{-11}	2.7×10^{-12}
	4,3	1.2×10^{-8}	1.2×10^{-9}	1.3×10^{-10}
	4,4	.	-	†
	4,5	2.6×10^{-10}	2.6×10^{-11}	2.6×10^{-12}
	5,2	3.2×10^{-7}	3.2×10^{-8}	3.2×10^{-9}
	5,3	1.1×10^{-8}	1.1×10^{-9}	1.1×10^{-10}
	5,4	5.0×10^{-11}	5.7×10^{-12}	1.2×10^{-12}
	5,5	4.7×10^{-11}	4.7×10^{-12}	5.2×10^{-13}

[*] For one-tenth computed damping value given in Table 2b.

[**] For computed damping value given in Table 2b.

[***] For ten times computed damping value given in Table 2b.

. Computer error (recomputation not made).

7
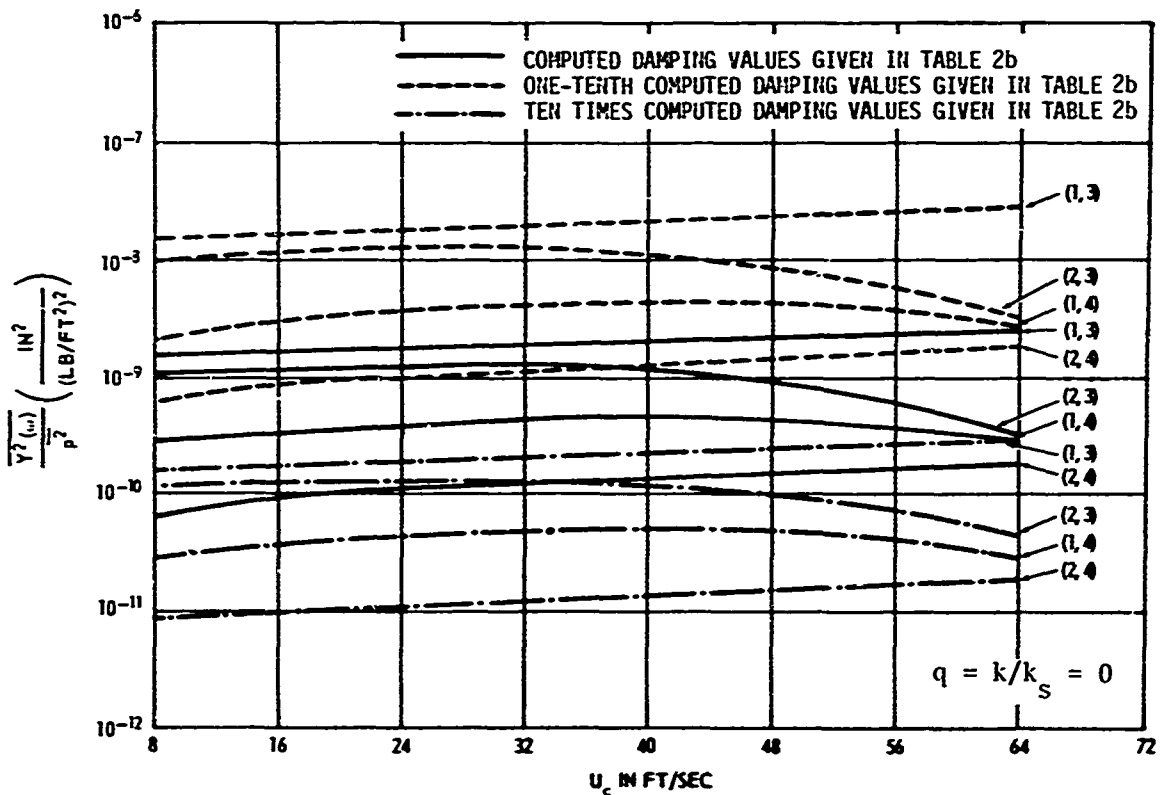
Figure 1 - Normalized Modal Mean Square Displacement of
Simply Supported Aluminum Plate with Fluid Loading
Effects Included

The response results computed at NSRDC and plotted in
Figure 1 were duplicated by Mr. Lucio Maestrello and Mrs.
Christene Brown who assisted the author by performing
similar computations on their computer at Langley Research
Center NASA, using the author's program. Their more ex-
tensive results are tabulated in Table 2c.

8

TABLE 3

Input Data for Computing Normalized Modal Mean Square Displacement $\overline{Y^2(\omega)}/\overline{p^2}$
for Simply Supported Steel Plate in Water

TABLE 3a
Computed Natural Frequencies and Total Damping for
Simply Supported Steel Plate in Air

Mode Number (m,n)	f(Hz) Warburton	ω_{mn}(rad/sec) Warburton	$\delta_{mn} = 0.5/f_{mn}$	$a_{mn} = \dfrac{\delta_{mn}\,\omega_{mn}}{2}$ (1/sec)
1,1	3.37	21.16	0.1483	0.5π
2,1	13.37	83.98	0.0373	
3,1	30.03	188.68	0.0166	
4,1	53.36	335.25	0.0093	
5,1	83.35	523.71	0.0059	
6,1	120.01	754.05	0.0041	
7,1	163.33	1026.26	0.0030	
8,1	213.32	1340.35	0.0023	
9,1	269.98	1596.33	0.0018	
10,1	333.30	2094.18	0.0015	
11,1	403.28	2533.91	0.0012	
12,1	479.93	3015.52	0.0010	
13,1	563,25	2539.01	0.0008	
14,1	653.23	4104.38	0.0007	
15,1	749.88	4711.63	0.0006	
16,1	853.19	5360.75	0.00058	
17,1	963.17	6051.76	0.00051	
18,1	1079.81	6784.65	0.00046	
19,1	1203.12	7559.41	0.00041	
20,1	1333.09	8376.05	0.00037	0.5π

a   = 10 ft
b   = 97.39 ft
h   = 0.5 in.
E   = 30×10^6 lb/in.^{2}
σ = 0.30
$(\rho_w)_{\text{steel}}$ = 0.283 lb/in.^{3}
g   = 32.2 ft/sec^2 = 384.6 in./sec^2
κ = 1.204×10^{-2} ft
c_ℓ = 17,000 ft/sec

9

TABLE 3b

Input Data for Computing $\dfrac{\overline{\gamma^2(\omega)}}{\overline{p^2}}$ for Simply Supported Steel Plate in Water--

Frequency Computation by Method I; q = 0

Mode Number (m,n)	W_p (lb/ft²)	W_{mn} (lb/ft²)	$W'=W_p+W_{mn}$ (lb/ft²)	$(W')^2$ (lb/ft²)²	$\bar{f}_{mn}$ (hz)	$\bar{\omega}_{mn}$ (rad/sec)	$\bar{a}_{mn}$ (1/sec)	$\bar{\delta}_{mn}$
1,1	20.4	406.57	426.97	182303.38	0.74	4.62	0.0748	0.03238
2,1		204.09	224.49	50395.76	4.03	25.33	0.1425	0.01125
3,1		136.16	156.56	24511.03	10.85	68.13	0.2045	0.00600
4,1		102.14	122.54	15016.05	21.79	136.83	0.2612	0.00381
5,1		81.72	102.12	10428.49	37.28	234.14	0.3135	0.00267
6,1		68.11	88.51	7834.02	57.66	362.12	0.3617	0.00199
7,1		58.38	78.78	6206.28	83.18	522.39	0.4064	0.00155
8,1		51.08	71.48	5109.39	114.05	716.23	0.4479	0.00125
9,1		45.41	65.81	4330.95	150.43	944.72	0.4865	0.00102
10,1		40.87	61.27	3754.01	192.47	1208.72	0.5226	0.00086
11,1		37.15	57.55	3312.00	240.28	1508.97	0.5564	0.00073
12,1		34.06	54.46	2975.70	293.97	1846.10	0.5879	0.00063
13,1		31.44	51.84	2687.38	353.60	2220.64	0.6177	0.00055
14,1		29.19	49.59	2459.16	419.27	2633.03	0.6457	0.00049
15,1		27.25	47.65	2270.52	491.03	3083.68	0.6721	0.00043
16,1		25.54	45.94	2110.48	568.94	3572.93	0.6966	0.00038
17,1		24.04	44.54	1983.81	653.04	4101.07	0.7190	0.00035
18,1		22.71	43.21	1867.10	743.37	4668.38	0.7411	0.00031
19,1		21.51	41.91	1756.44	839.98	5275.09	0.7641	0.00028
20,1	20.4	20.43	40.93	1675.26	942.90	5921.40	0.7824	0.00026

results for modes of interest

a = 10 ft

b = 97.39 ft

h = 0.5 in.

$\kappa = \dfrac{h}{2\sqrt{3}}$ = 1.204 x 10⁻² ft

c_ℓ = 17,000 ft/sec

$x = x'$ = 5.0 ft

$y = y'$ = 48.695 ft

W' (lb/ft²) (see Column E)

σ = 0.30

E = 30 x 10⁶ lb/in.²

$(\rho_w)_{steel}$ = 0.283 lb/in.³

g = 384.6 in./sec²

$\overline{p^2}$ = 1.0 (lb/ft²)²

τ_w = 0.323 lb/ft²

$(\rho_w)_{water}$ = 64.2 lb/ft³ = 0.037 lb/in.³

α = 2.0

i	A_i	K_i
1	1.6	0.47
2	7.2	3.0
3	12.0	14.0

U_c (ft/sec)	θ (sec)	δ^* (ft)
8	2.25 x 10⁻³	0.044
16		0.041
32		0.038
64	2.25 x 10⁻³	0.035

Note: $\bar{a}_{mn} = a_{mn} (W_p/W') = (0.5\pi)\left(\dfrac{20.4}{20.4 + W_{mn}}\right)$

$\bar{\delta}_{mn} = \dfrac{2\,\bar{a}_{mn}}{\bar{\omega}_{mn}}$

Note: In computing f_{mn} or ω_{mn} (see Program C' in Section 3 of Appendix H) the program input is in lb/in.³ units for $(\rho_w)_{steel}$. In computing $\bar{f}_{mn}$ or $\bar{\omega}_{mn}$ (see Program B' in Section 3 of Appendix H) the program input is in lb/ft³ units for both $(\rho_w)_{steel}$ and $(\rho_w)_{water}$.

q = 0.3

Mode Number (m,n)	W_p(lb/ft^2)	W_{mn}(lb/ft^2)	$W'=W_p+W_{mn}$ (lb/ft^2)	$(W')^2$(lb/ft^2)^2	$\bar{f}_{mn}$(Hz)	$\bar{\omega}_{mn}$(rad/sec)	$\bar{a}_{mn}$(1/sec)	$\bar{\delta}_{mn}$
1,1	20.4	426.20	446.60	199451.56	0.72	4.52	0.0715	0.03163
2,1		213.94	234.34	54915.24	3.95	24.79	0.1365	0.01101
3,1		142.73	163.13	26611.40	10.63	66.74	0.1962	0.00587
4,1		107.08	127.48	16251.15	21.36	134.16	0.2512	0.00374
5,1		85.67	106.07	11250.84	36.58	229.75	0.3019	0.00262
6,1		71.40	91.80	8427.24	56.62	355.58	0.3488	0.00196
7,1		61.20	81.60	6658.56	81.73	513.29	0.3925	0.00152
8,1		53.55	73.95	5468.60	112.13	704.19	0.4330	0.00122
9,1		47.60	68.00	4624.00	147.99	929.36	0.4710	0.00101
10,1		42.84	63.24	3999.30	189.45	1189.72	0.5063	0.00085
11,1		38.95	59.35	3522.42	236.62	1486.00	0.5396	0.00072
12,1		35.70	56.10	3147.21	289.63	1818.85	0.5708	0.00062
13,1		32.96	53.36	2847.29	348.54	2188.83	0.6002	0.00054
14,1		30.60	51.00	2601.00	413.44	2596.40	0.6280	0.00048
15,1		28.56	48.96	2397.08	484.39	3041.98	0.6540	0.00042
16,1		26.78	47.18	2225.95	561.45	3525.93	0.6787	0.00038
17,1		25.20	45.60	2079.36	644.68	4048.56	0.7022	0.00034
18,1		23.80	44.20	1953.64	734.10	4610.15	0.7245	0.00031
19,1		22.54	42.94	1843.84	829.77	5210.94	0.7457	0.00028
20,1		21.42	41.82	1748.91	931.71	5851.16	0.7658	0.00026

results for modes of interest

q = 0.6

Mode Number (m,n)	W_p(lb/ft^2)	W_{mn}(lb/ft^2)	$W'=W_p+W_{mn}$ (lb/ft^2)	$(W')^2$(lb/ft^2)^2	$\bar{f}_{mn}$(Hz)	$\bar{\omega}_{mn}$(rad/sec)	$\bar{a}_{mn}$(1/sec)	$\bar{\delta}_{mn}$
1,1	20.4	508.21	528.61	279428.53	0.66	4.16	0.0604	0.02903
2,1		255.11	275.51	75905.76	3.64	22.86	0.1161	0.01015
3,1		170.20	190.60	36328.36	9.83	61.75	0.1679	0.00543
4,1		127.68	148.08	21927.69	19.82	124.48	0.2161	0.00347
5,1		102.16	122.56	15020.95	34.04	213.74	0.2612	0.00244
6,1		85.14	105.54	11138.69	52.80	331.63	0.3033	0.00182
7,1		72.98	93.38	8719.82	76.41	479.83	0.3428	0.00142
8,1		63.86	84.26	7099.75	105.05	659.73	0.3800	0.00115
9,1		56.76	77.16	5953.67	138.93	872.47	0.4149	0.00095
10,1		51.09	71.49	5110.82	178.19	1119.03	0.4479	0.00080
11,1		46.44	66.84	4467.59	222.97	1400.24	0.4791	0.00068
12,1		42.57	62.97	3965.22	273.38	1716.80	0.5085	0.00059
13,1		39.30	59.70	3564.09	329.51	2069.34	0.5364	0.00051
14,1		36.49	56.89	3236.47	391.46	2458.40	0.5628	0.00045
15,1		34.06	54.46	2965.89	459.31	2884.45	0.6104	0.00042
16,1		31.93	52.33	2738.43	533.11	3347.90	0.6119	0.00036
17,1		30.05	50.45	2545.20	612.92	3849.13	0.6347	0.00032
18,1		28.38	49.28	2428.52	698.80	4388.49	0.6498	0.00029
19,1		26.89	47.29	2236.34	790.80	4966.20	0.6771	0.00027
20,1		25.54	45.94	2110.48	888.95	5582.60	0.6970	0.00024

results for modes of interest

11

TABLE 3e (Continued)

q = 0.9

Mode Number	W_p (lb/ft^2)	W_{mn} (lb/ft^2)	$W' = W_p + W_{mn}$ (lb/ft^2)	$(W')^2$ (lb/ft^2)^2	$\bar{f}_{mn}$ (Hz)	$\bar{\omega}_{mn}$ ($\frac{rad}{sec}$)	$\bar{a}_{mn}$ (1/sec)	$\bar{\delta}_{m,n}$
1,1	20.4	932.74	953.14	908475.86	0.49	3.10	0.0335	0.02161
2,1		468.20	488.60	238729.96	2.734	17.17	0.0654	0.00761
3,1		312.36	332.76	111394.74	7.44	46.93	0.0962	0.00415
4,1		234.33	254.73	64887.37	15.11	94.91	0.1256	0.00264
5,1		187.49	207.89	43218.25	26.13	164.11	0.1540	0.00187
6,1		156.25	176.65	31205.22	40.82	256.33	0.1811	0.00141
7,1		133.93	154.33	23817.75	59.43	373.24	0.2073	0.00111
8,1		117.20	137.60	18933.76	82.21	516.27	0.2326	0.00090
9,1		104.18	124.58	15520.18	109.34	686.68	0.2570	0.00074
10,1		93.76	115.16	13261.83	141.01	885.56	0.2780	0.00062
11,1		85.24	105.64	11159.81	177.37	1113.88	0.3031	0.00054
12,1		78.13	98.53	9708.16	218.56	1372.53	0.3249	0.00047
13,1		72.12	92.52	8559.95	264.70	1662.28	0.3460	0.00041
14,1		66.97	87.37	7633.52	315.90	1983.85	0.3664	0.00036
15,1		62.51	82.91	6874.07	372.27	2337.86	0.3862	0.00033
16,1		58.60	79.00	6241.00	433.90	2724.91	0.4053	0.00029
17,1		55.15	75.55	5707.80	500.88	3145.53	0.4239	0.00026
18,1		52.09	72.49	5254.80	573.28	3600.20	0.4417	0.00024
19,1		49.35	69.85	4879.02	651.18	4089.38	0.4584	0.00022
20,1		46.88	67.28	4526.90	734.63	4613.47	0.4760	0.00020

results for modes of interest

TABLE 3f (Continued)

q = 0.995

Mode Number	$\bar{f}_{mn}$ (Hz)
1,1	0.237
2,1	1.325
3,1	3.638
4,1	7.445
5,1	12.972
6,1	20.410
7,1	29.331
8,1	41.691
9,1	55.831
10,1	72.482
11,1	91.765
12,1	113.795
13,1	138.678
14,1	166.517
15,1	197.405
16,1	231.433
17,1	268.69
18,1	309.256
19,1	353.209
20,1	400.626

results for modes of interest

Note: No computations of $\dfrac{\overline{\gamma^2(\omega)}}{\overline{p}^2}$ were made for q = 0.995.

12

TABLE 3g

Computation of Normalized Modal Mean Square

Displacement $\overline{Y^2(\omega)}/\overline{p^2}$ for Simply Supported
Steel Plate in Water

Note: The extensive results for the response obtained by Mr. Lucio Maestrello and Mrs. Christine Brown at Langley Research Center, NASA, using the authors program, are tabulated in Tables 3g-3i.

q = 0   STEEL PLATE

U_c (ft/sec)	Mode Number (m,n)	$\dfrac{\overline{Y^2(\omega)}}{\overline{p^2}}$ *	$\dfrac{\overline{Y^2(\omega)}}{\overline{p^2}}$ **	$\dfrac{\overline{Y^2(\omega)}}{\overline{p^2}}$ ***
8	8,1	4.4×10^{-9}	4.4×10^{-10}	4.4×10^{-11}
	9,1	1.7×10^{-9}	1.7×10^{-10}	1.7×10^{-11}
	10,1	7.1×10^{-10}	7.1×10^{-11}	7.1×10^{-12}
	11,1	3.0×10^{-10}	3.0×10^{-11}	3.0×10^{-12}
	12,1	1.4×10^{-10}	1.4×10^{-11}	1.4×10^{-12}
	13,1	6.4×10^{-11}	6.4×10^{-12}	6.4×10^{-13}
	14,1	3.0×10^{-11}	3.0×10^{-12}	3.1×10^{-13}
	15,1	1.6×10^{-11}	1.6×10^{-12}	1.7×10^{-13}
	16,1	9.3×10^{-12}	9.3×10^{-13}	9.4×10^{-14}
	17,1	5.1×10^{-12}	5.1×10^{-13}	5.2×10^{-14}
	18,1	3.1×10^{-12}	3.1×10^{-13}	3.1×10^{-14}
	19,1	1.8×10^{-12}	1.8×10^{-13}	1.9×10^{-14}
	20,1	1.0×10^{-12}	1.0×10^{-13}	1.1×10^{-14}
16	8,1	4.2×10^{-9}	4.2×10^{-10}	4.2×10^{-11}
	9,1	1.7×10^{-9}	1.7×10^{-10}	1.7×10^{-11}
	10,1	7.5×10^{-10}	7.5×10^{-11}	7.6×10^{-12}
	11,1	3.1×10^{-10}	3.1×10^{-11}	3.1×10^{-12}
	12,1	1.4×10^{-10}	1.4×10^{-11}	1.4×10^{-12}
	13,1	6.8×10^{-11}	6.8×10^{-12}	6.8×10^{-13}
	14,1	3.9×10^{-11}	3.9×10^{-12}	3.9×10^{-13}
	15,1	2.3×10^{-11}	2.3×10^{-12}	2.3×10^{-13}
	16,1	1.2×10^{-11}	1.2×10^{-12}	1.2×10^{-13}
	17,1	5.7×10^{-12}	5.7×10^{-13}	5.7×10^{-14}
	18,1	3.1×10^{-12}	3.1×10^{-13}	3.2×10^{-14}
	19,1	1.9×10^{-12}	1.9×10^{-13}	2.0×10^{-14}
	20,1	1.2×10^{-12}	1.2×10^{-13}	1.2×10^{-14}
32	8,1	3.2×10^{-9}	3.2×10^{-10}	3.2×10^{-11}
	9,1	1.1×10^{-9}	1.1×10^{-10}	1.1×10^{-11}
	10,1	4.6×10^{-10}	4.6×10^{-11}	4.7×10^{-12}

13

Table 3g (Continued)

STEEL PLATE (Continued)

q = 0

U_c (ft/sec)	Mode Number (m,n)	$\dfrac{\overline{\gamma^2(\omega)}}{\overline{p^2}}$ *	$\dfrac{\overline{\gamma^2(\omega)}}{\overline{p^2}}$ **	$\dfrac{\overline{\gamma^2(\omega)}}{\overline{p^2}}$ ***
	11,1	2.2×10^{-10}	2.2×10^{-11}	2.2×10^{-12}
	12,1	1.3×10^{-10}	1.3×10^{-11}	1.3×10^{-12}
	13,1	8.9×10^{-11}	8.9×10^{-12}	9.0×10^{-13}
	14,1	6.7×10^{-11}	6.7×10^{-12}	6.7×10^{-13}
	15,1	4.5×10^{-11}	4.5×10^{-12}	4.5×10^{-13}
	16,1	2.3×10^{-11}	2.3×10^{-12}	2.3×10^{-13}
	17,1	9.5×10^{-12}	9.5×10^{-13}	9.5×10^{-14}
	18,1	4.1×10^{-12}	4.1×10^{-13}	4.2×10^{-14}
	19,1	1.7×10^{-12}	1.7×10^{-13}	1.7×10^{-14}
	20,1	5.8×10^{-13}	5.8×10^{-14}	6.0×10^{-15}
64	8,1	3.5×10^{-9}	3.5×10^{-10}	3.5×10^{-11}
	9,1	1.3×10^{-9}	1.3×10^{-10}	1.3×10^{-11}
	10,1	5.0×10^{-10}	5.0×10^{-11}	5.1×10^{-12}
	11,1	2.1×10^{-10}	2.1×10^{-11}	2.1×10^{-12}
	12,1	7.1×10^{-11}	7.1×10^{-12}	7.2×10^{-13}
	13,1	1.8×10^{-11}	1.8×10^{-12}	1.9×10^{-13}
	14,1	†	†	†
	15,1	†	†	†
	16,1	†	†	†
	17,1	†	†	†
	18,1	1.0×10^{-12}	1.0×10^{-13}	1.0×10^{-14}
	19,1	1.2×10^{-12}	1.2×10^{-13}	1.2×10^{-14}
	20,1	1.0×10^{-12}	1.0×10^{-13}	1.1×10^{-14}

*For one-tenth computed damping value given in Table 3b.

**For computed damping value given in Table 3b.

***For ten times computed damping value given in Table 3b.

†Computer error (recomputation not made).

TABLE 3h

STEEL PLATE

q = 9.5

U_c (ft/sec)	Mode Number (m,n)	$\dfrac{\overline{\gamma^2(\omega)}}{\overline{p^2}}$*	$\dfrac{\overline{\gamma^2(\omega)}}{\overline{p^2}}$**	$\dfrac{\overline{\gamma^2(\omega)}}{\overline{p^2}}$***
8	8,1	4.5×10^{-9}	4.5×10^{-10}	4.6×10^{-11}
	9,1	1.7×10^{-9}	1.7×10^{-10}	1.8×10^{-11}
	10,1	7.3×10^{-10}	7.3×10^{-11}	7.3×10^{-12}
	11,1	3.1×10^{-10}	3.1×10^{-11}	3.1×10^{-12}
	12,1	1.4×10^{-10}	1.4×10^{-11}	1.5×10^{-12}
	13,1	6.5×10^{-11}	6.5×10^{-12}	6.6×10^{-13}
	14,1	3.2×10^{-11}	3.2×10^{-12}	3.2×10^{-13}
	15,1	1.7×10^{-11}	1.7×10^{-12}	1.7×10^{-13}
	16,1	9.5×10^{-12}	9.5×10^{-13}	9.6×10^{-14}
	17,1	5.4×10^{-12}	5.4×10^{-13}	5.5×10^{-14}
	18,1	3.2×10^{-12}	3.2×10^{-13}	3.2×10^{-14}
	19,1	1.9×10^{-12}	1.9×10^{-13}	1.9×10^{-14}
	20,1	1.1×10^{-12}	1.1×10^{-13}	1.1×10^{-14}
16	8,1	4.3×10^{-9}	4.3×10^{-10}	4.3×10^{-11}
	9,1	1.8×10^{-9}	1.8×10^{-10}	1.8×10^{-11}
	10,1	7.7×10^{-10}	7.7×10^{-11}	7.7×10^{-12}
	11,1	3.2×10^{-10}	3.2×10^{-11}	3.2×10^{-12}
	12,1	1.4×10^{-10}	1.4×10^{-12}	1.4×10^{-12}
	13,1	6.8×10^{-11}	6.8×10^{-12}	6.9×10^{-13}
	14,1	3.9×10^{-11}	3.9×10^{-12}	4.0×10^{-13}
	15,1	2.4×10^{-11}	2.4×10^{-12}	2.4×10^{-13}
	16,1	1.2×10^{-11}	1.2×10^{-12}	1.2×10^{-13}
	17,1	6.1×10^{-12}	6.1×10^{-13}	6.1×10^{-14}
	18,1	3.2×10^{-12}	3.2×10^{-13}	2.3×10^{-14}
	19,1	2.0×10^{-12}	2.0×10^{-13}	2.0×10^{-14}
	20,1	1.2×10^{-12}	1.2×10^{-13}	1.3×10^{-14}
32	8,1	3.3×10^{-9}	3.3×10^{-10}	3.3×10^{-11}
	9,1	1.2×10^{-9}	1.2×10^{-10}	1.2×10^{-11}
	10,1	4.7×10^{-10}	4.7×10^{-11}	4.7×10^{-12}
	11,1	2.2×10^{-10}	2.2×10^{-11}	2.3×10^{-12}

$$f_c = \frac{c^2}{2\pi\kappa c_\ell}$$

aluminum 243,000

steel 19,400

15

Table 3h (Continued)

STEEL PLATE (Continued)

$q = 0.3$

U_c (ft/sec)	Mode Number (m,n)	$\dfrac{\overline{\gamma^2(\omega)}}{\overline{p^2}}$[*]	$\dfrac{\overline{\gamma^2(\omega)}}{\overline{p^2}}$[**]	$\dfrac{\overline{\gamma^2(\omega)}}{\overline{p^2}}$[***]
	12,1	1.3×10^{-10}	1.3×10^{-11}	1.3×10^{-12}
	13,1	8.8×10^{-11}	8.8×10^{-12}	8.8×10^{-13}
	14,1	6.6×10^{-11}	6.6×10^{-12}	6.6×10^{-13}
	15,1	4.7×10^{-11}	4.7×10^{-12}	4.7×10^{-13}
	16,1	2.5×10^{-11}	2.5×10^{-12}	2.5×10^{-13}
	17,1	1.0×10^{-11}	1.0×10^{-12}	1.0×10^{-13}
	18,1	4.4×10^{-12}	4.4×10^{-13}	4.5×10^{-14}
	19,1	1.8×10^{-12}	1.8×10^{-13}	1.9×10^{-14}
	20,1	6.0×10^{-13}	6.1×10^{-14}	6.3×10^{-15}
64	8,1	3.6×10^{-9}	3.6×10^{-10}	3.6×10^{-11}
	9,1	1.4×10^{-9}	1.4×10^{-10}	1.4×10^{-11}
	10,1	5.2×10^{-10}	5.2×10^{-11}	5.3×10^{-12}
	11,1	2.1×10^{-10}	2.1×10^{-11}	2.2×10^{-12}
	12,1	7.7×10^{-11}	7.7×10^{-12}	7.8×10^{-13}
	13,1	2.2×10^{-11}	2.2×10^{-12}	2.3×10^{-13}
	14,1	†	†	†
	15,1	†	†	†
	16,1	†	†	†
	17,1	†	†	†
	18,1	†	†	†
	19,1	†	†	†
	20,1	†	†	†

[*] For one-tenth computed damping value given in Table 3b.

[**] For computed damping value given in Table 3b.

[***] For ten times computed damping value given in Table 3b.

†Computer error (recomputation not made).

16

TABLE 5i

STEEL PLATE

$q = 0.6$

U_c (ft/sec)	Mode Number (n,n)	$\dfrac{\overline{Y^2(\omega)}}{\overline{p^2}}$ *	$\dfrac{\overline{Y^2(\omega)}}{\overline{p^2}}$ **	$\dfrac{\overline{Y^2(\omega)}}{\overline{p^2}}$ ***
8	8,1	4.9×10^{-9}	4.9×10^{-10}	4.9×10^{-11}
	9,1	1.9×10^{-9}	1.9×10^{-10}	1.9×10^{-11}
	10,1	7.9×10^{-10}	7.9×10^{-11}	8.0×10^{-12}
	11,1	3.5×10^{-10}	3.5×10^{-11}	3.5×10^{-12}
	12,1	1.6×10^{-10}	1.6×10^{-11}	1.6×10^{-12}
	13,1	7.3×10^{-11}	7.3×10^{-12}	7.4×10^{-13}
	14,1	3.7×10^{-11}	3.8×10^{-12}	3.8×10^{-13}
	15,1	1.9×10^{-11}	1.9×10^{-12}	1.9×10^{-13}
	16,1	1.0×10^{-11}	1.0×10^{-12}	1.0×10^{-13}
	17,1	5.6×10^{-12}	5.6×10^{-13}	5.7×10^{-14}
	18,1	3.2×10^{-12}	3.2×10^{-13}	3.2×10^{-14}
	19,1	1.9×10^{-12}	1.9×10^{-13}	1.9×10^{-14}
	20,1	1.3×10^{-12}	1.3×10^{-13}	1.3×10^{-14}
16	8,1	4.5×10^{-9}	4.5×10^{-10}	4.5×10^{-11}
	9,1	1.9×10^{-9}	1.9×10^{-10}	1.9×10^{-11}
	10,1	8.4×10^{-10}	8.4×10^{-10}	8.5×10^{-12}
	11,1	3.7×10^{-10}	3.7×10^{-11}	3.8×10^{-12}
	12,1	1.6×10^{-10}	1.6×10^{-11}	1.6×10^{-12}
	13,1	7.3×10^{-11}	7.3×10^{-12}	7.4×10^{-13}
	14,1	4.1×10^{-11}	4.1×10^{-12}	4.2×10^{-13}
	15,1	2.4×10^{-11}	2.4×10^{-12}	2.4×10^{-13}
	16,1	1.4×10^{-11}	1.4×10^{-12}	1.4×10^{-13}
	17,1	7.1×10^{-12}	7.1×10^{-13}	7.1×10^{-14}
	18,1	3.5×10^{-12}	3.5×10^{-13}	3.5×10^{-14}
	19,1	2.0×10^{-12}	2.0×10^{-13}	2.0×10^{-14}
	20,1	1.3×10^{-12}	1.3×10^{-13}	1.4×10^{-14}
32	8,1	3.6×10^{-9}	3.6×10^{-10}	3.6×10^{-11}
	9,1	1.3×10^{-9}	1.3×10^{-10}	1.3×10^{-11}
	10,1	5.0×10^{-10}	5.0×10^{-11}	5.1×10^{-12}

Table 3i (Continued)

STEEL PLATE (Continued)

$q = 0.6$

U_c (ft/sec)	Mode Number (m,n)	$\dfrac{\overline{\gamma^2(\omega)}}{\overline{p^2}}$ *	$\dfrac{\overline{\gamma^2(\omega)}}{\overline{p^2}}$ **	$\dfrac{\overline{\gamma^2(\omega)}}{\overline{p^2}}$ ***
	11,1	2.3×10^{-10}	2.3×10^{-11}	2.3×10^{-12}
	12,1	1.3×10^{-10}	1.3×10^{-11}	1.3×10^{-12}
	13,1	8.1×10^{-11}	8.1×10^{-12}	8.2×10^{-13}
	14,1	6.0×10^{-11}	6.0×10^{-12}	6.0×10^{-13}
	15,1	4.4×10^{-11}	4.4×10^{-12}	4.4×10^{-13}
	16,1	3.0×10^{-11}	3.0×10^{-12}	3.0×10^{-13}
	17,1	1.5×10^{-11}	1.5×10^{-12}	1.5×10^{-13}
	18,1	6.1×10^{-12}	6.1×10^{-13}	5.2×10^{-14}
	19,1	2.7×10^{-12}	2.7×10^{-13}	2.8×10^{-14}
	20,1	1.1×10^{-12}	1.1×10^{-13}	1.2×10^{-14}
64	8,1	3.9×10^{-9}	3.9×10^{-10}	4.0×10^{-11}
	9,1	1.5×10^{-9}	1.5×10^{-10}	1.5×10^{-11}
	10,1	6.0×10^{-10}	6.0×10^{-11}	6.0×10^{-12}
	11,1	2.5×10^{-10}	2.5×10^{-11}	2.5×10^{-12}
	12,1	9.9×10^{-11}	9.9×10^{-12}	1.0×10^{-12}
	13,1	3.6×10^{-11}	3.6×10^{-12}	3.7×10^{-13}
	14,1	4.8×10^{-12}	4.9×10^{-13}	5.3×10^{-14}
	15,1	÷	÷	÷
	16,1	÷	÷	÷
	17,1	÷	÷	÷
	18,1	÷	÷	÷
	19,1	÷	÷	÷
	20,1	÷	÷	÷

*For one-tenth computed damping value given in Table 3b.

**For computed damping value given in Table 3b.

***For ten times computed damping value given in Table 3b.

÷Computer error (recomputation not made).

18

TABLE 3j

STEEL PLATE

q = 0.9

U_c (ft/sec)	Mode Number (m,n)	$\dfrac{\overline{r^2(\omega)}}{\overline{p^2}}$ *	$\dfrac{\overline{r^2(\omega)}}{\overline{p^2}}$ **	$\dfrac{\overline{r^2(\omega)}}{\overline{p^2}}$ ***
8	8,1	---	---	---
	9,1	2.7×10^{-9}	2.7×10^{-10}	2.7×10^{-11}
	10,1	1.1×10^{-9}	1.1×10^{-10}	1.1×10^{-11}
	11,1	5.1×10^{-10}	5.1×10^{-11}	5.1×10^{-12}
	12,1	2.4×10^{-10}	2.4×10^{-11}	2.4×10^{-12}
	13,1	1.1×10^{-10}	1.1×10^{-11}	1.1×10^{-12}
	14,1	5.7×10^{-11}	5.7×10^{-12}	5.7×10^{-13}
	15,1	3.0×10^{-11}	3.0×10^{-12}	3.0×10^{-13}
	16,1	1.5×10^{-11}	1.5×10^{-12}	1.5×10^{-13}
	17,1	8.6×10^{-12}	8.6×10^{-13}	8.7×10^{-14}
	18,1	5.1×10^{-12}	5.1×10^{-13}	5.1×10^{-14}
	19,1	3.1×10^{-12}	3.1×10^{-13}	3.1×10^{-14}
	20,1	1.9×10^{-12}	1.9×10^{-13}	1.9×10^{-14}
16	8,1	---	---	---
	9,1	2.5×10^{-9}	2.5×10^{-10}	2.5×10^{-11}
	10,1	1.1×10^{-9}	1.1×10^{-10}	1.1×10^{-11}
	11,1	5.5×10^{-10}	5.5×10^{-11}	5.5×10^{-12}
	12,1	2.7×10^{-10}	2.7×10^{-11}	2.8×10^{-12}
	13,1	1.3×10^{-10}	1.3×10^{-11}	1.3×10^{-12}
	14,1	5.9×10^{-11}	6.0×10^{-12}	6.0×10^{-13}
	15,1	2.9×10^{-11}	2.9×10^{-12}	2.9×10^{-13}
	16,1	1.6×10^{-11}	1.6×10^{-12}	1.6×10^{-13}
	17,1	1.1×10^{-11}	1.1×10^{-12}	1.1×10^{-13}
	18,1	7.0×10^{-12}	7.0×10^{-13}	7.1×10^{-14}
	19,1	4.0×10^{-12}	4.0×10^{-13}	4.0×10^{-14}
	20,1	2.1×10^{-12}	2.2×10^{-13}	2.2×10^{-14}
32	8,1	---	---	---
	9,1	2.0×10^{-9}	2.0×10^{-10}	2.0×10^{-11}
	10,1	7.9×10^{-10}	7.9×10^{-11}	8.0×10^{-12}

19

STEEL PLATE (Continued)

q = 0.9

U_c (ft/sec)	Mode Number (n,n)	$\overline{\dfrac{Y^2(\omega)}{p^2}}$ *	$\overline{\dfrac{Y^2(\omega)}{p^2}}$ **	$\overline{\dfrac{Y^2(\omega)}{p^2}}$ ***
	11,1	3.2×10^{-10}	3.2×10^{-11}	3.2×10^{-12}
	12,1	1.4×10^{-10}	1.4×10^{-11}	1.4×10^{-12}
	13,1	7.4×10^{-11}	7.4×10^{-12}	7.5×10^{-13}
	14,1	4.6×10^{-11}	4.6×10^{-12}	4.6×10^{-13}
	15,1	3.0×10^{-11}	3.0×10^{-12}	3.1×10^{-13}
	16,1	2.4×10^{-11}	2.4×10^{-12}	2.4×10^{-13}
	17,1	2.1×10^{-11}	2.1×10^{-12}	2.1×10^{-13}
	18,1	1.6×10^{-11}	1.6×10^{-12}	1.6×10^{-13}
	19,1	9.4×10^{-12}	9.4×10^{-13}	9.4×10^{-14}
	20,1	4.4×10^{-12}	4.4×10^{-13}	4.4×10^{-14}
64			Not Computed	
	9,1	2.3×10^{-9}	2.3×10^{-10}	2.3×10^{-11}
	10,1	9.5×10^{-10}	9.5×10^{-11}	9.6×10^{-12}
	11,1	4.1×10^{-10}	4.1×10^{-11}	4.2×10^{-12}
	12,1	1.8×10^{-10}	1.8×10^{-11}	1.8×10^{-12}
	13,1	8.5×10^{-11}	8.5×10^{-12}	8.6×10^{-13}
	14,1	3.9×10^{-11}	3.9×10^{-12}	3.9×10^{-13}
	15,1	1.4×10^{-11}	1.4×10^{-12}	1.4×10^{-13}
	16,1	2.8×10^{-12}	2.9×10^{-13}	3.0×10^{-14}
	17,1	÷	÷	÷
	18,1	÷	÷	÷
	19,1	÷	÷	÷
	20,1	÷	÷	÷

*For one-tenth computed damping value given in Table 3b.

**For computed damping value given in Table 3b.

***For ten times computed damping value given in Table 3b.

---Computation not made for 8,1 mode because for q = 0.9, $\tilde{f}_{8,1}$ < 100 Hz (see Table 3e).

÷Computer error (recomputation not made).

Figure 2 - Normalized Modal Mean Square Displacement of Simply Supported Steel Plate with Fluid Loading Effects Included

The response results computed at NSRDC and plotted in
Figure 2 were duplicated by Mr. Lucio Maestrello and Mrs.
Christene Brown who assisted the author by performing
similar computations on their computer at Langley Research
Center NASA, using the author's program. Their more extensive results are tabulated in Tables 3g-3j.
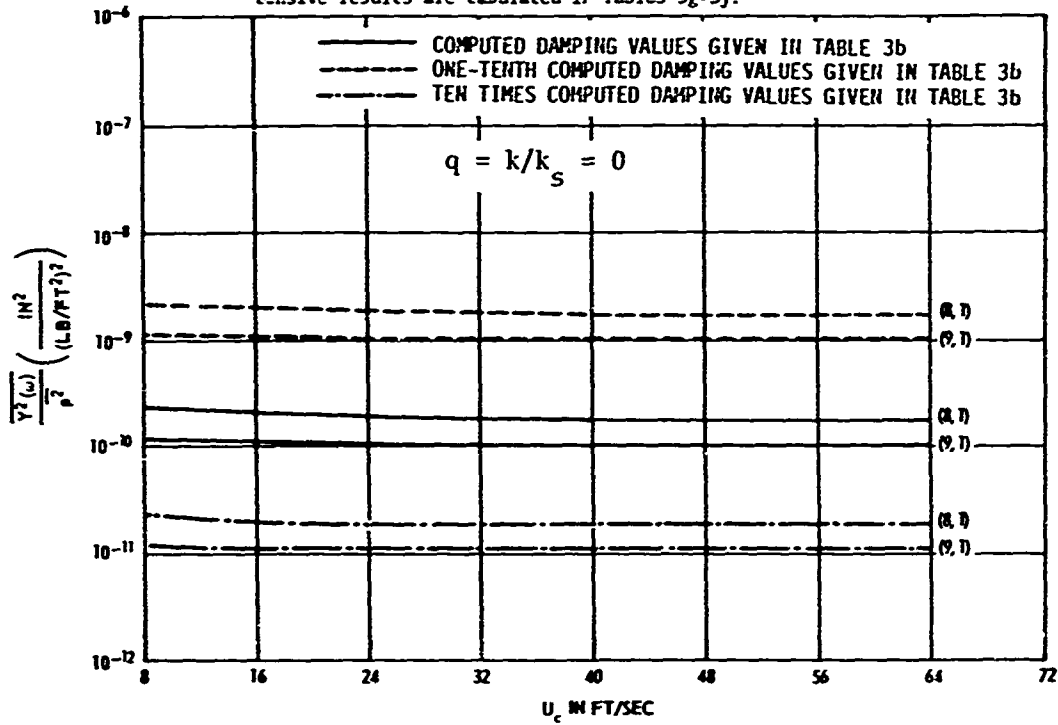
Figure 2a

Figure 2b

21
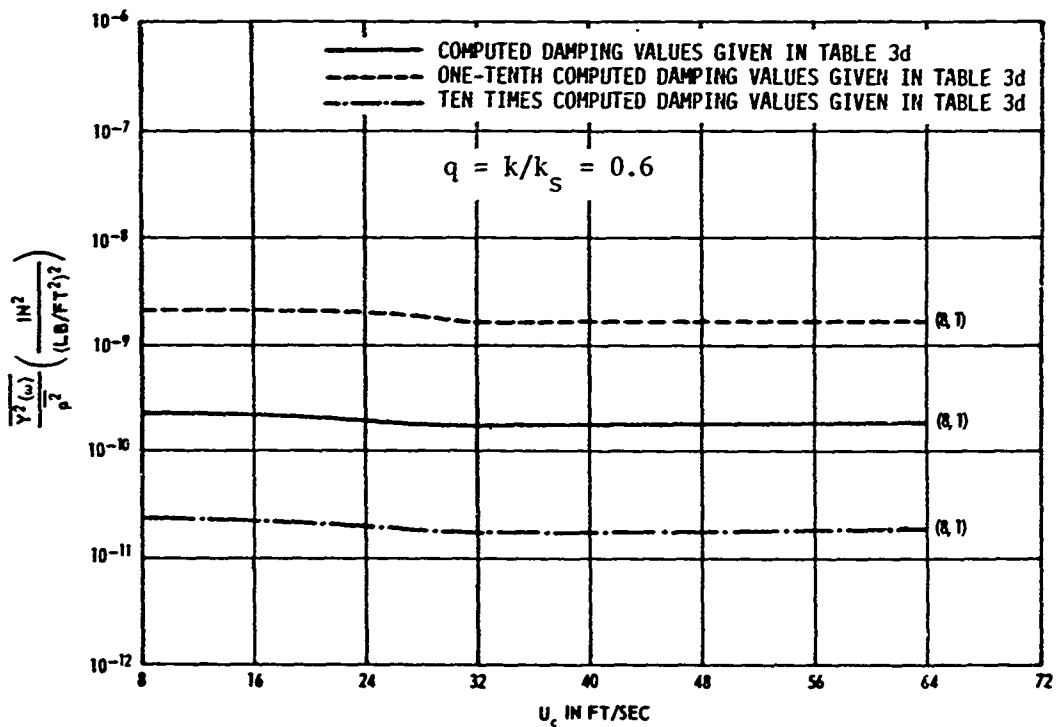
Figure 2c

Figure 2d
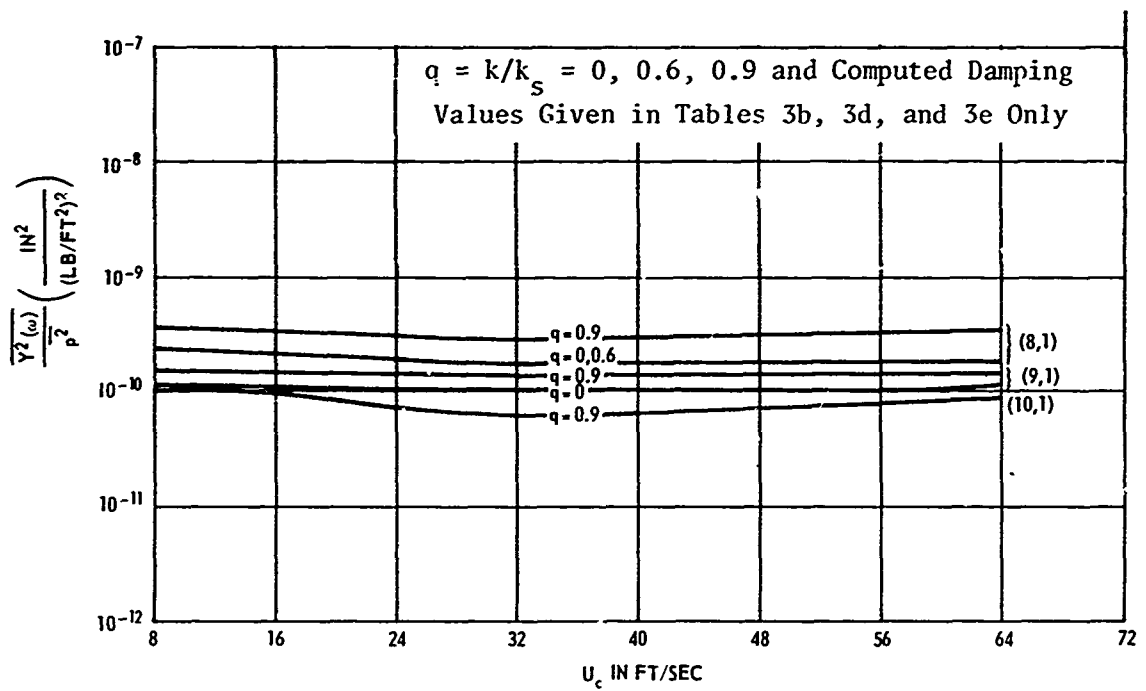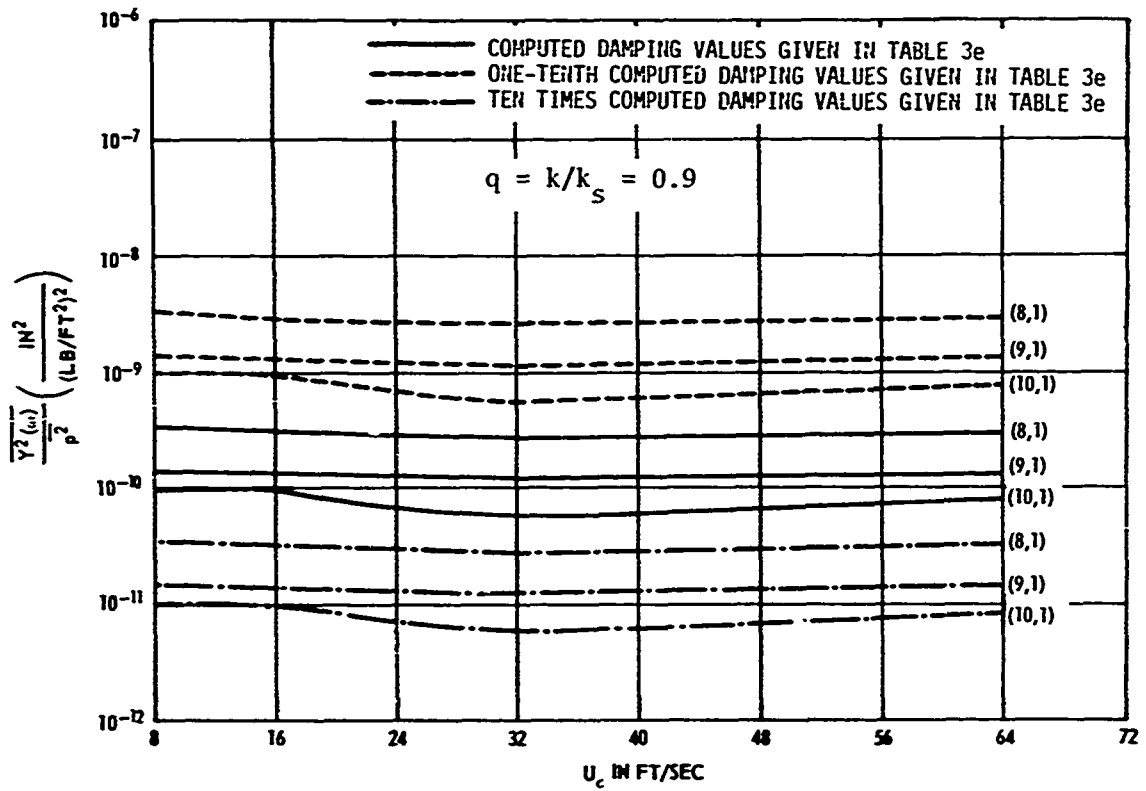
Note: Results for one-tenth and ten times the computed
damping values are obtainable by multiplying and dividing
the vertical scale by a factor of 10, respectively.

22

CALCULATIONS AND RESULTS

The analytical results for a fluid-loaded plate are presented in a series of Appendixes (A-G). The salient features of this study are summarized in Table 1 for the convenience of the reader.

In addition, computer results were obtained for the vibratory response of a water-loaded, simply supported, rectangular-aluminum isotropic plate and for a water-loaded, simply supported, rectangular-steel isotropic plate subject to turbulence excitation. The computer results were obtained by modifying *the updated version of the original formulation devised by Maestrello*[1] with the fluid loading program devised here. The corresponding mathematical analysis, methods for determining the input data, and computer program documentation are given in Appendix H.* Results are now presented for the aluminum and steel plates.

ALUMINUM PLATE

Table 2a presents the natural frequencies and total damping ratio of a simply supported aluminum plate in *air* for several modes of vibration.

The natural frequencies were computed by use of the Warburton method (see Reference 3 for the associated computer program) and were checked by use of the simple frequency expression $\omega_{mn} = \kappa c_\ell \left[\left(\frac{m\pi}{a} \right)^2 + \left(\frac{n\pi}{b} \right)^2 \right]$ for simply supported plates. The corresponding natural frequencies in *water*, as well as other relevant input data required for the computation of the normalized modal mean square displacement $\frac{\overline{Y^2(\omega)}}{\overline{p^2}}$, are tabulated in Table 2b.** The normalized modal mean square displacements $\frac{\overline{Y^2(\omega)}}{\overline{p^2}}$ for the simply supported aluminum plate in water are tabulated in Table 2c. All of these data are computed in accordance with the detailed procedure given in Appendix H.

---

*Both the updated program (designated MTURAD) which supercedes the original Maestrello program (designated TURAD) and the fluid loading program (Option 3) are presented in Appendix H.

**The Maestrello method[1] for obtaining $\overline{p^2}$ is given in Appendix H. Dyer (page 32 of Reference 1) uses $\overline{p^2} = [6 \times 10^{-3} \cdot \frac{1}{2} \rho U_\infty^2]^2$ and Jacobs (page 301 of Reference 1) used $\overline{p^2} = 3.1 \tau_w$. Here $\overline{p^2}$ is the mean square turbulence pressure, ρ is the fluid density, U_∞ is the free-stream velocity, and τ_w is the local wall shear stress (see Appendix H for further discussion).

Figure 1 is a plot of some of the computed results for the normalized modal mean square displacements $\overline{Y^2(\omega)}/\overline{p^2}$ of a simply supported, water-loaded aluminum plate subject to turbulence excitation over a range of convection velocities U_c for various values of damping and $q = k/k_s = 0$ only (see notation for Appendix H).[*] More extensive results are tabulated in Table 2c. The computer procedure used for the calculations is given in Appendix H.

STEEL PLATE

Table 3a tabulates the natural frequencies of a simply supported steel plate in *air* for several modes of vibration as computed by use of the Warburton method (see Reference 3 for the associated computer program). The corresponding natural frequencies in *water* as well as other relevant input data required for the computation of the normalized modal mean square displacement $\overline{Y^2(\omega)}/\overline{p^2}$ are tabulated in Tables 3b-3f. The normalized modal mean square displacements $\overline{Y^2(\omega)}/\overline{p^2}$ for the simply supported steel plate in water are tabulated in Tables 3g-3j.

Figures 2a-2d are plots of some of the computed results for the normalized modal mean square displacement $\overline{Y^2(\omega)}/\overline{p^2}$ of a simply supported, water-loaded steel plate subject to turbulence excitation over a range of convection velocities U_c for various values of damping[*] and $q = k/k_s < 1$ (see notation for Appendix H). More extensive results are tabulated in Tables 3g-3j. The computer procedure used for the calculations is given in Appendix H.

DISCUSSION AND EVALUATION

This section discusses (1) the analytical results, (2) the computational results, and (3) the turbulence-vibroacoustic relationships.

---

[*]For the present problem, the contribution of radiation damping but not added mass is excluded in the (acoustically slow) region for which the computations are applicable; see Appendix H for a more detailed discussion of this point. Simple equations for determining the radiation damping contributions for inclusion in the computer program will appear in a companion report.

ANALYTICAL RESULTS

Table 1 identifies and compares the various methods of computation. Notation pertinent to each method is found in Appendixes A-G inclusive. The results have been included in the overall computer program (see Appendix H).

From the summary for Appendix C given in Table 1, we observe that the solution to the Feit-Junger basic equations has been extended to include the added mass results for *coupled modes* in addition to their results for *uncoupled modes* presented in Appendix A; the extended results are then identical to corresponding results obtained by Davies in Appendix B. The physicomathematical basis clarifying the plate-fluid coupling mechanism is discussed in Appendix A. In general, results can be classified both in terms of modes in wave number space according to their radiation characteristics and in terms of frequency band.

It is interesting to note that despite the variety of analytical methods used, the results obtained in Appendixes A-E are identical for the *uncoupled modes*. As discussed in Appendixes A-C, the results for these modes are considered to be dominant with respect to the results for coupled modes. Moreover, we perceive from the discussion in Appendix D that for the *uncoupled (dominant) modes*, the methods of Appendixes A-D are applicable, with minor modification, to low wave numbers (m,n=(1,1) (1,2) (2,1)...) as well as to high wave numbers.

The results presented in Table 1 for Appendixes A-E are based on analyses which assume a plate with simple supports for the boundary condition. However, with proper modification and interpretation, these results can be used to yield corresponding results for fluid-loaded clamped plates, at least for the dominant modes. Following the method and using the computer program (Option 2) described in Reference 3, we first obtain the *in vacuo* natural circular frequency $\omega_{mn} \rightarrow (\omega_{mn})_{\text{clamped}}$ for a *clamped-clamped* plate.[*] The frequency for the *fluid-loaded clamped-clamped plate* is

---

[*] $\omega_{mn} \rightarrow (\omega_{mn})_{\text{clamped}}$ means $\omega_{mn} \equiv (\omega_{mn})_{\text{clamped}}$ and similarly for $(\bar{\omega}_{mn})_{\text{clamped}}$.

25

then computed from the equation for $\bar{\omega}_{mn} \rightarrow (\bar{\omega}_{mn})_{clamped}$ given in Table 1 where now, in this equation, $\omega_{mn} \rightarrow (\omega_{mn})_{clamped}$ is the previously computed *in-vacuo frequency for a clamped-clamped plate*. Finally to obtain the response of a *fluid-loaded clamped-clamped plate* subject to turbulence excitation, we use $(\bar{\omega}_{mn})_{clamped}$ but *mode shapes* corresponding to *simply supported end conditions*. In extending the method of Reference 3 to the case of fluid-loaded *clamped-clamped plates*, we assume that the sensitivity of the fluid loading to the change in boundary conditions is sufficiently small so that the preceding procedure will yield approximately correct results for the response of clamped-clamped plates.

Using an entirely different theoretical approach, Appendixes F and G (see Table 1) give directly obtainable results for both simply supported and clamped plates. Again the results depend on the mode numbers. Appendix G presents a relatively simple formulation relevant for low frequencies.

If we treat the radiation of boundary layer noise into a closed rectangular cavity as well as into free space (see Dyer Model,[*] Appendix A of Reference 1), then the approximate value of the added mass due to the enclosed fluid is given as

$$m_{cavity} = \frac{\rho \, \tanh \left| k_{mn} \, L_z \right|}{\left| k_{mn} \right|} \text{ if } \omega_{mn} > \omega_c$$

and

$$m_{cavity} = \frac{\rho}{k_{mn}} \tan k_{mn} \, L_z \text{ if } \omega_{mn} < \omega_c$$

The total added mass is then the sum of the added mass of the enclosed fluid and the free (half) space added mass given in Table 1.

---

[*] In the Dyer Model all interior surfaces except the plate are assumed to be pressure release surfaces.

COMPUTATIONAL RESULTS

For the results shown in Figures 1 and 2, which include the effects of fluid loading, we make the following observations; of course evaluation of the theoretical results requires a comparison between theory and experiment in water.*

To compute the normalized modal mean sequare displacement $\overline{Y^2(\omega)}/\overline{p^2}$ of a water-loaded plate subject to turbulence excitation, we require the corresponding modal frequencies. Appendix H presents two methods, designated Methods 1 and 2 for computing the natural frequencies of a plate in water. Method 1 (Equation (H3)) is based on the analyses in Appendixes A-E whereas Method 2 (Equation (H6)) is based on the analyses in Appendixes F and G. Computations show that the frequencies computed by Method 2 are significantly greater than those computed by Method 1 and this difference increases at higher modes.** The discrepancy is attributed to the less sophisticated assumptions involved in deriving Equation (H6); see Appendix F. Consequently, we consider the results obtained by Method 2 to be less valid (i.e., more inaccurate) than those obtained by Method 1, and use only Method 1 for the computations of $\overline{Y^2(\omega)}/\overline{p^2}$ now presented.

For the fluid-loaded *aluminum* plate, Figure 1 shows the contributions of the lowest modes to the normalized modal mean square displacement $\overline{Y^2(\omega)}/\overline{p^2}$ for both the range of convection velocities considered ($0 \leq U_c \leq 64$ ft/sec) and the range of modal frequencies of interest ($100 \leq \overline{f}_{mn} \leq 1000$ Hz); see Table 2. It is evident from the figure that for any damping value considered, the contribution of the modes to the total normalized mean square displacement $(\overline{Y_{13}^2} + \overline{Y_{23}^2} + \overline{Y_{14}^2} + \overline{Y_{24}^2})+\dots)/\overline{p^2}$ decreases with successive mode orders (1,2), (2,3), (1,4), and (2,4). The major contributors are the (1,3) and (2,3) modes; the relative contribution of the latter mode

_____

*The fluid loading does not include the influence of hydrostatic pressure. The effect of hydrostatic pressure on the natural frequencies is discussed in Appendix I.

**As shown in Appendixes F, G, and H, the data given in Table 4 are used in computing the frequencies by Method 2.

27

TABLE 4

Modal Values of A_{ij} and β_{ij} for Clamped and
Simply Supported Plates

Mode	Clamped Plate		Simply Supported Plate	
	A_{ij}	β_{ij}	A_{ij}	β_{ij}
i = 1 j = 1	0.6904	1	0.4053	0.25
i = 1 j = 2	0	1	0	0.25
i = 1 j = 3	0.3023	1	0.1351	0.25
i = 1 j = 5	0.1924	1	0.0810	0.25
i = 3 j = 1	0.3023	1	0.1351	0.25
i = 3 j = 2	0	1	0	0.25
i = 3 j = 3	0.1324	1	0.0450	0.25

28

decreases for values of U_c approaching 64 ft/sec. However, we also ob-
serve that for given values of U_c and damping, the root mean square dis-
placement of each mode treated is of the same order of magnitude. We con-
clude therefore that each of the several modes considered makes a signi-
ficant contribution to the total vibratory displacement.

A comparison of the curves of Figure 1 also indicates that the
character of the curves is essentially independent of the damping values
and that the values for the modal amplitudes decrease with increasing
values of the damping. If the damping is sufficiently small and/or $\overline{p^2}$ is
sufficiently large, we may expect the turbulence excitations to produce
undesirably large magnitudes of plate vibration.

For the *steel* plate (Figure 2), similar results were obtained for
the lowest modes for various values of $q = k/k_s$; see Table 3. Again, we
observe that for any value of q, each of the several modes considered makes
a significant contribution to the total vibratory displacement, the modal
amplitudes decrease with increasing values of damping, and the character
of the curves is essentially independent of the damping values. In
addition, we observe that the response increases with increasing values of
q. For $q = 0.995$, Table 3b shows a significant increase in the mode
numbers corresponding to the frequency range of interest ($100 \leq \bar{f}_{mn} \leq$
1000 Hz). Once more we conclude that if the damping is sufficiently small
and/or $\overline{p^2}$ is sufficiently large, we may expect the turbulence excitations
to produce undesirably large magnitudes of plate vibration; the magnitudes
are enhanced, but not radically, at sufficiently large values of q. Hence
in computations it appears practical to use a single representative value
for q for the range of turbulence frequencies distributed about $\omega = U_c k_T$
$= k c$, corresponding to $0 \leq q = k/k_s \leq 1.0$.[*] A practical alternative would
be to select the average of the mean square displacement responses computed
for small and large values of q.

---

[*] These relationships are discussed in the following section.

TURBULENCE-VIBROACOUSTIC RELATIONSHIPS

Background material is cited in the bibliography.

For the convenience of the reader, we list the notation commonly used in this section.

a,b	Length and width of the plate, respectively
B	Plate bending stiffness equal to $E h^3/12(1-\sigma^2)$
C_B	Trace speed of the plate bending wave in the direction of flow or free flexural phase velocity for a thin plate equal to $\omega^{1/2} (B/M)^{1/4}$
c	Velocity of sound
c_ℓ	Compressional wave velocity of the plate equal to $[E/\rho_s(1-\sigma^2)]^{1/2}$
E	Young's modulus
f, f_c, f_h	Natural, acoustic coincidence or critical, and hydrodynamic coincidence or critical frequencies, respectively
h	Plate thickness
k	Acoustic wave number equal to ω/c
k_1, k_3	Wave number components lying along the x- and y-axes, respectively
k_m, k_n	Modal wave numbers equal to $m\pi/a$ and $n\pi/b$, respectively
k_{mn}, k_s	Wave numbers equal to $\sqrt{k_m^2 + k_n^2}$
k_p	Free plate bending wave number equal to $(\omega/\kappa c_\ell)^{1/2}$
k_T	Turbulence wave number
M, m_p	Plate structural mass per unit area
M'	Effective mass per unit area (i.e., mass per unit area of fluid-loaded plate) equal to $m_p + m_{mn}$
m_{mn}	Added mass per unit area (or apparent mass or virtual mass per unit area)
m,n	Mode numbers
q	Equal to k/k_s
U	Free-stream velocity
U_c	Convection velocity equal to 0.8 U
v	Mean convection speed along the flow direction
v_o	Hydrodynamic coincidence speed
α	Equal to 1 for fluid loading on one side of plate only; equal to 2 for fluid loading on both sides of plate
κ	Radius of gyration equal to $h/2\sqrt{3}$

ρ Mass density of fluid medium

ρ_s Mass density of plate

σ Poisson's ratio

ω Circular frequency equal to $2\pi f$

ω_c Acoustic coincidence or critical frequency equal to $2\pi f_c$

ω_h Hydrodynamic coincidence or critical frequency equal to $2\pi f_h$

ω_{mn} Plate resonance frequency equal to $2\pi f_{mn}$

——   Bar over quantity denotes quantity for water-loaded plate

The convection properties of the turbulence pressure field relate the circular frequency ω and the turbulence wave number k_T by the equation

$$k_T U_c \cong \omega \tag{1}$$

The approximation obtains because, in actuality, a range of wave numbers contributes to the frequency spectral density of the turbulent pressures (e.g., see Equation (B60) of Reference 1). Alternatively stated, for a turbulent field, a particular wave number component is generally associated with a distribution of frequencies and/or convection speeds.

Following Dyer (see page 18 of Reference 1), the hydrodynamic coincidence speed v_o is defined as the speed at which the magnitude of the mean flow convection velocity U_c along the flow direction is equal to the trace speed of the bending wave C_B in the direction of flow, i.e., $v = v_o = C_B$.[*] The frequency at which this occurs is a significant parameter because it represents a value at which we can expect a large vibratory response due to increased amplitudes of the modal forcing function for the panel. This parameter is called the hydrodynamic coincidence frequency ω_h and is given by the equation

$$\omega_h = k_p C_B = k_p U_c \tag{2}$$

Thus from Equations (1) and (2), $k_T = k_p = \omega_h/U_c$ at the hydrodynamic coincidence frequency.

---

[*] The bending wave is also referred to as the free flexural phase velocity and free plate bending velocity.

Here

$$k_p = \left(\frac{\omega}{\kappa\, c_\ell}\right)^{\frac{1}{2}} = \left(\frac{M}{B}\right)^{\frac{1}{4}} \omega^{\frac{1}{2}} \qquad (3)$$

because (see pages 18 and 28 of Reference 1)

$$C_B = \frac{\omega}{k_p} = \omega^{\frac{1}{2}} \left(\frac{B}{M}\right)^{\frac{1}{4}} \; ; \; \omega = \omega_h \text{ at hydrodynamic coincidence} \qquad (4)$$

and

$$\left(\frac{B}{M}\right)^{\frac{1}{2}} = \frac{h\, c_\ell}{\sqrt{12}} = \kappa\, c_\ell \qquad (5)$$

The region within which hydrodynamic coincidence can exist is defined by a semicircle in k space represented by $(k_m - U_c/2\kappa\, c_\ell)^2 + k_n{}^2 = (U_c/2\kappa\, c_\ell)^2$. For the plate coordinate system shown in Figure 3, the corresponding classification of plate modes in wave number space is shown in Figure 4. For low convection velocities $U_c \ll C_B$, the locus of the hydrodynamic coincidence (HC) curve collapses to the origin and the response is composed entirely of hydrodynamically fast (HF) modes.

From these equations we obtain the significant relationship from which we can determine ω_h for a given plate material and value of U_c, namely,

$$\omega_h = \frac{C_B{}^2}{\left(\frac{B}{M}\right)^{1/2}} = \frac{U_c{}^2}{\kappa\, c_\ell} \qquad (6)$$

The hydrodynamic critical frequency is now defined as the resonance frequency of the plate mode with bending wave velocity equal to the convection velocity. Table 5a presents values of the hydrodynamic critical frequency[*] $f_h = \omega_h/2\pi$ computed for the fluid-loaded, simply supported aluminum and steel plates for values of U_c used in the previous computations

---

[*] The condition of hydrodynamic coincidence has been used by Maestrello[1] in obtaining computer solutions $\overline{Y^2}(\omega)/\overline{p^2}$ (see Appendix H).

Note: The dense fluid occupies the space $x_2 > 0$.
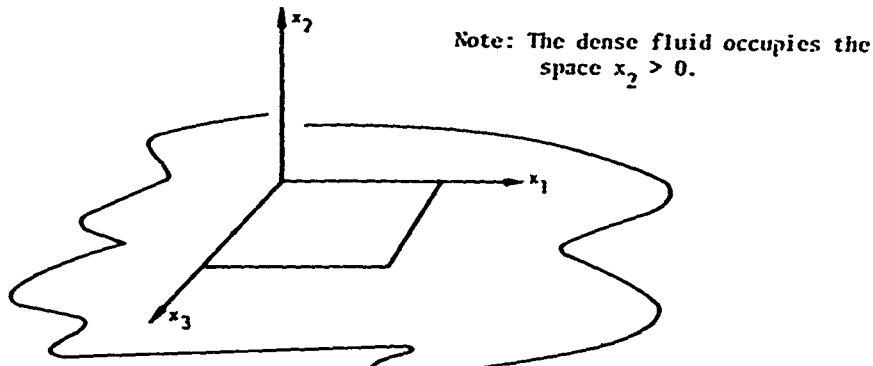
Figure 3 - Plate with Coordinate System
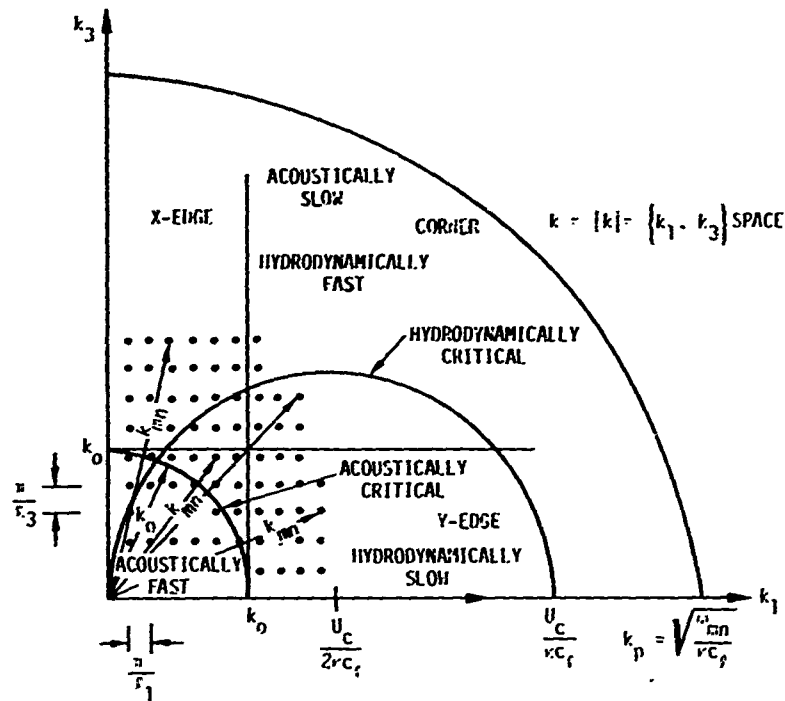
Notes: 1. For any value of k_{mn} in the modal lattice, the projection of k_{mn} on k_1 is $k_m = m\pi/\ell_1$ and the projection of k_{mn} on k_3 is $k_n = n\pi/\ell_3$.

2. For an infinite plate the curves in $\{k_1,\omega\}$ space show that above ω_h hydrodynamic coincidence does not occur for any wavenumber. At very high frequencies the sonic curve intersects the free wave curve because $\frac{\omega}{c}$ increases faster than $\left(\frac{\omega}{\kappa c_\ell}\right)^{1/2}$, and acoustic coincidence occurs.

For additional details on corresponding relationships in $\{\kappa_1,\kappa_3\}$ space see Bibliography (White, P.H.)
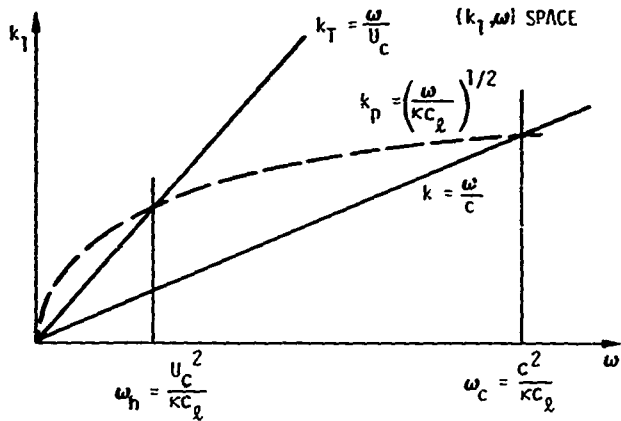
Figure 4 - Classification of Modes in Wave Number Space
and Turbulence Vibroacoustic Relationships
in Wave Number-Frequency Space

33

TABLE 5

Computation of Hydrodynamic Critical Frequencies and Acoustic Critical Frequencies for Fluid-Loaded, Simply Supported Aluminum and Steel Plates

TABLE 5a

Computation of Hydrodynamic Critical Frequencies for Aluminum and Steel Plates

U_c (ft/sec)	$f_h = \dfrac{U_c^2}{2\pi\kappa c_\ell}$ (Hz) alum. plate	$f_h = \dfrac{U_c^2}{2\pi\kappa c_\ell}$ (Hz) steel plate
8	0.62	0.05
16	2.48	0.20
32	9.95	0.79
64	39.87	3.17

ALUMINUM: $\kappa = 9.64 \times 10^{-4}$ ft
$c_\ell = 17,000$ ft/sec

Steel : $\kappa = 1.204 \times 10^{-2}$ ft
$c_\ell = 17,000$ ft/sec

c_{water} : $= 5,000$ ft/sec

TABLE 5b

Computation of Acoustic Critical Frequencies for Aluminum and Steel Plates

Material	$f_c = \dfrac{c^2}{2\pi\kappa c_\ell}$ (Hz)
Aluminum	243,000
Steel	19,400

of the plate response. The results were obtained by use of Equation (6).
For a finite plate at resonance, $k_p^2 \equiv k_s^2 \equiv k_{mn}^2 = [(m\pi/a)^2 + (n\pi/b)^2]$.
For air (or *in vacuo*) loading

$$\omega \to \omega_{mn} = \kappa\, c_\ell \left[\left(\frac{m\pi}{a}\right)^2 + \left(\frac{n\pi}{b}\right)^2\right] \tag{7}$$

the equation $\omega_{mn} = \kappa\, c_\ell\, (m\pi/a)^2 = (m\pi/a)\, U_c$ represents the hydrodynamic
coincidence condition for the finite plate at resonance because U_c is the
convection velocity in the flow direction only (see page 132) and

$$C_B = \frac{\omega_{mn}}{k_p} \text{ or } U_c = \frac{\omega_{mn}}{k_{mn}} = \kappa\, c_\ell\, k_{mn}$$
$$\longrightarrow \kappa\, c_\ell \left(\frac{m\pi}{a}\right) \text{ at } \omega = \omega_h \tag{8}$$

For water loading (see Equation (113))

$$\omega \to \bar{\omega}_{mn} = \omega_{mn} \left[1 + \frac{\alpha\, \rho}{\rho_s\, k_s h\, [1-\varsigma^2]^{1/2}}\right]^{-\frac{1}{2}} \tag{9}$$

The *radiative* properties of the plate *immersed in a fluid* relate the
given frequency ω (Equation (1)) and the acoustic wave number k by the
equation:

$$kc = \omega \tag{10}$$

From Equations (1) and (10), we obtain:

$$k \cong \frac{U_c}{c}\, k_T \cong 0.8\, k_T \cdot \frac{U_c}{c} = 0.8\, k_T \cdot \text{Mach No.} \tag{11}$$

These last two relations are given to add to the theoretical picture. How-
ever, no computations for the radiation of plates were made for the present
report.

On page 24 of Reference 1, we defined the sound coincidence or cutoff
or critical frequency $\omega = \omega_c$ as corresponding to $c = C_B$, i.e., the fre-
quency at which the flexural wavelength of a thin plate equals the acoustic
wavelength in water.[*] At this frequency we expect a greatly increased
acoustic response.

---

[*]The critical frequency is used for a resonant plate.

35

Moreover since at this frequency (see page 27 of Reference 1)

$$c = C_B = \omega_c^{1/2} \left(\frac{B}{M}\right)^{\frac{1}{4}} \qquad (12)$$

Then

$$\omega_c = c^2 \left(\frac{M}{B}\right)^{\frac{1}{2}} = \frac{c^2}{\kappa\, c_\ell} \qquad (13)$$

Table 5b presents values of $f_c = \omega_c/2\pi$ computed for the fluid-loaded, simply supported aluminum and steel plates. The results were obtained by use of Equation (13). Obviously there is one and only one sound coincidence (or critical frequency) for each plate material.

According to Leehey (see Bibliography), the frequency range of interest for sonar self-noise application is

$$\omega_n = \frac{U_c^{\,2}}{\kappa\, c_\ell} < \omega < \omega_c = \frac{c^2}{\kappa\, c_\ell}$$

Hydrodynamic coincident effects are not important for this range (see Tables 2 and 3), and the radiated power per unit area is associated with both the decay of turbulence and the presence of plate boundaries.

We observe that the near field in the vicinity of the panel represents the predominant portion of the transduced pressure spectrum. This spectrum is composed of nonpropagating components caused by hydrodynamic coincidence effects. Thus, the wave numbers chiefly in evidence are those in the immediate vicinity of the hydrodynamic coincidence curve which corresponds to an excitation field progressing in the flow direction with velocity U_c and frequency ω; see Figure 4. The spectrum of boundary layer pressure is distributed about $k_1 = k_T = \omega/U_c$ with most of the energy at rather low values of k_3. As we proceed into the far field, the near-field components decay and only the wave numbers at or below the sonic line, represented in Figure 4 by a circle $k = k_0 = \omega/c$ is present.

We now show that at sufficiently low wave numbers, the added mass (or near field) of a fluid-loaded plate subject to turbulence excitation may contribute significantly to the vibroacoustic response of a structure in its vicinity and, in turn, may also be significantly affected by that response.

36

The added mass or fluid inertial loading of a flexurally vibrating plate represents the imaginary or reactive part of the impedance associated with the reaction of the fluid to the vibrating plate. The corresponding fluid pressure is considered to be effective over a distance $d \approx \frac{\lambda}{6}$ from the plate; the distance $d = \frac{\lambda}{6}$ is called the near field. Thus, at sufficiently small wave numbers ($d \leq \lambda/6$ or $kd \leq 1$), the near field will exert a pressure on an adjacent structure lying within the effective bounds of the field. If the structure is flexible, we will then have a complex coupled vibro-acoustic system involving the plate, the adjacent structure, and the inter-vening fluid medium. The interaction would in general couple the near- and far-field (or radiation) pressures on both plate and adjacent structure and would include the phenomena of reflections, scattering, etc. We explain this by recognizing that each flexible body or source works against its own sound pressure which represents the reaction of the medium to its motion as well as against the sound pressure that is generated by the adjacent source (e.g., the opposing body). Thus, two sound sources (i.e., flexible bodies) in close proximity ($d \leq \frac{\lambda}{6}$) react with each other and the sources may generate considerably more sound energy than if they were further apart. Sound sources of this type in close proximity are said to be dependent, and the power that each source generates individually cannot simply be added to yield the actual or total power of the system which is due to the interaction effects associated with the near field.

37

CONCLUSIONS

The chief conclusions drawn from this investigation are:

1. The added mass and corresponding natural frequency of a fluid-loaded rectangular plate are more significant for the *uncoupled* modes and are easily computed using the results given in Table 1. For a first approximation, only the results for *uncoupled* modes need to be considered in vibroacoustic computations.

2. The added mass results for the *coupled modes* can be computed (using the results in Table 1) and added to the results for the *uncoupled modes* to refine the accuracy of the computation for the natural frequency or to determine the effect of these modes on the natural frequency and vibro-acoustic response.

3. Separate results for the added mass and natural frequencies of only the *uncoupled modes* can be computed (using the results in Table 1) to determine the absolute numerical contribution of these modes to the vibro-acoustic response or to identify a corresponding response.

4. The methods of analysis used in Appendixes A-E yield the *same* added mass and natural frequency results for *uncoupled modes* and are applicable, in their essence, to both high and low wave numbers and for low and high frequencies (see the remarks column of Table 1 relative to Appendix B; see also Appendix E).

5. The Feit-Junger method of analysis used in Appendix A can be extended by the methods of Leibowitz presented in Appendix C to yield the same added mass and natural frequency results for the *coupled modes* as obtained by Davies (Appendix B).

6. The results obtained in Appendixes A-E for the added mass and natural frequency of a fluid-loaded, *simply supported* plate can be extended to yield corresponding results for a fluid-loaded *clamped-clamped* plate by using the Leibowitz-Wallace methods given in Reference 3. The results obtained by Greenspon and Leibowitz in Appendixes F and G can be used directly to compute the added mass and natural frequency of either a *simply supported* or *clamped-clamped* plate; the results for Appendix G are particularly applicable to the low frequency response. The Greenspon-Leibowitz results are considered to be less accurate than the former results.

7. The total mass and corresponding natural frequency for a plate radiating into free (half) space as well as into a closed rectangular space can be computed using the results presented in Table 1 and the results obtained from Appendix A of Reference 1 given in the Discussion.

8. The computed results for both the aluminum and steel plates show that the contribution of the higher modes to the total vibratory response is not negligible e.g., for the aluminum plate, the magnitudes of the root mean square displacement for the (1,4) and (2,4) modes are of the same order as that for the (1,3) and (2,3) modes for a given value of convection velocity and damping. Thus, determination of the total vibratory displacement requires that the computations include the contributions of the several modes of vibration deemed to be significant.

9. Turbulence-induced plate vibration may be of significant magnitude for small damping and/or sufficiently large mean square pressure fluctuations; the magnitude is enhanced, but not radically, at sufficiently large values of $q = k/k_s$. Hence in computation it appears practical to use a single representative value for q for the range of turbulence frequencies distributed about $\omega = U_c k_T = kc$ corresponding to $0 \leq q = k/k_s \leq 1.0$. A practical alternative would be to select the average of the mean square displacement responses computed for small and large values of q.

RECOMMENDATIONS

To simplify the computational procedure (and the computer program) and to achieve reasonably accurate vibroacoustic results for a vibrating plate fluid loaded on one side, the following recommendations are made. Note, however, that the user who wishes to refine the accuracy of computations, determine the coupled mode contribution, identify a coupled mode response, or treat a closed rectangular cavity can incorporate the additional relevant results presented here into the computer program.

1. It is recommended, as a first approximation, that the equations for the added mass and corresponding natural frequency of only the *uncoupled* or self (dominant) modes of a fluid-loaded, *simply supported* rectangular plate be used in making vibroacoustic computations. This includes the *uncoupled* mode equation common to all of the results obtained in Appendixes A-E; see Appendix H for the corresponding computer program.

2. It is recommended that vibroacoustic computations for fluid-loaded, *clamped-clamped* rectangular plates be made (for *uncoupled* modes only) by extending the equation for a fluid-loaded, simply supported rectangular plate to include this case, in accordance with the Leibowitz-Wallace methods of Reference 3; see Appendix H for the corresponding computer program.

ACKNOWLEDGMENTS

APPENDIX A

THE FEIT-JUNGER METHOD

NOTATION

A	Amplitude of $\tilde{p}$
c	Velocity of sound in fluid medium
c_p	Compressional wave velocity of the plate equal to $\left[\dfrac{E}{\rho_s(1-\nu^2)}\right]^{1/2}$
D	Flexural rigidity of plate equal to $\dfrac{c_p^2\,\rho_s h^3}{12} = \dfrac{Eh^3}{12(1-\nu^2)}$
E	Young's modulus
e	Equal to 2.718; base for natural or Naperian system of logarithms
F(x,y)	Driving force applied at coordinates x, y, z = 0
F_{mn}	Generalized force for the mn mode
h	Plate thickness
I_{mnpq}	Defined by Equation (A17b)
i	Equal to $\sqrt{-1}$
k	Acoustic wave number equal to ω/c
k_m, k_n, k_p, k_q	Modal wave numbers defined by Equation (A3)
k_s	Surface wave number equal to $(k_m^2 + k_n^2)^{1/2}$
L_x, L_y	Half length and half width of plate, respectively
M_p	Total plate structural mass
m, n, p, q	Mode numbers
m_{mn}	Added modal mass per unit area
m_{mnpq}	Added mass of coupled modes mnpq per unit area
p(x, y, z > 0)	Pressure in fluid
p(x, y, z = 0)	Pressure on surface of plate
$\tilde{p}(\Upsilon_x, \Upsilon_y, z)$	Double inverse Fourier transform in Υ_x and Υ_y
r_{mn}	Radiation modal damping
r_{mnpq}	Mutual specific acoustic resistance for coupled modes mnpq

41

r_s	Structural modal resistance
w_{mn}, w_{pq}	Displacement amplitude of vibration of a plate for the mn and pq modes of vibration, respectively
$w_{mn}(x,y)$	Modal displacement at surface of plate
$w(x,y, z=0)$	Fluid particle displacement at surface of plate equal to plate displacement
$\tilde{w}(\gamma_x, \gamma_y)$	Transform of displacement $w(x, y, z = 0)$; equal to a series of modal transforms
$\tilde{w}_{pq}(\gamma_x, \gamma_y)$	Modal transform of displacement at the surface of plate
x, y, z	Rectangular coordinates; x and y are in the plane of the plate and z is normal to the plate
∇^2	Equal to $\dfrac{\partial^2}{\partial x^2} + \dfrac{\partial^2}{\partial y^2} + \dfrac{\partial^2}{\partial z^2}$
$\delta(k_i - \gamma_j')$	Delta function; $\displaystyle\int \delta(k_i - \gamma_j)d_{\gamma_j} = \begin{cases} 1, & \gamma_j = k_i \\[2mm] 0, & \gamma_j \neq k_i \end{cases}$
γ_x, γ_y	Wave numbers which are the coordinates in Fourier transform space
ε	A small quantity
η_s	Structural loss factor equal to $r_s \omega / \omega_{mn}^2 \rho_s h$
ν	Poisson's ratio
ρ	Mass density of fluid medium
ρ_a	Added mass density of fluid per unit volume equal to m_{mn}/h
ρ_e	Sum of mass densities of plate and fluid equal to $\rho_s + \rho_a$
ρ_s	Mass density of the plate
ω	Natural circular frequency of vibration
ω_c	Coincidence frequency equal to $c^2 \Big/ \left(\dfrac{h}{\sqrt{12}} c_p\right)$
ω_{mn}, $\bar{\omega}_{mn}$	*In vacuo* and submerged natural circular frequency, respectively, for the mn mode of vibration i.e., resonance frequency for the *in vacuo* and submerged plate, respectively

42

DERIVATION

From Reference 4, the *even* modes of a simply supported rectangular plate vibrating *in vacuo* have a configuration described by[*]

$$w_{mn}(x,y) = W_{mn} \cos k_m x \cos k_n y, \quad |x| < L_x, \; |y| < L_y$$
$$= 0 \qquad\qquad\qquad |x| \geq L_x, \; |y| \geq L_y \tag{A1}$$

with boundary conditions

$$\cos k_m L_x = \cos k_n L_y = 0$$
$$\sin k_m L_x = (-1)^m \tag{A2}$$
$$\sin k_n L_y = (-1)^n$$

The boundary conditions restrict the wave numbers k_m, k_n, or k_s to the values

$$k_m L_x = (2m + 1)\frac{\pi}{2} \qquad ; \; m,n = 0,\, 1,\, 2\cdots$$
$$k_n L_y = n$$

$$k_s = \left(k_m^2 + k_n^2\right)^{1/2} = \frac{\pi}{2}\left[\left(\frac{2m+1}{L_x}\right)^2 + \left(\frac{2n+1}{L_y}\right)^2\right]^{1/2} ; \; m,n=0,\, 1,\, 2\cdots \tag{A3}$$

Also $k_s^2 > k^2$ for $\omega_{mn} < \omega_c = c^2/\left(h/\sqrt{12}\right)c_p$ (see Reference 4) so that each wave is characterized by one pair of wave numbers k_m and k_n, i.e., the normal modes of a plate vibrating *in vacuo* are described in terms of a discrete wave number spectrum. The modal configurations are defined to be orthogonal to each other so that each mode can be excited independently by a suitable distribution of the load.

For the *submerged* plate (exposed to water on one side), however, each of the originally normal (k_m, k_n) modes generates an acoustic pressure in the plane of the plate (which can be represented as an inverse Fourier

---

[*]This configuration is of practical importance because it matches the modes of vibration of a simply supported, rectangular plate driven at the center.

transform) whose wave number spectrum is *continuous* and thereby encompasses the *discrete* wave numbers of the other originally (i.e., *in vacuo*) normal modes. The resulting pressure distribution due to a single mode is not orthogonal to the other modes. This causes the modal configurations to couple, and thereby to lose their normal mode character. Thus if we attempt to formulate the problem in terms of *in vacuo* normal modes, we shall find that these modes become coupled; the subsequent discussion will clarify these features. The modes also lose their standing wave character in the range $k_s^2 > k^2$ because the plate boundaries are energy sinks.

For a distributed load, the forced equation of motion for the $(m,n)^{th}$ mode of an *undamped* thin rectangular plate extending from $-L_x$ to L_x and $-L_y$ to L_y is[4-6]

$$L_x L_y \rho_s h \left[\omega_{mn}^2 - \omega^2 \right] W_{mn} = F_{mn} \tag{A4}$$

Here, $L_x L_y \rho_s h = M_p/4$ where M_p is the mass of the plate,
$\omega_{mn} = \dfrac{h c_p}{\sqrt{12}} (k_m^2 + k_n^2) = \left(\dfrac{D}{\rho_s h} \right)^{1/2} [k_m^2 + k_n^2]$ is the *in vacuo* natural frequency of this particular mode,* F_{mn} is the generalized force associated with a concentrated driving force applied at $x=0$, $y=0$, and the surface pressure $p(x,y,0)$ is represented by

$$F_{mn} = F(0,0) - \int_{-L_x}^{L_x} \int_{-L_y}^{L_y} p(x,y,0) \cos k_m x \cos k_n y \, dx \, dy \tag{A5}$$

To obtain an explicit expression for $p(x,y,0)$ as a double integral, the surface pressure, which is *spatially aperiodic* in x and y, is written as a double inverse transform in γ_x and γ_y.

---

*With inclusion of a structural loss factor
$$\omega_{mn} = \dfrac{h|c_p|}{\sqrt{12}} [k_m^2 + k_n^2] \left(1 - \dfrac{\eta_s}{2} \right) \text{ (see Reference 4).}$$

$$\tilde{p}(\gamma_x, \gamma_y; z) = \int_{-\infty}^{\infty} \int_{-\infty}^{\infty} p(x,y,z) \, e^{[-i(\gamma_x x + \gamma_y y)]} \, dx \, dy \qquad (A6)$$

$$p(x, y; z) = \frac{1}{(2\pi)^2} \int_{-\infty}^{\infty} \int_{-\infty}^{\infty} \tilde{p}(\gamma_x, \gamma_y; z) \, e^{[i(\gamma_x x + \gamma_y y)]} \, d\gamma_x \, d\gamma_y \qquad (A7)$$

Now the three-dimensional Helmholtz wave equation is

$$\left[\frac{\partial^2}{\partial x^2} + \frac{\partial^2}{\partial y^2} + \frac{\partial^2}{\partial z^2} + k^2 \right] p(x,y;z) = [\nabla^2 + k^2] \, p(x,y;z) = 0 \qquad (A8)$$

The double transform of the foregoing equation is[*]

$$\left(k^2 - \gamma_x^2 - \gamma_y^2 + \frac{\partial^2}{\partial z^2} \right) \tilde{p}(\gamma_x, \gamma_y \, z) = 0 \qquad (A9)$$

Assuming a solution of the form $\tilde{p} = Ae^{i\alpha z}$, the solution of Equation (A9) is

$$\tilde{p}(\gamma_x, \gamma_y; z) = Ae^{i(k^2 - \gamma_x^2 - \gamma_y^2)^{1/2} z} \qquad (A10)$$

where the boundary condition $\partial p/\partial z = \rho\omega^2 w$ at z=0 yields the value (see Chapter IV of Reference 4)

---

[*]The Fourier transform of the term $\dfrac{\partial^2}{\partial x^2} p(x,y;z)$ is obtained by integrating by parts and setting p and its derivative equal to zero at the limits $x = \pm \infty$. This yields $\int_{-\infty}^{\infty} \partial^2 p/\partial x^2 \, e^{-i\gamma_x x} \, dx = -\gamma_x^2 \, p(\gamma_x, y; z)$. Also because $\partial^2/\partial y^2$, $\partial^2/\partial z^2$, and k^2 are independent of x, they can be taken outside the integral sign so that $(\partial^2/\partial y^2 + \partial^2/\partial x^2 + k^2)\int_{-\infty}^{\infty} p(x,y;z)e^{-i\gamma_x x} \, dx$ $= (\partial^2/\partial y^2 + \partial^2/\partial z^2 + k^2) \, \tilde{p}(\gamma_x, y; z)$. The procedure is now repeated for $\dfrac{\partial^2}{\partial y^2} \tilde{p}(\gamma_x, y; z)$ to obtain Equation (A9).

45

$$A = \frac{-i\rho\omega^2 \, \tilde{w}(\Upsilon_x, \Upsilon_y)}{(k^2 - \Upsilon_x^2 - \Upsilon_y^2)^{1/2}} \tag{A11}$$

Substituting Equation (A11) in Equation (A10) and the result in Equation (A7), then letting z=0, and considering even modes only, we get

$$p(x,y,0) = \frac{-i\rho c^2 k^2}{4\pi^2} \int_{-\infty}^{\infty} \int_{-\infty}^{\infty} \frac{\tilde{w}(\Upsilon_x, \Upsilon_y) \cos \Upsilon_x x \cos \Upsilon_y y}{(k^2 - \Upsilon_x^2 - \Upsilon_y^2)^{1/2}} \, d\Upsilon_x \, d\Upsilon_y \tag{A12}$$

where $\tilde{w}(\Upsilon_x, \Upsilon_y)$ is the series of modal transforms

$$\tilde{w}(\Upsilon_x, \Upsilon_y) = \sum_{pq} \tilde{w}_{pq}(\Upsilon_x, \Upsilon_y) \tag{A13}$$

Substituting Equation (A13) in Equation (A12) and the result in Equation (A5), we get

$$F_{mn} = F(0,0) + \frac{i\rho c^2 k^2}{4\pi^2} \sum_{pq} \int_{-L_x}^{L_x} \int_{-L_y}^{L_y} \left[\iint_{-\infty}^{\infty} \frac{\tilde{w}_{pq}(\Upsilon_x, \Upsilon_y) \cos \Upsilon_x x \cos \Upsilon_y y \, d\Upsilon_x \, d\Upsilon_y}{(k^2 - \Upsilon_x^2 - \Upsilon_y^2)^{1/2}} \right] \cdot \tag{A14}$$

$$\cdot \cos k_m x \cos k_n y \, dx \, dy$$

The double Fourier transform of Equation (A1) yields

$$\left. \begin{array}{l} \tilde{\dot{w}}_{mn} = \dot{W}_{mn} \displaystyle\int_{-L_x}^{L_x} \int_{-L_y}^{L_y} \cos \Upsilon_x x \cos k_m x \cos \Upsilon_y y \cos k_n y \, dx \, dy \\[20pt] = \dfrac{4 \, \dot{W}_{mn} \, k_m k_n \, (-1)^{m+n} \cos \Upsilon_x L_x \cos \Upsilon_y L_y}{(k_m^2 - \Upsilon_x^2)(k_n^2 - \Upsilon_y^2)} \end{array} \right\} \tag{A15}$$

46

Substituting the time integral of the first of Equations (A15) in Equation (A14), we get

$$F_{mn} = F(0,0) + \frac{i\rho c^2 k^2}{4\pi^2 W_{mn}} \sum_{pq} \iint_{-\infty}^{\infty} \frac{\tilde{w}_{pq}(\gamma_x, \gamma_y) \, \tilde{w}_{mn}(\gamma_x, \gamma_y)}{(k^2 - \gamma_x^2 - \gamma_y^2)^{1/2}} \, d\gamma_x d\gamma_y \qquad (A16)$$

Using the time integral of the second of Equations (A15) for both $\tilde{w}_{mn}$ and $\tilde{w}_{pq}$, we get

$$F_{mn} = F(0,0) + \frac{i4\rho c^2 k^2 k_m k_n \, (-1)^{m+n}}{\pi^2} \sum_p \sum_q W_{pq} k_p k_q (-1)^{p+q} \iint_{-\infty}^{\infty}$$

$$\qquad (A17)$$

$$\frac{\cos^2 \gamma_x L_x \, \cos^2 \gamma_y L_y \, d\gamma_x d\gamma_y}{(k^2 - \gamma_x^2 - \gamma_y^2)^{1/2} (k_m^2 - \gamma_x^2)(k_n^2 - \gamma_y^2)(k_p^2 - \gamma_x^2)(k_q^2 - \gamma_y^2)}$$

The exact solution of Equation (A17) requires a numerical integration of the branch cut integral. Reference 4 avoids the determination of the exact solution by evaluating the integral for the *high wave numbers* (short wavelength) limit only. This simplifies the analysis, and the final expression is considered to hold for a finite rectangular plate over a particular wave number and frequency range.

Write

$$F_{mn} = F(0,0) + i\omega \sum_{pq} I_{mnpq} W_{pq} \qquad (A17a)$$

where we define

$$I_{mnpq} = \frac{4\rho\omega k_m k_n (-1)^{m+n}}{\pi^2} \sum_{pq} (-1)^{p+q} k_p k_q \cdot \qquad (A17b)$$

47

(Equation continued from page 47)

$$\left\{ \iint_{-\infty}^{\infty} \frac{\cos^2 \gamma_x L_x \cos^2 \gamma_y L_y \, d\gamma_x \, d\gamma_y}{\left(k^2-\gamma_x^2-\gamma_y^2\right)^{1/2}\left(k_m^2-\gamma_x^2\right)\left(k_n^2-\gamma_y^2\right)\left(k_p^2-\gamma_x^2\right)\left(k_q^2-\gamma_y^2\right)} \right\}$$ (A17b) Cont'd

$$= \left(r_{mnpq} - i\omega m_{mnpq} \right) L_x L_y$$

Thus the complex quantity I_{mnpq} is the product of $L_x L_y$ and the sum of the mutual specific acoustic resistance r_{mnpq} and the reactance $- i\omega m_{mnpq}$, also referred to as modal coupling coefficients, where

$$r_{mnpq} = \text{Re} \ (I_{mnpq})$$

$$m_{mnpq} = - \frac{1}{\omega} \text{Imag} \ (I_{mnpq})$$

Then

$$F_{mn} = F(0,0) + i\omega \sum_{pq} L_x L_y \left(r_{mnpq} - i\omega m_{mnpq} \right) W_{pq}$$

$$= F(0,0) + i\omega L_x L_y \left(r_{mn} - i\omega m_{mn} \right) W_{mn} + \sum_{pq \neq mn} i\omega L_x L_y \left(r_{mnpq} - i\omega m_{mnpq} \right) W_{pq}$$

$$= F(0,0) + L_x L_y \left(\omega^2 m_{mn} + i\omega r_{mn} \right) W_{mn} + \sum_{pq \neq mn} \left(\omega^2 m_{mnpq} + i\omega r_{mnpq} \right) W_{pq}$$

For the simplified analysis, we write the Lagrange equation for the forced motion of a mode, replacing Equations (A4) and (A5) by (note that harmonic time dependence is in the form $e^{-i\omega t}$)

$$L_x L_y \rho_s h \left[\omega_{mn}^2 - \omega^2 \right] W_{mn} - i\omega \left(\frac{L_x L_y \rho_s h \omega_{mn}^2 \eta_s}{\omega} \right) W_{mn}$$

(A18)

$$= F(0,0) + L_x L_y \left(\omega^2 m_{mn} + i\omega r_{mn} \right) W_{mn} + \sum_{pq \neq mn} L_x L_y \left(\omega^2 m_{mnpq} + i\omega r_{mnpq} \right) W_{pq} = F_{mn}$$

48

where the left member now includes a term for the structural resistance $r_s = \omega_{mn}^2 \rho_s h \eta_s / \omega$ expressed in terms of a structural loss factor η_s and the radiation loading portion of the generalized forces are written as two terms. The first of these terms represents the uncoupled (added mass and radiation) damping, i.e., the self-impedance due to radiation loading whereas the second of these terms represents the coupled added mass and radiation damping i.e., the mutual impedance due to radiation loading. If included in the computation, the coupled terms must be evaluated numerically.

Transferring the radiation-loading portion of the generalized forces to the left member of Equation (A18), the Lagrange equation becomes

$$\left[-\omega^2 \left(\rho_s h + m_{mn} \right) - i\omega \left(\frac{\rho_s h \omega_{mn}^2 \eta_s}{\omega} + r_{mn} \right) + \omega_{mn}^2 \rho_s h \right] W_{mn}$$

$$- \sum_{pq \neq mn} \left(\omega^2 m_{mnpq} + i\omega r_{mnpq} \right) W_{pq} = \frac{F}{L_x L_y} \tag{A19}$$

which is a doubly infinite set of equations for the unknowns W_{mn} coupled by the terms m_{mnpq} and r_{mnpq}. Thus I_{mnpq} is a coupling coefficient linking an (m,n) mode to a (p,q) mode.

For kL_x, $kL_y > 3$ which for $\omega \ll \omega_c$, is equivalent to $k_m L_x$, $k_n L_y \gg 1$ (i.e., the criteria for large plates), see Equation (A3), the coupling terms are much smaller than the self-impedance components so that they can be ignored in making an approximate evaluation of the far field.

Feit et al. now proceed to solve the integral Equation (A14) for the case $k_m L_x$ and $k_n L_y$ approaching infinity in order to gain some insight into the above approximation.[*] In this case the orthogonality of the cosines in Equation (A14) yields

---

[*] However, even without going to the limit of infinite $k_m L_x$, $K_n L_y$, the pq summation is small when $k_m L_x$, $k_n L_y$ is large; see Reference 7.

49

$$\lim_{\substack{k_m L_x \to \infty \\ k_n L_y \to \infty}} \int_{-L_y}^{L_y} \int_{-L_x}^{L_x} \cos \gamma_x x \, \cos k_m x \, \cos \gamma_y y \, \cos k_n y \, dx dy = 4\pi^2 \, \delta(k_m - \gamma_x) \delta(k_n - \gamma_y)$$

(A20)

Using these δ functions in Equation (A14), we find

$$F_{mn} = F(0,0) + i\rho c^2 k^2 \sum_{pq} \iint_{-\infty}^{\infty} \frac{\tilde{w}_{pq}(\gamma_x, \gamma_y) \delta(k_m - \gamma_x) \delta(k_n - \gamma_y) d\gamma_x d\gamma_y}{(k^2 - \gamma_x^2 - \gamma_y^2)^{1/2}}$$

(A21)

or

$$F_{mn} = F(0,0) + \frac{i\rho c^2 k^2 \displaystyle\sum_{pq} \tilde{w}_{pq}(k_m, k_n)}{(k^2 - k_m^2 - k_n^2)^{1/2}}$$

(A22)

Using the second of Equations (A15), Equation (A22) becomes: (In Equation (A15), let $m \to p$, $n \to q$, $x \to m$, $y \to n$.)

$$F_{mn} = F(0,0) + \frac{i4\rho c^2 \displaystyle\sum_{pq} W_{pq} k_p k_q (-1)^{p+q} \cos k_m L_x \, \cos k_n L_y}{(k^2 - k_m^2 - k_n^2)^{1/2} (k_p^2 - k_m^2)(k_q^2 - k_n^2)}$$

(A23)

The second term in the right member vanishes when $k_p \neq k_m = \gamma_x$, $k_q \neq k_n = \gamma_y$ (see Appendix B). For $k_p = k_m = \gamma_x$, $k_q = k_n = \gamma_y$, the denominator vanishes but the second term is finite because the boundary conditions, Equation (A3), require that the numerator also vanish. Hence we evaluate the indeterminate quantity

$$\lim_{\substack{k_p - k_m \to 0 \\ k_q - k_n \to 0}} \left[\frac{\cos k_m L_x}{(k_p^2 - k_m^2)} \right] \left[\frac{\cos k_n L_y}{(k_q^2 - k_n^2)} \right]$$

50

For $\lim\limits_{k_p - k_m \to 0} \dfrac{\cos k_m L_x}{k_p^{\,2} - k_m^{\,2}}$ let $k_p = k_m + \varepsilon$, $k_p^{\,2} \approx k_m^{\,2} + 2\varepsilon k_m$

Then

$$\lim_{k_p - k_m \to 0} \frac{\cos k_m L_y}{k_p^{\,2} - k_m^{\,2}} \approx \lim_{\varepsilon \to 0} \frac{\cos (k_p - \varepsilon) L_x}{2\varepsilon k_m}$$

$$\approx \frac{\cos k_m L_x \cos \varepsilon L_x + \sin k_p L_x \sin \varepsilon L_x}{2\varepsilon k_m} \tag{A24}$$

$$\approx \frac{(-1)p\varepsilon L_x}{2\varepsilon k_m} = \frac{(-1)p L_x}{2k_m}$$

Similarly,

$$\lim_{k_q - k_n \to 0} \frac{\cos k_n L_y}{k_q^{\,2} - k_n^{\,2}} \approx \frac{(-1)^q L_y}{2k_n} \tag{A25}$$

Substituting Equations (A24) and (A25) in Equation (A23), setting $(-1)^{2p+2q} = 1$, letting $W_{pq} \to W_{mn}$, and dropping $\sum\limits_{pq}$ since the coupling terms vanish in the large $k_m L_x$, $k_n L_y$ limit, we obtain

$$F_{mn} = F(0,0) + \frac{i\rho c^2 k^2 \, W_{mn} L_x L_y}{(k^2 - k_m^{\,2} - k_n^{\,2})^{1/2}} \tag{A26}$$

Hence in the large $k_m L_x$, $k_n L_y$ limit

$$F_{mn} = F(0,0) + \left. \frac{\omega^2 \rho \, L_x L_y \, W_{mn}}{(k_m{}^2 + k_n{}^2 - k^2)^{1/2}} \right\} \quad (k_m{}^2 + k_n{}^2) > k^2 \qquad (A27)$$

$$= F(0,0) + \omega^2 L_x L_y \, m_{mn} \, W_{mn} \qquad \omega < \omega_c$$

where (see Equation (A18))

$$m_{mn} = \frac{\rho}{(k_m{}^2 + k_n{}^2 - k^2)^{1/2}} = \frac{\rho}{(k_s{}^2 - k^2)^{1/2}} \approx \frac{\rho}{k_s} \qquad (A27a)$$

is the added mass per unit area which is shown in Reference 4 to correspond to an infinite train of straight-crested parallel waves or of straight-crested orthogonal waves. Feit and Junger assume that this added mass will hold for a finite rectangular plate, i.e., the added mass of a finite plate whose dynamic configuration embodies many nodal lines is effectively that of an infinite train of standing waves.

For the low frequency range where few modes contribute to the far field, a deterministic approach can be used. The resonance frequency for the submerged plate $\bar{\omega}_{mn}$ is then determined as follows:

$$\rho_a = \frac{m_{mn}}{h} = \frac{\rho}{(k_s{}^2 - k^2)^{1/2} h} \; ; \; k_s > k \qquad (A28)$$

Therefore

$$\rho_e = \rho_s + \rho_a = \rho_s + \frac{\rho}{(k_s{}^2 - k^2)^{1/2} h} \; ; \; k_s > k \qquad (A29)$$

$$\frac{\rho_e}{\rho_s} = 1 + \frac{\rho}{\rho_s (k_s{}^2 - k^2)^{1/2} h} = 1 + \frac{m_{mn}}{\rho_s h} \qquad (A30)$$

52

Since $\omega_{mn} \propto \sqrt{\dfrac{1}{\rho_s h}}$ (see notation) and $\bar{\omega}_{mn}$ occurs at the frequency computed

by the addition of the added mass to the mass of the plate, i.e.,

$\bar{\omega}_{mn} \propto \sqrt{\dfrac{1}{\rho_s h + m_{mn}}}$ then

$$\frac{\omega_{mn}}{\bar{\omega}_{mn}} = \sqrt{1 + \frac{m_{mn}}{\rho_s h}} \qquad (A31)$$

or

$$\bar{\omega} = \omega_{mn} \left(1 + \frac{m_{mn}}{\rho_s h}\right)^{-1/2} \qquad (A32)$$

$$= \omega_{mn} \left[1 + \frac{\rho}{\rho_s (k_m^2 + k_n^2 - k^2)^{1/2} h}\right]^{-1/2} \qquad (A33)$$

$$\approx \omega_{mn} \left[1 + \frac{\rho}{\rho_s (k_m^2 + k_n^2)^{1/2} h}\right]^{-1/2} = \omega_{mn} \left[1 + \frac{\rho}{\rho_s k_s h}\right]^{-1/2} ; \ k_s^2 >> k^2 \quad (A34)$$

53

APPENDIX B

THE DAVIES METHOD

NOTATION

A_p	Area of plate equal to $\ell_1 \ell_3$
B_{mn}	Coefficient of v_{mn} defined by Equations (B46) and (B47)
c_o	Velocity of sound in fluid medium
D	Flexural rigidity
e	Equal to 2.718; base for natural or Naperian system of logarithms
$I_{mq}(k_1), I_{nr}(k_3)$	Functions defined by Equations (B23) and (B26), respectively
$I_{mm}(k_1)$	Function defined by Equation (B24)
i	Equal to $\sqrt{-1}$
k	Wave number equal to $\lvert \underline{k} \rvert = k_1^2 + k_3^2$
$\underline{k}$	Wave number vector with components $\{k_1, k_3\}$
k_o	Acoustic wave number equal to ω/c_0
k_1	Component of $\underline{k}$ lying along x_1 axis
k_3	Component of $\underline{k}$ lying along x_3 axis
k_m	Wave number equal to $m\pi/\ell_1$
k_n	Wave number equal to $n\pi/\ell_3$
k_{mn}	Surface wave number equal to $\sqrt{k_m^2 + k_n^2}$
ℓ_1, ℓ_3	Length and width of plate, respectively
M_p	Total mass per unit area represented by Equation (B49)
m_p	Mass per unit area of panel
m_{mn}	Added mass or fluid loading per unit area
m, n, q, r	Mode numbers
P	Acoustic pressure generated by motion of panel
P_{mn}	Acoustic modal pressure defined by Equation (B8)
p	Pressure field driving panel
p_{mn}	Driving modal pressure defined by Equation (B7)

55

$R_{mnqr}(\omega)$	Coupling coefficient connecting the m,n mode with the q,r mode
$S_{mn}(\underline{k})$	Shape function
S_{mnqr}	Modal radiation coupling term
T_{mnqr}	Modal mass loading coupling term
t	Time
v	Panel normal velocity displacement
v_{mn}	Modal velocity amplitude
x_1, $x_2, x_3 \equiv \underline{x}, x_2$	Rectangular coordinates; x_2 is normal to the panel and the origin is at one corner of the panel; $\underline{x} \equiv \{x_1, x_3\}$
$y(x,t)$	Panel normal displacement
$Z(\underline{k},w)$	Radiation impedance
$\text{sgn } \omega$	Equal to -1 for $\omega < 0$, $+1$ for $\omega > 0$
$*$	Denotes complex conjugate
β	Coefficient accounting for mechanical damping of panel
∇^4	Equal to $D\left(\dfrac{\partial^4 y}{\partial x^4} + \dfrac{2\partial^4 y}{\partial x^2 \partial y^2} + \dfrac{\partial^4 y}{\partial y^4}\right)$ for isotropic plate
$\delta(k_i - k_j)$	Delta function: $\displaystyle\iint_{-\infty}^{\infty} \delta(k_i - k_j)dk_i = 1$ for $k_i = k_j$ $= 0$ for $k_i \neq k_j$
δ_{ij}	Kronecker delta equal to 1 for i=j, equal to 0 otherwise
η_{mn}	Modal structural loss factor
ρ_o	Mass density of fluid medium
$\Psi_{mn}(\underline{x})$	Normalized characteristic functions
ω	Natural circular frequency of vibration

DESCRIPTION

Reference 7 treats a simply supported, thin, rectangular plate inserted in an infinite rigid baffle and loaded with a dense fluid on one side. The normal vibration velocity field of the plate is expanded in a series of *in vacuo* normal modes.[*] The effect of structure-fluid interaction leads to the coupling of *in vacuo* modes represented by an infinite set of simultaneous linear equations to be solved for the infinite number of unknown modal response amplitudes. Fluid loading terms or coefficients in these equations are defined by integrals which are evaluated approximately for various regimes of frequency. Coupled and uncoupled plate modes are included. The imaginary part of the coefficients associated with these modes leads to a virtual mass which is added to the plate mass. This causes a decrease in the modal resonance frequencies.

DERIVATION

Assume that neither the panel vibration nor the acoustic field affects the applied external force acting on the thin panel (Figure 3). The equation of motion representing the normal displacement of the panel driven by a pressure field is then

$$D\nabla^4 y + m_p \beta \frac{\partial y}{\partial t} + m_p \frac{\partial^2 y}{\partial t^2} = p(\underline{x},t) - P(\underline{x},x_2 = 0,t) \qquad (B1)$$

---

[*] As discussed in Appendix A, the wave number spectrum of the structure is discrete and that of the acoustic field is continuous. Hence for the submerged plate, *in vacuo* normal modes do not exist. However, the expansion of the velocity response of the structure in terms of its *in vacuo* modes is still valid. For convenience, we refer to these functions as modes and also refer to the resonance frequencies of these modes. Thus, we do not refer to a frequency associated with some natural mode of vibration but rather to a frequency corresponding to a maximum value of the amplitude response of a mode. The coupling together of the *in vacuo* modes by the structure-field interaction is a significant aspect of this problem. The effective coupling depends on both wave number matching and resonance frequency proximity and, therefore, on the relative magnitudes of the widths of the resonance peaks and the frequency spacing of the resonances.

The modal equation for the frequency Fourier transform of panel velocity is then

$$[Dk_{mn}^4 - \omega^2 m_p - i\omega^2 m_p \eta_{mn} \, \text{sgn} \, \omega] v_{mn}(\omega) = -i\omega p_{mn} + i\omega P_{mn} \qquad (B2)$$

obtained by use of the following relationships

$$v(x,\omega) = \int_{-\infty}^{\infty} v(x,t) e^{-i\omega t} \, dt \qquad (B3)$$

$$= \sum_{m,n=1}^{\infty} v_{mn}(\omega) \, \Psi_{mn}(\underline{x}) \qquad (B4)$$

where

$$\Psi_{mn}(\underline{x}) = \frac{2}{\sqrt{A_p}} \sin k_m x_1 \sin k_n x_3 \qquad (B5)$$

is a normal mode of a simply supported panel. Here $k_m = \frac{m\pi}{\ell_1}$, $k_n = \frac{n\pi}{\ell_3}$, $A_p = \ell_1 \ell_3$, and $k_{mn}^2 = k_m^2 + k_n^2$. Also

$$\beta = \eta_s |\omega| = \eta_s \, \omega \, \text{sgn} \, \omega \qquad (B6)$$

and (see Chapter V of Reference 8)

$$p_{mn}(\omega) = \int_{A_p} p(\underline{x},\omega) \, \Psi_{mn}(\underline{x}) \, d\underline{x} \qquad (B7)$$

$$P_{mn}(\omega) = \int_{A_p} P(\underline{x},0,\omega) \, \psi_{mn}(\underline{x}) \, d\underline{x} \qquad (B8)$$

where $d\underline{x} = dx_1 dx_3$

The boundary condition in the plane of the plate relating the *acoustic pressure* and panel velocity $v(\underline{x},t) = \partial y/\partial t$ is

$$\frac{\partial P(\underline{x}, x_2, t)}{\partial x_2}\Bigg|_{x_2 = 0} = -\rho_0 \frac{\partial v(\underline{x}, t)}{\partial t} \tag{B9}$$

so that

$$\frac{\partial P(\underline{x}, x_2, \omega)}{\partial x_2}\Bigg|_{x_2 = 0} = i\omega\rho_0 v(\underline{x}, \omega) \tag{B10}$$

Using Equation (B10) together with the wave equation for $P(\underline{x}, x_2, \omega)$ in an acoustic medium, the wave number-frequency transform relating the acoustic pressure to the panel velocity (see Equation (D10), Appendix D) is

$$P(\underline{k}, x_2, \omega) = Z(\underline{k}, \omega) v(\underline{k}, \omega) \varepsilon^{ix_2\sqrt{k_0^2 - k^2}} \tag{B11}$$

where the radiation impedance $Z(\underline{k}, \omega)$ is given by

$$Z(\underline{k}, \omega) = \rho_0 c_0 \left(1 - \frac{k^2}{k_0^2}\right)^{-1/2} \tag{B12}$$

Here $k = |\underline{k}|$ and $k_0 = \frac{\omega}{c_0}$.

After some rearrangement, we obtain from the above definitions

$$P_{mn}(\omega) = \frac{1}{(2\pi)^2} \sum_{q,r=1}^{\infty} v_{qr}(\omega) \iint_{-\infty}^{\infty} Z(\underline{k}, \omega) S_{mn}(\underline{k}) S_{qr}^{*}(\underline{k}) d\underline{k} \tag{B13}$$

$$= \sum_{q,r=1}^{\infty} R_{mnqr}(\omega) v_{qr}(\omega) \tag{B14}$$

where $d\underline{k} = dk_1 dk_2$ and $S_{mn}(\underline{k})$ is a shape function defined by

59

$$S_{mn}(\underline{k}) = \int_{A_p} \Psi_{mn}(\underline{x}) \, e^{i\underline{k} \cdot \underline{x}} \, d\underline{x} \qquad \text{(B15)}$$

and R_{mnqr} the coupling coefficient connecting the (m,n) mode and the (q,r) mode is defined by

$$R_{mnqr}(\omega) = \frac{1}{(2\pi)^2} \iint_{-\infty}^{\infty} Z(\underline{k},\omega) \, S_{mn}(\underline{k}) \, S_{qr}^*(\underline{k}) \, d\underline{k} \qquad \text{(B16)}$$

If $q \to m$ and $r \to n$, then the modal coupling coefficient becomes the modal radiation coefficient. The modal coupling coefficients connect the vibration of one plate mode with that of other plate modes because of plate-fluid interaction. The modal radiation coefficients, which can be obtained as special cases of the modal coupling coefficients, are a measure of how efficiently a particular mode shape resonates when no other modes are excited. The real parts of the coefficients are associated with a radiation damping effect on the plate response. The imaginary parts lead to a virtual mass to be added to the structural mass of the plate, thereby diminishing the modal resonance frequencies. The coupling coefficients can therefore be written

$$R_{mnqr} = S_{mnqr} + i T_{mnqr} \qquad \text{(B17)}$$

and the equations of motion can be written

$$[Dk_{mn}^4 - \omega^2 m_p - i\omega^2 m_p \, \eta_{mn} \, \text{sgn} \, \omega] \, v_{mn}(\omega) - i\omega \sum_{q,r} R_{mnqr} v_{qr} = -i\omega p_{mn}(\omega) \qquad \text{(B18)}$$

Approximate values of $T_{mnqr} = -\omega m_{mnqr}$ are now obtained for (1) the entire frequency range, (2) the low frequency range, and (3) the high frequency range. Moreover, for these frequencies, values of T_{mnqr} are obtained for various wave number domains, i.e., for edge and corner modes. Finally, we observe that the acoustically slow edge modes are the major contributors to the virtual mass (see Figure 4).

60

ENTIRE FREQUENCY RANGE

The shape functions used in Equation (B16) are:

$$S_{mn} = \int_{A_p} \Psi_{mn}(\underline{x}) e^{i\underline{k}\cdot\underline{x}} \, d\underline{x} = \frac{2k_m k_n [(-1)^m e^{-ik_1\ell_1}-1][(-1)^n e^{-ik_3\ell_3}-1]}{\sqrt{A_p}\,(k_1^2-k_m^2)(k_3^2-k_n^2)} \tag{B19}$$

Hence the integrand of Equation (B16) includes terms of the form

$$1 + (-1)^{q+m} - (-1)^q e^{ik_1\ell_1} - (-1)^m e^{-ik_1\ell_1} = \begin{cases} 2[1-(-1)^m \cos k_1\ell_1] & \text{for } m,q \\ & \text{both odd or even;} \\ 0 & \text{otherwise} \end{cases} \tag{B20}$$

(An analogous equation holds for n and r.) Each mode is thus coupled to at most only one-quarter of all the other modes. The coupling coefficients are then written

$$R_{mnqr} = S_{mnqr} + iT_{mnqr} = \frac{64\rho_o c_o k_o k_m k_n k_q k_r k_o}{(2\pi)^2 A_p}$$

$$\iint_0^\infty \frac{[1-(-1)^m \cos k_1\ell_1][1-(-1)^n \cos k_3\ell_3] \, dk_1 \, dk_3}{(k_1^2-k_m^2)(k_1^2-k_q^2)(k_3^2-k_n^2)(k_3^2-k_r^2)(k_o^2-k_1^2-k_3^2)^{1/2}} \tag{B21}$$

We consider only the imaginary part of the integral which is the mass loading coupling term T_{mnqr}. This part of the integration is performed over all values $|k| > k_o$, i.e., the region containing acoustically slow modes. Inspection of the integrand indicates that the largest coefficients are those having either m=q or n=r, or both. In Equation (B21) we let $(k_o^2-k_1^2-k_3^2)^{1/2} \rightarrow -i(k_1^2+k_3^2-k_o^2)^{1/2}$. The region of integration for Equation (B21) is now divided into three regions *covering acoustically slow modes*, i.e., exterior to the acoustically fast region (see Figure 4).

$$\iint_{|\underline{k}|>k_o} d\underline{k} = \int_{k_o}^\infty dk_3 \int_0^\infty dk_1 + \int_0^{k_o} dk_3 \int_{k_o}^\infty dk_1 + \int_0^{k_o} dk_3 \int_{\sqrt{k_o^2-k_1^2}}^{k_o} dk_1 \tag{B22}$$

61

Edge Modes

It is clear from Figure 4 that the first of the integrals given in the right member of Equation (B22) are the dominant ones for the two X-type edge modes. We first perform the k_1 integration. Let

$$I_{mq}(k_1) = \frac{[1-(-1)^m \cos k_1 \ell_1]}{(k_1{}^2-k_m{}^2)(k_1{}^2-k_q{}^2)} \qquad (B23)$$

A graph of this function is plotted in Figure 5. The function is such that

$$\int_0^\infty I_{mq}(k_1)dk_1 = 0 \text{ for } m{\neq}q$$

and

$$I_{mn}(k_1) \approx \frac{\pi\ell_1}{4k_m{}^2} \delta(k_1-k_m) \text{ for } m=q \qquad (B24)$$

Hence

$$T_{mnmr} = \frac{-4\rho_o c_o k_o k_n k_r k_o \ell_1}{\pi A_p} \int_{k_o}^\infty \frac{I_{nr}(k_3)dk_3}{[k_3{}^2-(k_o{}^2-k_m{}^2)]^{1/2}} \qquad (B25)$$

where $I_{nr}(k_3)$ as defined by Equation (B23) is

$$I_{nr}(k_3) = \frac{[1-(-1)^n \cos k_3 \ell_3]}{(k_3{}^2-k_n{}^2)(k_3{}^2-k_r{}^2)} \qquad (B26)$$

Explicitly,

$$T_{mnmr} = \frac{-4\rho_o c_o k_o k_n k_r k_o \ell_1}{\pi A_p} \int_{k_o}^\infty \frac{[1-(-1)^n \cos k_3 \ell_3] \, dk_3}{(k_3{}^2-k_n{}^2)(k_3{}^2-k_r{}^2)\left[k_3{}^2-(k_o{}^2-k_m{}^2)\right]^{1/2}} \qquad (B27)$$

62
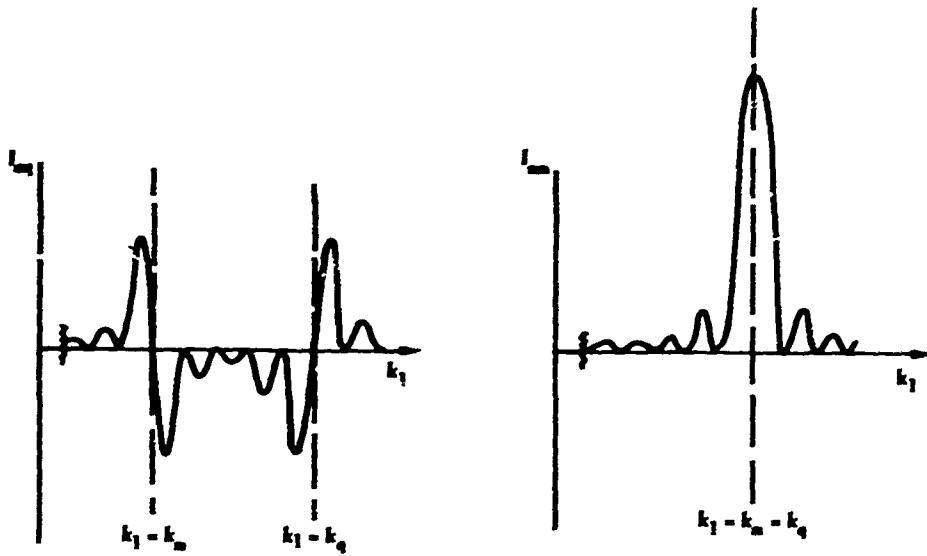
Figure 5 - Graph of $I_{mq}(k_1) = \dfrac{\left[(1-(-1)^m \cos k_1 \ell_1\right]}{(k_1{}^2 - k_m{}^2)(k_1{}^2 - k_q{}^2)}$

We observe that there is no contribution from the singularities at $k_3 = k_n \neq k_r$ or $k_3 = k_r \neq k_n$ for $n \neq r$ since in that case the term in brackets in the numerator of Equation (B27) becomes zero and $I_{nr}(k_3) \to o$. Hence the only singularity of the integrand is the root singularity.

We now treat the terms 1 and $(-1)^n \cos k_3 \ell_3$ separately as Cauchy principal values. We make the approximation $k_3^2 - k_n^2 \approx -k_n^2$ and $k_3^2 - k_r^2 \approx -k_r^2$ (since there is little contribution from $k_3 \sim k_n$, $k_3 \sim k_r$ we consider $k_n, k_r > k_3$ from which the approximation follows). We write for the first principal value

$$\int_{k_o}^{\infty} \frac{1}{(k_3^2 - k_n^2)(k_3^2 - k_r^2)[k_3^2 - (k_o^2 - k_m^2)]^{1/2}} \, dk_3 \approx \frac{1}{k_n^2 k_r^2} \int_{k_o}^{k_n} \frac{dk_3}{[k_3^2 - (k_o^2 - k_m^2)]^{1/2}} \quad \text{(B28)}$$

$$= \frac{1}{k_n^2 k_r^2} \ln \left[\frac{k_n + \sqrt{k_n^2 - (k_o^2 - k_m^2)}}{k_o + \sqrt{k_o^2 - (k_o^2 - k_m^2)}} \right] \quad \text{(B29)}$$

$$\approx \frac{1}{k_n^2 k_r^2} \ln \frac{2k_n}{k_o} \quad \text{(B30)}$$

for $k_n^2 \gg k_o^2 - k_m^2$, $2k_n \gg k_o + k_m$. For coupling between resonant edge modes only, that is for modes close together in wave number space,

$$\ln \frac{2k_n}{k_o} \approx \ln \frac{2k_r}{k_o} \quad \text{(B31)}$$

The integral associated with the $(-1)^n \cos k_3 \ell_3$ term is shown in Reference 7 to lead to an asymptotic result due to the square root singularity. The magnitude of this result can be ignored in comparison with the dominant term given by Equation (B30). Hence for the edge modes, since $k_n^2 = k_{mn}^2 - k_m^2 \approx k_{mn}^2$

64

$$T_{mnmr} = \frac{-4\rho_o c_o}{\pi A_p} \frac{k_o \ell_1}{k_n k_r} \ln \frac{2k_{mn}}{k_o} \tag{B32}$$

Finally *when n=r* so that $k_n = k_r$, Equation (B27) becomes for *acoustically slow modes*

$$T_{mnmn} = \frac{-4\rho_o c_o k_n k_r k_o \ell_1}{\pi A_p} \left[\frac{\pi \, \ell_3}{4k_n^2} \int_{k_o}^{\infty} \frac{\delta(k_3 - k_n) \, dk_3}{[k_3^2 - (k_o^2 - k_m^2)]^{1/2}} \right. \tag{B33}$$

$$\approx \frac{-\rho_o c_o k_o}{k_{mn}} \text{ for } k_{mn}^2 \gg k_o^2 \tag{B34}$$

by virtue of the analog of Equation (B24) for $I_{nn}(k_3)$.

Corner Modes

For corner modes, $k_o^2 \ll k_m^2$ and since

$$\int_{k_o}^{\infty} dk_3 = \int_{o}^{\infty} dk_3 - \int_{o}^{k_o} dk_3 \approx \int_{o}^{\infty} dk_3$$

the integral in Equation (B27) becomes

$$\int_{o}^{\infty} \frac{I_{nr}(k_3) \, dk_3}{(k_3^2 + k_m^2)^{1/2}} = \int_{o}^{k_n} \frac{[1 - (-1)^n \cos k_3 \ell_3] \, dk_3}{(k_3^2 - k_n^2)(k_3^2 - k_r^2)(k_3^2 + k_m^2)^{1/2}} \tag{B35}$$

$$\approx \frac{1}{k_m^2 k_n^2} \qquad ; \ (n \neq r) \tag{B36}$$

65

following a procedure similar to that used in evaluating the integral for the edge modes. Hence Equation (B27) yields

$$T_{mnmr} = \frac{-4\rho_o c_o}{\pi A_p} \cdot \frac{k_n k_r k_o \ell_1}{k_{mn}^2 k_{mr}^2} \cdot \delta_{mq} \tag{B37}$$

Finally when $n=r$ so that $k_n = k_r$, Equation (B27) becomes for *acoustically slow modes*

$$T_{mnmn} \approx \frac{-4\rho_o c_o}{\pi A_p} k_n k_r k_o \ell_1 \left[\frac{\pi \ell_3}{4k_n^2} \cdot \int_o^\infty \frac{\delta(k_3 - k_n) dk_3}{(k_3^2 + k_m^2)^{1/2}} \right] \tag{B38}$$

$$= -\rho_o c_o \frac{k_o}{k_{mn}} \text{ for } k_{mn}^2 \gg k_o^2 \tag{B39}$$

Moreover, inspection shows that the mass coupling T_{mnmn} is negligibly small for two acoustically fast modes.

Retaining only the dominant terms, Reference 7 summarizes the values of T_{mnqr} as follows:

For (m,n) an X-type edge mode and (q,r) an edge mode.

$$T_{mnqr} = -\frac{4\rho_o c_o}{\pi A_p} \frac{k_o \ell_1}{k_n k_r} \ell n \frac{2k_{mn}}{k_o} \delta_{mq} - \frac{4\rho_o c_o}{\pi A_p} k_o \ell_3 \frac{k_m k_q}{k_{mn}^2 k_{qn}^2} \delta_{qn} \tag{B40}$$

For large inertial coupling between modes, it is necessary that two mode numbers be the same so that the modes vibrate in the same shape in one direction. This is symbolized by the Kronecker delta functions.

66

For (m,n) an X-type edge mode and (q,r) a corner mode.

$$T_{mnqr} = - \frac{4\rho_o c_o}{\pi A_p} k_o \ell_3 \frac{k_m k_q}{k_{mn}^2 k_{qr}^2} \delta_{nr} \tag{B41}$$

For (m,n) an X-type edge mode and (q,r) an acoustically fast mode.

$$T_{mnqr} = - \frac{4\rho_o c_o}{A_p} k_o \ell_1 \frac{k_r}{k_n k_o^2} \delta_{mq} \tag{B42}$$

For (m,n) and (q,r) corner modes.

$$T_{mnqr} = - \frac{4\rho_o c_o}{\pi A_p} k_o \ell_1 \frac{k_n k_r}{k_{mn}^2 k_{mr}^2} \delta_{mq} - \frac{4\rho_o c_o}{\pi A_p} k_o \ell_3 \frac{k_m k_q}{k_{mn}^2 k_{qn}^2} \delta_{nr} \tag{B43}$$

For all modes in $\underline{K}$ space for which $|k| > k_o$ the self-inertia term is

$$T_{mnmn} = \begin{cases} -\rho_o c_o \dfrac{k_o}{k_{mn}} , & k_{mn} > k_o \\[2mm] 0 , & k_{mn} < k_o \end{cases} \tag{B44}$$

Equations (B43) and (B44) may be combined to give the following result valid for all corner modes

$$T_{mnqr} = - \rho_o c_o \frac{k_o}{k_{mn}} \delta_{mq} \delta_{nr} - \frac{4\rho_o c_o}{\pi A_p} k_o \ell_1 \frac{k_n k_r}{k_{mn}^2 k_{mr}^2} \delta_{mq} - \frac{4\rho_o c_o}{\pi A_p} k_o \ell_3 \cdot$$
$$\frac{k_m k_q}{k_{mn}^2 k_{qn}^2} \delta_{nr} \tag{B44a}$$

That is, T_{mnmn} is the same for all acoustically slow modes and T_{mnqr} is of the same form for all cases treated, irrespective of the division by radiation characteristics into edge and corner modes. Equation (B18) is now written as

67

$$B_{mn} v_{mn} - i\omega \sum_{q,r} S_{mnqr} v_{qr} + \omega \sum_{q,r} T_{mnqr} v_{qr} = -i\omega p_{mn} \tag{B45}$$

Here

$$B_{mn} = Dk_{mn}^4 - \omega^2 M_p - i\omega^2 m_p \eta_{mn} \, \text{sgn} \, \omega \tag{B46}$$

where

$$M_p = \begin{cases} m_p \left(1 + \dfrac{\rho_o}{m_p k_{mn}}\right), & k_{mn} > k_o \\[2em] m_p, & k_{mn} < k_o \end{cases} \tag{B47}$$

We observe that the term $\rho_o c_o \dfrac{k_o}{k_{mn}}$ of Equation (B39) is included in B_{mn} and T_{mnqr} is defined solely as in Equations (B40) to (B43). The solution of the set of Equations (B45) is discussed in detail in Reference 7. It is shown that in Equation (B45), the total effect of the reactive coupling terms is considerably less than the modal self-inertia term, Equation (B44). The main reactive effect of the fluid is therefore the modal self-inertia term which acts to decrease the modal resonance frequencies.

The inertia terms for the low and high frequency limits obtained in Reference 7 by solving Equation (B45) are now presented.

LOW FREQUENCY LIMIT

At frequencies such that $k_o \ell_1$, $k_o \ell_3 < \pi$, all modes are of corner mode radiation character. For these frequencies

$$M_p \approx m_p \left(1 + \frac{\rho_o c_o}{\omega m_p} \frac{k_o}{k_{mn}}\right) \tag{B48}$$

HIGH FREQUENCY LIMIT

At high frequencies, $k_o \ell_1$, $k_o \ell_3 \gg \pi$, the radiation and coupling characteristics of the modes are not the same for all modes as in the low frequency case. The important inertia term is the self-inertia defined by Equation (B44) so that

$$
\begin{aligned}
M_p &= m_p \left(1 + \frac{\rho_o}{m_p k_{mn}} \right) ; \quad k_{mn} > k_o \\
&= m_p \quad\quad\quad\quad\quad ; \quad k_{mn} < k_o
\end{aligned}
\tag{B49}
$$

The high frequency analysis was restricted to frequencies below the acoustic critical frequency, that is, the resonant modes considered all have wave speeds on the plate less than the acoustic wave speed. Hence the case of resonantly excited acoustically fast modes are not treated. Since, however, the acoustic critical frequency for a 1/4 in. steel plate in water is about 40,000 Hz, the restriction is of no great practical significance.

For still greater refinements than the results presented here, the reader is referred to Reference 7; the refinements, however, do not significantly alter the results presented here.

69

APPENDIX C

THE LEIBOWITZ METHOD I

NOTATION

A_p	Area of plate
c	Velocity of sound in fluid medium
$F(0,0)$	Driving force applied at coordinates x=o, y=o (also z=o) i.e., origin of coordinate system, used in Appendix A, on plate surface
F_{mnpq}	Generalized force for coupled mnpq modes
I	Integral defined by Equation (C2)
$I_{mq}(k_1)$	Defined by Equation (B23) of Appendix B
k	Acoustic wave number equal to ω/c
k_m, k_n, k_p, k_q	Modal wave numbers defined by Equation (A5)
k_{mn}	Surface wave number equal to $\sqrt{k_m^2 + k_n^2}$
k_3	Wave number in the direction of the ordinate (defined as in notation for Appendix B)
ℓ_x, ℓ_y	Half length and half width of plate, respectively
ℓ_1, ℓ_3	Equal to $2\ell_x$ and $2\ell_y$, respectively
m, n, p, q	Mode numbers
m_{mn}	Added mass per unit area
m_{mnpq}	Mass of coupled modes mnpq per unit area
T_{mnpq}	Modal mass coupling term
W_{pq}	Displacement amplitude of vibration of a plate for the pq mode
$\delta(\gamma_i - k_j)$	Delta function; $\displaystyle\int_{-\infty}^{\infty} \delta(\gamma_i - k_j)d\gamma_i = \begin{cases} 1, & \gamma_i = k_j \\ 0, & \gamma_i \neq k_j \end{cases}$
δ_{ij}	Kronecker delta equal to 1 for i=j; equal to 0 otherwise
γ_x, γ_y	Wave numbers which are the coordinates in Fourier transform space
ρ	Mass density of fluid medium
ω	Natural circular frequency of vibration

71

DESCRIPTION

It was indicated in Appendix A that Feit and Junger avoided the determination of the exact solution of Equation (A17). They obtained an approximate solution by evaluating the integral of the equivalent Equation (A14) for the high wave number limit and $\omega < \omega_c$. In the present Appendix we attempt to obtain approximate solutions directly from Equation (A17) using with some modifications the methods and results of Davies given in Appendix B. Thus with proper interpretation of the results as applicable to various modal regions, the work of Appendices A and B can be interrelated.

DERIVATION

For a *single mode*, the double integral of Equation (A17) may be rewritten in the following form;[*] note that for a single mode the summation $\sum\limits_{pq}$ is dropped and wave numbers k_p, k_q are considered as known quantities corresponding to any particular set of prescribed mode numbers pq. Thus Equation (Ci) represents the contribution of a single prescribed pq mode to F_{mn} (see footnote to sentence above Equation (C29)).

$$F_{mn} = F(0,0) + \frac{4\rho c^2 k^2 k_m k_n k_p k_q (-1)^{m+n+p+q}}{\pi^2} \bar{W}_{pq} \int\int_0^\infty \frac{dY_x dY_y}{[Y_x^2 - (k^2 - Y_y^2)]^{1/2}} \cdot \quad (C1)$$

$$\left[\frac{(1 + \cos 2Y_x \ell_x)}{(k_m^2 - Y_x^2)(k_p^2 - Y_x^2)}\right]\left[\frac{(1 + \cos 2Y_y \ell_y)}{(k_n^2 - Y_y^2)(k_q^2 - Y_y^2)}\right]$$

---

[*] The problem is first discussed in terms of the results for various modal regions. Subsequently, it is shown that for the even modes, the general integral expressions for the virtual mass (or mass reactance) obtained from Equations (A17) and (B21) are identical.

since all terms in the integrand are even functions in Y_x and Y_y. For convenience let

$$I = \iint\limits_0^{\infty} \frac{dY_x dY_y}{[Y_x^2 - (k^2 - Y_y^2)]^{1/2}} \left[\frac{(1 + \cos 2Y_x \ell_x)}{(k_m^2 - Y_x^2)(k_p^2 - Y_x^2)} \right] \left[\frac{1 + \cos 2Y_y}{(k_n^2 - Y_y^2)(k_q^2 - Y_y^2)} \right] \quad (C2)$$

We evaluate I for the following cases:

Case I: $m \neq p$, $n \neq q$

We observe that for $m \neq p$ there is no contribution to the integral from the singularities at $Y_x = k_m \neq k_p$ or $Y_x = k_p \neq k_m$ because in that case the term in the numerator of the first bracket of Equation (C2) becomes zero (see Equation (A3)). Evaluation of the resultant indeterminate quantity, using L'Hospitals rule, yields a null result, i.e.,

$$\lim_{\substack{Y_x - k_m \to 0 \\ k_m \neq k_p}} \left(\frac{1}{k_p^2 - k_m^2} \cdot \frac{1 + \cos 2Y_x \ell_x}{k_m^2 - Y_x^2} \right) = \frac{\ell_x}{k_p^2 - k_m^2} \cdot \frac{\sin 2k_m \ell_x}{k_m}$$

$$= \frac{\ell_x}{k_p^2 - k_m^2} \frac{\sin (2m+1)\pi}{k_m} , \quad m=0,1,2\cdots$$

$$= 0 \text{ for all } k_m$$

A similar result is obtained for all k_n for $n \neq q$. Thus we conclude that the singularities at $Y_x = k_m \neq k_p$ or $Y_x = k_p \neq k_m$ and $Y_y = k_n \neq k_q$ or $Y_y = k_q \neq k_n$ make no contribution to the integral.

Moreover when $Y_x = k_m \neq k_p$, then in the first bracket of Equation (C2), $\cos 2Y_x \ell_x = \cos 2k_m \ell_x = \cos (2m+1)\pi = -1$ for all m. Since $\cos (2m+1)\pi = -(-1)^m \cos m\pi$, then

73

$$\frac{(1 + \cos 2\gamma_x \ell_x)}{(k_m^2 - \gamma_x^2)(k_p^2 - \gamma_x^2)} + \frac{[1-(-1)^m \cos 2k_m \ell_x]}{(\gamma_x^2 - k_m^2)(\gamma_x^2 - k_p^2)} \equiv 0 \quad \text{for } \gamma_x = k_m \neq k_p \text{ only} \quad (C3)$$

Similar relationships obtain for $\gamma_x = k_p \neq k_m$, $\gamma_y = k_n \neq k_q$, and $\gamma_y = k_q \neq k_n$. For $\gamma_x \neq k_m$, the form of the left member of Equation (C3) differs from the form of $I_{mq}(k_1)$ ($= I_{mp}(\gamma_x)$ here) given by Equation (B23) of Appendix B and plotted in Figure 5, only for even values of m by the sign in the numerator preceding $\cos 2\gamma_x \ell_x$. Thus, by analogy with the work in Appendix B and from an inspection of Figure 5, it is apparent that the integrated contribution is very small over the range $0 < \gamma_x \leq \infty$.

The foregoing is compatible with the statement made in Appendix B to the effect that the largest contributors to the integral occur when either/ or $m=p$ and $n=q$. Appendixes A and B also indicate that the dominant contribution occurs for $m=p$ and $n=q$, i.e., the important inertia term is the self-inertia term. These cases are discussed next.

Case II: $m=p$, $n \neq q$ or $n=q$, $m \neq p$
_____

For $m=p$, $n \neq q$ we use the methods of Appendix B. For this case we have, using Equation (B24)[*]

$$\frac{(1 + \cos 2\gamma_x \ell_x)}{(k_m^2 - \gamma_x^2)(k_p^2 - \gamma_x^2)} \equiv \frac{[1-(-1)^m \cos 2k_m \ell_x]}{(\gamma_x^2 - k_m^2)(\gamma_x^2 - k_p^2)} \approx \frac{\pi 2\ell_x}{4k_m^2} \delta(\gamma_x - k_m) \text{ for}$$
$$\gamma_x = k_m = k_p \qquad (C4)$$

Equation (C2) then becomes

$$I = \frac{\pi 2\ell_x}{4k_m^2} \int_0^\infty \left[\frac{1 + \cos 2\gamma_y \ell_y}{(k_n^2 - \gamma_y^2)(k_q^2 - \gamma_y^2)} \right] \frac{d\gamma_y}{[\gamma_y^2 - (k^2 - k_m^2)]^{1/2}} \qquad (C5)$$

_____

[*] In Equation (B24), let $\ell_1 = 2\ell_x$ and $k_1 \rightarrow \gamma_x$; for later use, we note that $\ell_3 = 2\ell_y$.

74

For the *X-type edge modes*

$$I \approx \frac{\pi 2 \ell_x}{4k_m^2} \int_{k_o}^{\infty} \frac{[1 + \cos 2\gamma_y \ell_y]}{[(k_n^2 - \gamma_y^2)(k_q^2 - \gamma_y^2)]} \frac{d\gamma_y}{[\gamma_y^2 - (k^2 - k_m^2)]^{1/2}} \quad (C6)$$

neglecting as in Appendix B the contribution of acoustically fast modes occurring in the region $0 < \gamma_y < k_o$. The integral in Equation (C6) is similar in form to that of Equation (B27). Using the Cauchy principal value for the terms 1 and $\cos 2\gamma_y \ell_y$ in Equation (C6), we find as before that the integrated contribution of the $\cos 2\gamma_y \ell_y$ term can be ignored. Similar results are obtained for n=q, m≠p. Hence the results obtained for *edge modes* in Appendix B can be used directly.

Similarly for the *corner modes* when $k^2 \ll k_m^2$, Equation (C4) is written as

$$I = \frac{\pi 2 \ell_x}{4k_m^2} \int_0^{\infty} \left[\frac{1 + \cos 2\gamma_y \ell_y}{(k_n^2 - \gamma_y^2)(k_q^2 - \gamma_y^2)} \right] \frac{d\gamma_y}{[\gamma_y^2 + k_m^2]^{1/2}} \quad (C7)$$

The integral is similar in form to the left member of Equation (B35). Hence using the Cauchy principal value for the term 1 and $\cos 2\gamma_y \ell_y$ in Equation (C7), we find that, as before, the integrated contribution of the $\cos 2\gamma_y \ell_y$ term can be ignored. Similar results are obtained for n=q, m≠p. Hence the results obtained for *corner modes* in Appendix B can be used directly.

Using Equations (B40)-(B43) we now find values of I, F_{mn}, and m_{mn} for various cases of modal coupling. Substituting Equation (C2) in Equation (C1), we have

$$F_{mn} = F(0,0) + \frac{4\rho c^2 k^2 k_m k_m k_p k_q (-1)^{m+n+p+q}}{\pi^2} W_{pq} \cdot I \quad (C8)$$

Inspection of the first two members of Equation (C4) indicates that for $\gamma_x = k_m = k_p$, $k_n \neq k_q$, the integrand of Equation (C1) and of Equation (B21) times -i are identical if, when using the Cauchy principal values, we

neglect the cos $2\gamma_y \ell_y$ and cos $k_3 \ell_3$ terms. A similar identity exists for $\gamma_y = k_n = k_q$, $k_m \neq k_p$. Hence substituting Equation (C2) in Equation (B21), we get

$$(\text{Imag})\ I = \frac{\dfrac{T_{mnpq}}{64\rho c k\, k_m k_n k_p k_q}}{(2\pi)^2\ A_p}\ ;\quad A_p = (2\ell_x)(2\ell_y) = 4\ell_x \ell_y \tag{C9}$$

where we have considered only the imaginary part of the integral in Equation (B21).

Substitution of Equation (C9) in Equation (C8) yields

$$F_{mn} = F(0,0) - \frac{ck(-1)^{m+n+p+q}\ A_p}{4}\ W_{pq}\ T_{mnpq} \tag{C10}$$

where T_{mnpq} is given by Equations (B40)-(B43). (Note: Davies symbol $q \rightarrow p$ and $r \rightarrow q$ here; m, p stay the same, and all odd mode numbers used with respect to Davies origin for the plate represent even modes with respect to the Feit-Junger origin for the plate; see Appendix D.)

For (m,n) an X-type edge mode and (p,q) an edge mode.

$$F_{mn} = F(0,0) - \frac{ckA_p}{4}\left[-(-1)^{n+q}\frac{4\rho c}{\pi A_p}\frac{k2\ell_x}{k_n k_q}\ \ell n\ \frac{2k_{mn}}{k}\ W_{pq}\ \delta_{mp}\ -(-1)^{m+q}\cdot\right.$$

$$\tag{C11}$$

$$\left.\frac{4\rho c}{\pi A_p}k2\ell_y\ \frac{k_m k_p}{k_{mn}^2 k_{pn}^2}\ W_{pq}\ \delta_{pn}\right]$$

$$= F(0,0) + \frac{2\rho c^2 k^2}{\pi}\left[(-1)^{n+q}\ell_x\ \ell n\ \frac{2k_{mn}}{k}\ W_{pq}\ \delta_{mp}\ +\ \frac{(-1)^{m+q}\ell_y k_m k_p}{k_{mn}^2 k_{pn}^2}W_{pq}\ \delta_{pn}\right] \tag{C12}$$

Hence

76

$$m_{mnpq} = \frac{2\rho}{\pi}\left[\frac{(-1)^{n+q}}{\ell_y k_n k_q} \ell_n \frac{2k_{mn}}{k} \delta_{mp} + \frac{(-1)^{m+q}k_m k_p}{\ell_x k_{mn}^2 k_{pn}^2} \hat{\delta}_{pn}\right] \qquad (C13)$$

For (m,n) an X-type edge mode and (p,q) a corner mode.

$$F_{mn} = F(0,0) - \frac{ck(-1)^{m+p} A_p}{4}\left[\frac{-4\rho c}{\pi A_p} k2 \ell_y \frac{k_m k_p}{k_{mn}^2 k_{pn}^2} W_{pq} \delta_{nq}\right] \qquad (C14)$$

$$= F(0,0) + \frac{2\rho c^2 k^2 (-1)^{m+p}\ell_y k_m k_p}{\pi k_{mn}^2 k_{pn}^2} W_{pq} \hat{\delta}_{nq} \qquad (C15)$$

Hence

$$m_{mnpn} = \frac{2\rho}{\pi}\left[\frac{(-1)^{m+p}}{\ell_x} \frac{k_m k_p}{k_{mn}^2 k_{pn}^2} \delta_{nq}\right] \qquad (C16)$$

For (m,n) an X-type edge mode and (p,q) an acoustically fast mode.

$$F_{mn} = F(0,0) \frac{-ck(-1)^{n+q} A_p}{4}\left[\frac{-4\rho ck2\ell_x}{A_p} \frac{k_q}{k_n k^2} W_{pq} \delta_{mp}\right] \qquad (C17)$$

$$= F(0,0) + \frac{2\rho c^2 k^2 (-1)^{n+q}\ell_x k_q}{k_n k^2} W_{pq} \delta_{mp} \qquad (C18)$$

Hence

$$m_{mnmq} = 2\rho\left[\frac{(-1)^{n+q}}{\ell_y} \frac{k_q}{k_n k^2} \delta_{mp}\right] \qquad (C19)$$

77

For (m,n) and (p,q) corner modes.

$$F_{mn} = F(0,0) - \frac{ckA_p}{4}\left[\frac{-(-1)^{n+q}4\rho ck2\ell_x k_n k_q}{\pi A_p k_{mn}^2 k_{mq}^2} W_{pq}\,\delta_{mp} - (-1)^{m+p}\frac{4\rho ck2\ell_y k_m k_p}{\pi A_p k_{mn}^2 k_{pn}^2}\cdot W_{pq}\,\delta_{nq}\right]$$

(C20)

$$= F(0,0) + \frac{2\rho c^2 k^2}{\pi}\left[\frac{(-1)^{n+q}\ell_x k_n k_q}{k_{mn}^2 k_{mq}^2} W_{pq}\,\delta_{mp} - \frac{(-1)^{m+p}\ell_y k_m k_p}{k_{mn}^2 k_{pn}^2} W_{pq}\,\delta_{nq}\right]$$

(C21)

Hence

$$m_{mnpq} = \frac{2\rho}{\pi}\left[\frac{(-1)^{n+q}k_n k_q}{\ell_y k_{mn}^2 k_{mq}^2}\,\delta_{mp} + \frac{(-1)^{m+p}k_m k_p}{\ell_x k_{mn}^2 k_{pn}^2}\,\delta_{nq}\right]$$

(C22)

Equations (C13), (C16), (C19), (C22) are identical to corresponding results obtained from Appendix B and presented as results in Table 1 as Items 2-5 for the Davies method. Having obtained the results for the added mass of the coupled modes, i.e., the coupled inertia terms, we now consider the added mass of the uncoupled modes, i.e., the self-inertia terms.

Case III: m=p, n=q

At m=p, n=q there occurs a dominant contribution to the integral in Equation (C1) from the singularities at $\Upsilon_x = k_m = k_p$ and $\Upsilon_y = k_n = k_q$. For this case

$$\frac{(1 + \cos 2\Upsilon_x \ell_x)}{(k_m^2 - \Upsilon_x^2)^2} \to \frac{[1-(-1)\cos 2k_m\ell_x]}{(k_m^2 - \Upsilon_x^2)^2} = I_{mm}(\Upsilon_x) = \frac{\pi \cdot 2\ell_x}{4k_m^2}\delta(\Upsilon_x - k_m)$$

(C23)

78

$$\frac{(1 + \cos 2\gamma_y \ell_y)}{(k_n^2 - \gamma_y^2)^2} + \frac{[1 - (-1)^n \cos 2k_n \ell_y]}{(k_n^2 - \gamma_y^2)^2} = I_{nn}(\gamma_y) = \frac{\pi \cdot 2 \ell_y}{4k_n^2} \delta(\gamma_y - k_n) \quad \text{(C24)}$$

Hence Equation (C2) becomes

$$I = \frac{\pi^2 \ell_x \ell_y}{4k_m^2 k_n^2} \int\!\!\int_0^\infty \frac{\delta(\gamma_x - k_m) \, \delta(\gamma_y - k_n) \, d\gamma_x d\gamma_y}{[\gamma_x^2 - (k^2 - \gamma_y^2)]^{1/2}} \quad \text{(C25)}$$

$$= \frac{\pi^2 \ell_x \ell_y}{4k_m^2 k_n^2 [k_{mn}^2 - k^2]^{1/2}} \quad \text{(C26)}$$

Substituting Equation (C26) in Equation (C1), we get

$$F_{mn} = F(0,0) + \frac{\rho c^2 k^2 \ell_x \ell_y \, W_{mn}}{[k_{mn}^2 - k^2]^{1/2}} \quad \text{(C27)}$$

Equation (C27) is identical with Equation (A27). Hence the results given by Equations (A28)-(A34) apply here. We note that since the mass loading is associated with the imaginary part of the integral for which $\gamma_x^2 + \gamma_y^2 > k^2$ (i.e., acoustically slow modes) then from Equation (A28)

$$m_{mn} = \frac{\rho}{(k_{mn}^2 - k^2)^{1/2}} \approx \frac{\rho}{k_{mn}} \ , \ k_{mn}^2 > k^2 \quad \text{(C28)}$$

The approximation value of m_{mn} given by Equation (C28) agrees with the results obtained in Equation (B44) since $T_{mnmn} = -\omega m_{mn} = -kc m_{mn}$. The result is therefore identical to the corresponding results presented in Table 1 as Item 1 for the Davies method.

79

PROOF OF IDENTITY OF FEIT-JUNGER AND DAVIES GENERAL INTEGRAL EXPRESSIONS FOR THE VIRTUAL MASS (FOR EVEN MODES)

The double integral of Equation (A17) may be rewritten in the form[*]

$$F_{mn} = F(0,0) + \frac{i4\rho c^2 k^2 k_m k_n (-1)^{m+n}}{\pi^2} \sum_{p,q} W_{pq} k_p k_q (-1)^{p+q} \int_0^\infty \int \left[\frac{1 + \cos 2\gamma_x \ell_x}{(k_m^2 - \gamma_x^2)(k_p^2 - \gamma_x^2)} \right]$$

(C29)

$$\left[\frac{1 + \cos 2\gamma_y \ell_y}{(k_n^2 - \gamma_y^2)(k_q^2 - \gamma_y^2)} \right] \frac{d\gamma_x d\gamma_y}{[k^2 - \gamma_x^2 - \gamma_y^2]^{1/2}}$$

In Appendix A (Feit-Junger), the origin is taken at the center of the plate whereas in Appendix B (Davies) the origin is taken at a corner of the plate. As shown in Appendix D and Figure 11 (see Appendix D), the modes numbered $m = 1, 3\cdots$ odd with respect to Davies origin represent the even modes with respect to Feit-Junger origin. By the Feit-Junger stipulation, Equation (A1), these are the only modes to be considered; similar relations hold for n,p,q. Hence $[-1]^{m+n} \equiv [-1]^{p+q} \to 1$ and

$$\left[\frac{1 + \cos 2\gamma_x \ell_x}{(k_m^2 - \gamma_x^2)(k_p^2 - \gamma_x^2)} \right]_{\text{Feit-Junger}} \to \left[\frac{1 - (-1)^m \cos k_1 \ell_1}{(k_m^2 - k_1^2)(k_q^2 - k_1^2)} \right]_{\text{Davies}}$$

$$\left[\frac{1 + \cos 2\gamma_y \ell_y}{(k_n^2 - \gamma_y^2)(k_q^2 - \gamma_y^2)} \right]_{\text{Feit-Junger}} \to \left[\frac{1 - (-1)^n \cos k_3 \ell_3}{(k_n^2 - k_3^2)(k_r^2 - k_3^2)} \right]_{\text{Davies}}$$

---

[*] Here, in contrast to Equation (C1), the contributions of all (p,q) modes to F_{mn} are included.

where the Feit-Junger notation $m,n,p,q \to m,n,q,r$, respectively, and $2\ell x$, $2\ell y \to \ell_1$, ℓ_3, respectively. Also $Y_x, Y_y \to k_1$, k_3 = components of $\underline{k}$, $k \to k_o$, $\rho c \to \rho_o c_o$. Thus the imaginary part of Equation (C29) rewritten in Davies notation is:

$$\left(\text{for the imaginary part, } \iint\limits_{o}^{\infty} \to \iint\limits_{|\underline{k}| \geq k_o}^{\infty} \text{ and we let } (k_o^2 - k_1^2 - k_3^2)^{1/2} \to \right.$$

$$\left. -i(k_1^2 + k_3^2 - k_o^2)^{1/2} \right)$$

$$(\text{Imag}) \; F_{mn} = F(0,0) - \frac{4\rho_o c_o^2 k_o^2 k_m k_n}{\pi^2} \sum_{q,r} W_{qr} k_q k_r \iint\limits_{|\underline{k}| \geq k_o} \left[\frac{1 - (-1)^m \cos k_1 \ell_1}{(k_m^2 - k_1^2)(k_q^2 - k_1^2)} \right] \cdot$$

$$\left[\frac{1 - (-1)^n \cos k_3 \ell_3}{(k_n^2 - k_3^2)(k_r^2 - k_3^2)} \right] \frac{d\underline{k}}{[k_1^2 + k_3^2 - k_o^2]^{1/2}} \tag{C30}$$

In Davies notation the expression for the virtual mass in Equation (A18) may be written

$$(F_{mn}) = (\text{Imag}) \; F_{mn} = \frac{\ell_1}{2} \cdot \frac{\ell_3}{2} \sum_{q,r} W_{qr} \, \omega^2 m_{mnqr} = -\frac{A_p}{4} \sum_{q,r} W_{qr} \, \omega \, T_{mnqr}$$

Virtual
mass
part
only

$$\tag{C31}$$

where $A_p = \ell_1 \ell_3$, $T_{mnqr} = -\omega m_{mnqr} = -kcm_{mnqr}$ and where now T_{mnqr} includes $T_{mnmn} = -\omega m_{mnmn}$ ($\equiv -\omega m_{mn}$ in Equation (A18)) and q,r includes m,n in the summation.

Comparing Equation (C31) and (excluding the driving force $F(0,0)$) Equation (C30), we get

$$T_{mnqr} = \frac{64 \rho_o c_o k_m k_n k_q k_r k_o}{(2\pi)^2 A_p} \iint\limits_{|\underline{k}| \geq k_o}^{\infty} \left[\frac{1 - (-1)^m \cos k_1 \ell_1}{(k_m^2 - k_1^2)(k_q^2 - k_1^2)} \right] \left[\frac{1 - (-1)^n \cos k_3 \ell_3}{(k_n^2 - k_3^2)(k_r^2 - k_3^2)} \right] \cdot$$

$$\frac{d\underline{k}}{[k_1^2 + k_3^2 - k_o^2]^{1/2}} \tag{C32}$$

81

In Equation (B21) let $(k_o^2 - k_1^2 - k_3^2)^{1/2} \rightarrow -i(k_1^2 + k_3^2 - k_o^2)^{1/2}$. We then see that Equation (C32) is identical to the imaginary part of Equation (B21) which has the same integral limits. Hence for m,n,p,q equal to odd numbers, representing Feit-Jungers even modes, all solutions of Equation (B21) for T_{mnqr} obtained by Davies methods, applicable to various modal regions, are relevant as solutions to the Feit-Junger Equation (A17).

APPENDIX D

LEIBOWITZ METHOD II

NOTATION

A	Area of plate
c	Velocity of sound in fluid medium
c_ℓ	Compressional wave velocity of the plate equal to $\left[\dfrac{E}{\rho_s(1-\nu^2)}\right]^{1/2}$
c_p	Phase velocity
E	Young's modulus
e	Equal to 2.718; base for natural or Naperian system of logarithms
f_m^{rad}	Radiation force for the mth mode
F_m^{rad}	Magnitude of the radiation force of the mth mode; equal to $f_m^{rad}/e^{-i\omega t}$
I_1, I_2	Defined by equations below Equation (D36)
i	Equal to $\sqrt{-1}$
$K(k_s)$	Equal to $1/\sqrt{k_s^2 - k_o^2}$ in Equation (D38)
k_m, k_n	Modal wave numbers equal to $m\pi/\ell_1$ and $n\pi/\ell_2$, respectively
k_{mn}	Wave number equal to $\sqrt{k_m^2 + k_n^2}$
$\bar{k}_n$	Projection of $\bar{k}_o$ on a normal to a plane lying along x_3
k_o	Acoustic wave number equal to ω/c
$\bar{k}_o$	Wave vector equal to $k_o \bar{r}_o$
k_s	Arbitrary wave number equal to $2\pi/\lambda_p = \omega/c_p$; $k_s^2 = k_1^2 + k_2^2$
$\bar{k}_s$	Projection of $\bar{k}_o$ on a plane
k_{x_1}, k_{x_2}	Wave numbers in x_1- and x_2-directions, respectively
k_1, k_2, k_3	Wave numbers along the x_1-, x_2-, x_3-directions, respectively
$\bar{k}_1, \bar{k}_2, \bar{k}_3$	Vector wave numbers in the x_1-, x_2-, x_3-directions, respectively
ℓ_1, ℓ_2	Length and width of plate, respectively

L_x, L_y	Half length and half width of plate, respectively
$M_{loading}$	Total added (or virtual) mass
m_{mn}	Added modal mass per unit area
m, n	Mode numbers
P	Amplitude of acoustic pressure p
p	Acoustic pressure in fluid medium, i.e., in half-space $x_3 > 0$
p_m^{rad}	Radiation pressure for the mth mode
Q_j	Sound flux or source strength or volume velocity of jth source equal to the product of the velocity of the source and the surface area of the source
R	Distance from origin to a field or observation point
R_j	Distance from j^{th} source to the field or observation point; equal to $R - \bar{r}_o \cdot \bar{r}_j$ which is the projection of R_j on R (here $\bar{r}_o \cdot \bar{r}_j$ is a dot producted equal to the projected distance difference $R - R_j$)
$\bar{r}$	Rest position of the plate
$r_o, \bar{r}_o$	Magnitude of wave direction vector, and wave direction vector respectively; $\bar{r}_o$ is unit vector from origin to field or observation point
$r_j, \bar{r}_j$	Magnitude and vector for distance from origin to j^{th} source lying in the plane
t	Time
$V(\bar{r}, t)$	Instantaneous modal velocity of a point on the plane
$V(\bar{r})$	Velocity of plate at its rest position $\bar{r}$; equal to plate velocity at $x_3 = 0$
$V(\bar{k}_s)$	Distribution of traveling plane waves in an infinite plane, i.e., Fourier distribution of the velocity $V(\bar{r}, t)$ in the region of the plate
V_m	Complex amplitude of $V(\bar{r}, t)$; modal velocity
V_o	Root mean square of $|V(\bar{r})|$; see Equation (D22); equal to $|V_m|$
$x, x' = x - \frac{\ell}{2}$	Abscissa with origin at the corner and midpoint of the plate, respectively
x_1, x_2, x_3	Rectangular coordinates, x_1, x_2 lie along the length and width of the plate of the plate, respectively; x_3 is normal to the plate and the origin lies at one corner of the plate

Z_m^{rad}	Radiation impedance
$\Gamma_m(k_s)$	Modal coupling parameter or directivity
∇^2	Equal to $(\partial^2/\partial x^2) + (\partial^2/\partial y^2) + (\partial^2/\partial z^2)$
λ_p	Wavelength of plate equal to $2\pi/k_s = 2\pi c_p/\omega$
ν	Poisson's ratio
ρ_o	Mass density of fluid
ρ_s	Mass density of plate
$\Psi_m(\bar{r})$	Normal mode function
ω	Natural circular frequency of vibration
*	Denotes complex conjugate
$\lvert\ \rvert$	Denotes magnitude
$\langle\rangle_{\bar{r}}$	Denotes average value over $\bar{r}$

DERIVATION

Consider a simply supported plate in an infinite plane baffle immersed in a fluid. Plane flexural waves form a wave field on this plate. We treat therefore a two-dimensional problem, in which radiation in the half-space $x_3 > o$ is of interest. The instantaneous modal velocity of a point on the plate, whose rest position is $\bar{r}$ is given by[8] (see Figure 6)

$$V(\bar{r},t) = V_m \Psi_m(\bar{r})e^{-i\omega t} \tag{D1}$$

We expand $V(\bar{r},t)$ into a distribution $V(\bar{k}_s)$ of traveling plane waves in an infinite plane each of the form[9] ($e^{-i\omega t}$ is tacitly implied)

$$V(\bar{r}) = V(\bar{k}_s)e^{i\bar{k}_s \cdot \bar{r}} \tag{D2}$$

For a plate vibrating with arbitrary wave number $k_s = 2\pi/\lambda_p = \omega/c_p$ and at frequency ω, it seems logical to make the following formulation for the sound pressure in the half-space $x_3 > 0$ (see Figure 6)

$$p(\bar{r},x_3) = Pe^{i(\bar{k}_s \cdot \bar{r} + k_3 x_3)} \tag{D3}$$

We require that the sound pressure represent a solution of the Helmholtz wave equation[9]
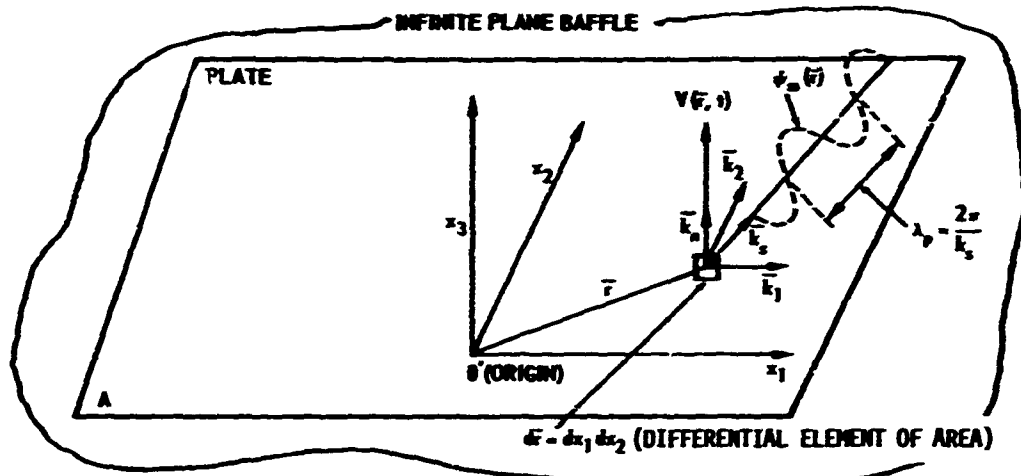
Figure 6a - Plan View
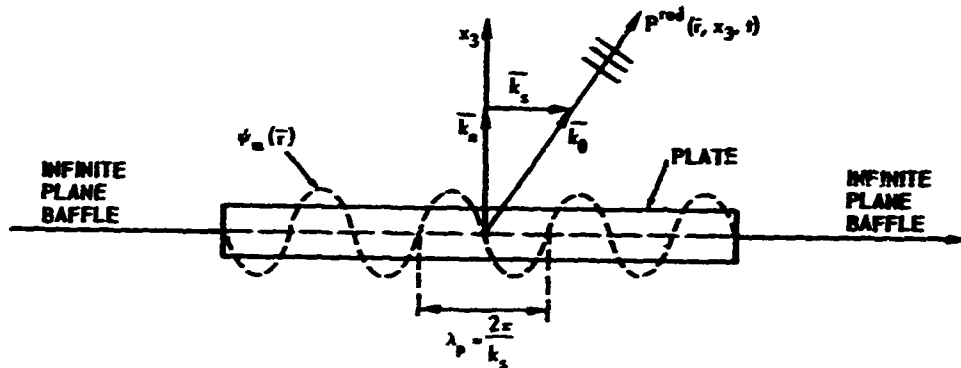
Figure 6b - Edge View Normal to $\bar{K}_s$; Vector Relations at $\bar{r}$

Figure 6 - Plan View and Edge View Normal to $\bar{K}_s$ of Plate in
Infinite Plane Baffle

Notes:

1. $\psi_m(\bar{r})$ and $V(\bar{r},t)$ are normal to plane; $+ V$ is out of plane, $- V$ is into plane

2. x_1, x_2, $\bar{k}_1$, $\bar{k}_2$, $\bar{k}_s$ lie in the plane, x_3, $\bar{k}_n$ are normal to the plane

3. $k_3 = |\bar{k}_n| = \sqrt{k_o^2 - k_s^2}$

4. $k_s = \dfrac{2\pi}{\lambda_p} = \dfrac{\omega}{c_p}$

86

$$\nabla^2 p + k_o{}^2 p = 0 \qquad (D4)$$

Substituting Equation (D3) in Equation (D4), we get

$$k_s{}^2 + k_3{}^2 = k_o{}^2 \qquad (D5)$$

We also require that the normal component of the sound velocity cal-
culated from Equation (D3) coincide at the boundary surface $x_3=0$ with the
plate velocity, i.e.,

$$V_{x_3 = 0} = V(\bar{r}) = \frac{1}{i\omega\rho_o}\left(\frac{\partial p}{\partial x_3}\right)_{x_3=0} = \frac{Pk_3}{\omega\rho_o} e^{i\bar{k}_s \cdot \bar{r}} \qquad (D6)$$

From Equations (D6) and (D2) we obtain

$$P = \frac{\omega\rho_o V(\bar{r})\, e^{-i\bar{k}_s \cdot \bar{r}}}{k_3} \qquad (D7)$$

$$= \frac{\rho_o c k_o V(\bar{k}_s)}{\sqrt{k_o{}^2 - k_s{}^2}} \qquad (D8)$$

$$= \frac{\rho_o c V(\bar{k}_s)}{\sqrt{1 - \dfrac{k_s{}^2}{k_o{}^2}}} \qquad (D9)$$

Substituting for P from Equation (D9) and for k_3 from Equation (D5)
into Equation (D3) and restoring the sinusoidal temporal variation yields
the following expression for the sound pressure radiated into the half-
space in front of the plate:

$$P_{\text{one wave}}^{\text{rad}}(\bar{r},x_3,t) = \frac{\rho_o c_o V(\bar{k}_s)}{\sqrt{1 - \dfrac{k_s{}^2}{k_o{}^2}}} e^{i\left(\bar{k}_s \cdot \bar{r} + \sqrt{k_o{}^2 - k_s{}^2}\, x_3 - \omega t\right)} \qquad (D10)$$

87

From Equation (D2) (with time factor included), the sum or integral of traveling plane waves in an infinite plane with amplitude distribution $V(\bar{k}_s)$ provides the velocity $V(\bar{r},t)$ in the region of the plate and zero outside the plate. The distribution $V(\bar{k}_s)$ must therefore satisfy the condition (note $d\bar{k}_s = dk_1 dk_3$)

$$V(\bar{r},t) = \int_{-\infty}^{\infty} V(\bar{k}_s)\, e^{i(\bar{k}_s \cdot \bar{r} - \omega t)} d\bar{k}_s \tag{D11}$$

Obviously $V(\bar{k}_s)$ is the Fourier distribution of the function $V(\bar{r},t)$ and we know, therefore, that such a distribution exists and that it can be calculated from the equation[*] (note $d\bar{r} = dx_1 dx_3$)

$$V(\bar{k}_s) = \frac{1}{(2\pi)^2} \int_A V(\bar{r},t)\, e^{-i(\bar{k}_s \cdot \bar{r} - \omega t)} d\bar{r} \tag{D12}$$

The corresponding total sound pressure obtained from the super-position of all traveling waves of the form represented by Equation (D10) is

$$p^{rad}(\bar{r},x_3,t) = \rho_o c_o \int_{-\infty}^{\infty} \frac{V(\bar{k}_s)}{\sqrt{1 - \dfrac{k_s^2}{k_o^2}}}\, e^{i\left(\bar{k}_s \cdot \bar{r} + \sqrt{k_o^2 - k_3^2}\, x_3 - \omega t\right)} d\bar{k}_s \tag{D13}$$

We are interested in the pressure on the surface of the plane. Hence setting $x_3 = 0$

$$p^{rad}(\bar{r},x_3=0,t) = \rho_o c_o \int_{-\infty}^{\infty} \frac{V(\bar{k}_s)}{\sqrt{1 - \dfrac{k_s^2}{k_o^2}}}\, e^{i(\bar{k}_s \cdot \bar{r} - \omega t)} d\bar{k}_s \tag{D14}$$

---

[*]No contribution to $V(\bar{k}_s)$ is rendered by the integral for the region external to the plate area.

Now substituting Equations (D1) in Equation (D12), we get

$$V(\bar{k}_s) = \frac{1}{(2\pi)^2} \int_{-\infty}^{\infty} V_m \bar{Y}_m(\bar{r}) e^{-i\bar{k}_s \cdot \bar{r}} \, d\bar{r} \tag{D15}$$

$$= \frac{V_m}{(2\pi)^2} \int_{-\infty}^{\infty} Y_m(\bar{r}) e^{-i\bar{k}_s \cdot \bar{r}} \, d\bar{r} \tag{D16}$$

We now prove that the integral is related to a quantity $[\Gamma_m*(\bar{k}_s)]/2$ where $\Gamma_m(\bar{k}_s)$ is called the modal coupling parameter or directivity. The functional forms and average values of $|\Gamma_m(\bar{k}_s)|^2$ described in some detail in Reference 8 are useful in making approximate computations.

PROOF

The pressure radiated into the half-space $x_3 > 0$ from an array of sources on an infinite rigid plane is[9] (see Figure 7)

$$p(R) = \frac{i\omega\rho_o}{2\pi} \sum_j \frac{Q_j}{R_j} e^{-ik_o R_j} \tag{D17}$$

Projecting R_j on R, we obtain $R_j \approx R - \bar{r}_o \cdot \bar{r}_j$ where $\bar{r}_o \cdot \bar{r}_j$, the projected distance difference, is a dot product (see Figure 8). Since $1/R_j =$

$$\frac{1}{R\left(1 - \dfrac{\bar{r}_o \cdot \bar{r}_j}{R}\right)} = \frac{1}{R}\left(1 + \frac{\bar{r}_o \cdot \bar{r}_j}{R} + \cdots\right) \approx 1/R \text{ then}$$

$$p(R,\bar{r}_o) = \frac{i\omega\rho_o}{2\pi R} e^{-ik_o R} \sum_j Q_j e^{i\bar{k}_o \cdot \bar{r}_j} \tag{D18}$$

where $\bar{k}_o = k_o \bar{r}_o$ is a wave vector = (wave number k_o) · (wave direction $\bar{r}_o$). If $\bar{k}_s \equiv$ projection of $\bar{k}_o$ on the plane and $\bar{k}_n \equiv$ projection of $\bar{k}_o$ on the normal to the plane, i.e., k_n lies along x_3, then $\bar{k}_o \cdot \bar{r}_j = \bar{k}_n \cdot \bar{r}_j + \bar{k}_s \cdot \bar{r}_j = \bar{k}_s \cdot \bar{r}_j$ since $\bar{k}_n \cdot \bar{r}_j = 0$ (see Figure 6). Hence Equation (D18) becomes

$$p(R,\bar{r}_o) = \frac{i\omega\rho_o}{2\pi R} e^{-ik_o R} \sum_j Q_j e^{i\bar{k}_s \cdot \bar{r}_j} \tag{D19}$$

89
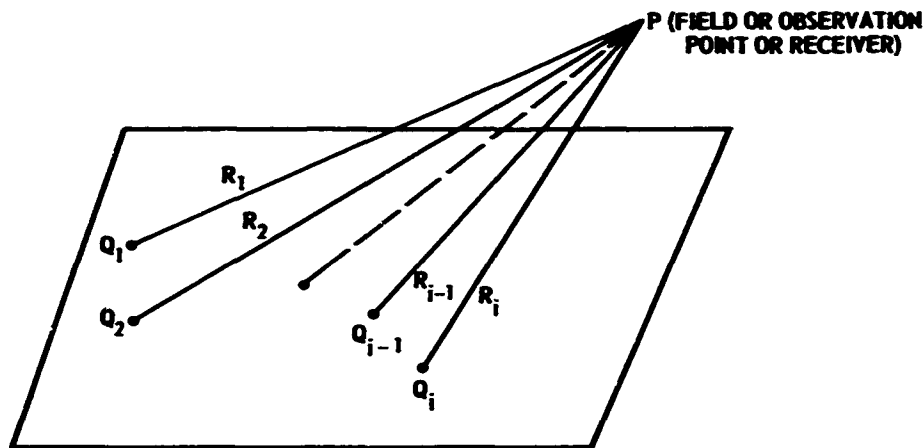
Figure 7 - Array of Point Sources in an Infinite Rigid Plane
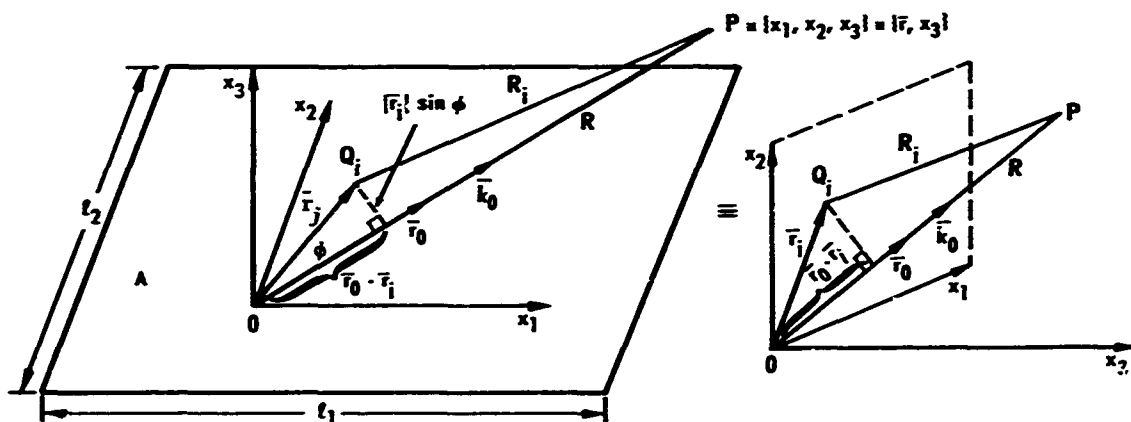
Figure 8 - Coordinate System Showing Vector Relationships

Notes:

1. x_1, x_2, $\bar{r}_j$ lie in plane of plate; x_3 is normal to plane,

   $\bar{r}_o$ and $\bar{k}_o$ are unit and acoustic spacevectors, respectively,

   $\bar{r}_o$, $\bar{k}_o$ and the distances (not vectors) R and R_j from the origin and source to the fluid point, respectively, are at arbitrary angles to the plane depending upon the position of the field point in space.

2. $R_j = R (1 - \bar{r}_o \cdot \bar{r}_j/R + \cdots\cdots)$

   $\approx R - \bar{r}_o \cdot \bar{r}_j$ for R, $R_j \gg |\bar{r}_j|$ or for $|\bar{r}_j|$ sin ϕ small,

   i.e., applicable to plate area A; which encloses all sources, for

   which $\sqrt{\ell_1^2 + \ell_2^2} \ll R, R_j$.

90

We now proceed to the calculation of the radiation from a plane surface with a continuous velocity distribution. Consider each *surface* element $d\bar{r}$ with a velocity $V(\bar{r})$ as a point source of sound with sound flux or differential source strength or differential volume velocity $dQ(\bar{r})$ equal to the differential area $(d\bar{r})$ times the velocity $V(\bar{r})$. Hence replacing the summation by the integration, we have

$$P(R,\bar{r}_o) = \frac{i\omega \rho_o}{2\pi R} e^{-ik_o R} \int_A V(\bar{r})\, e^{i(\bar{k}_s \cdot \bar{r})} d\bar{r} \tag{D20}$$

$$= -\frac{i\omega \rho_o V_o}{4\pi R} e^{-ik_o R} \left\{ \int_A (-2)\, \frac{V(\bar{r})}{V_o}\, e^{i(\bar{k}_s \cdot \bar{r})} d\bar{r} \right\} \tag{D21}$$

where the quantity in brackets is called the directivity or coupling parameter $\Gamma(\bar{k}_s)$. Thus

$$\Gamma(\bar{k}_s) = -2 \int_A \frac{V(\bar{r})}{V_o}\, e^{i(\bar{k}_s \cdot \bar{r})} d\bar{r} \tag{D22}$$

In Equations (D21) and (D22), $V_o^2 = <|V(\bar{r})|^2>_{\bar{r}} = <|V_m|^2 \Psi_m^2>_{\bar{r}} = |V_m|^2 < \Psi_m^2>_{\bar{r}} = |V_m|^2$ because[8] $<\Psi_m^2>_{\bar{r}} = \frac{1}{A} \int_A |\Psi_m^2(\bar{r})|d\bar{r} = 1$. Hence substituting Equation (D1) in Equation (D22) with $V_o = |V_m|$

$$\frac{\Gamma_m(\bar{k}_s)}{2} = \frac{-V_m}{|V_m|} \int_A \Psi_m(\bar{r})\, e^{i(\bar{k}_s \cdot \bar{r})} d\bar{r} \tag{D23}$$

$$\frac{\Gamma_m^*(\bar{k}_s)}{2} = \frac{-V_m^*}{|V_m|} \int_A \Psi_m(\bar{r})\, e^{-i(\bar{k}_s \cdot \bar{r})} d\bar{r} \tag{D24}$$

Equation (D24) represents the completion of our proof.

Substituting Equation (D24) in Equation (D16), we get

91

$$V(\bar{k}_s) = - \frac{V_m |V_m|}{(2\pi)^2 V_m{}^*} \frac{\Gamma_m{}^*(\bar{k}_s)}{2} \tag{D25}$$

Now substituting Equation (D25) in Equation (D14), we get

$$p_m^{rad}(\bar{r},t) = \frac{-\rho_o c}{8\pi^2} \frac{V_m |V_m|}{V_m{}^*} \int_{-\infty}^{\infty} \frac{\Gamma_m{}^* e^{i(\bar{k}_s \cdot \bar{r} - \omega t)}}{\sqrt{1 - \frac{k^2}{k_o{}^2}}} d\bar{k}_s \tag{D26}$$

The radiation force for the mth mode is[8] $\left(\text{noting that } p_m^{rad} = p_m^{rad} e^{-i\omega t} \right)$

$$f_m^{rad} = F_m^{rad} e^{-i\omega t} = \left[-\int_A p_m^{rad} \Psi_m(\bar{r}) d\bar{r} \right] e^{-i\omega t} = - \int p_m^{rad} \psi_m(\bar{r}) d\bar{r} \tag{D27}$$

Substituting Equation (D26) in Equation (D27),

$$F_m^{rad} = \frac{\rho_o c V_m |V_m|}{8\pi^2 V_m{}^*} \int_{-\infty}^{\infty} \frac{\Gamma_m{}^* d\bar{k}_s}{\sqrt{1 - \frac{k_s{}^2}{k_o{}^2}}} \int_A \Psi_m(\bar{r}) e^{i\bar{k}_s \cdot \bar{r}} d\bar{r} \tag{D28}$$

Using Equation (D23)

$$F_m^{rad} = \frac{1}{8\pi^2} \left(\frac{\rho_o c V_m |V_m|}{V_m{}^*} \right) \left(- \frac{|V_m|}{2V_m} \right) \int_{\infty}^{\infty} \frac{\Gamma_m{}^* \Gamma_m}{\sqrt{1 - \frac{k_s{}^2}{k_o{}^2}}} d\bar{k}_s \tag{D29}$$

and since $V_m{}^* V_m = |V_m{}^2|$, $\Gamma_m{}^* \Gamma_m = |\Gamma_m{}^2|$, then we find as a *basic working expression*

$$Z_m^{rad} = \frac{F_m^{rad}}{V_m} = \frac{\rho_o c}{16\pi^2} \int_{-\infty}^{\infty} \frac{|\Gamma_m|^2}{\sqrt{1 - \frac{k_s{}^2}{k_o{}^2}}} d\bar{k}_s \tag{D30}$$

92

We write this equation as the sum of real and imaginary terms:

$$Z_m^{rad} = \frac{\rho_o c}{16\pi^2} \int_{-k_o}^{k_o} \frac{|\Gamma_m|^2 d\bar{k}_s}{\sqrt{1 - \frac{k_s^2}{k_o^2}}} + \frac{i\rho_o c}{16\pi^2} \left[\int_{-\infty}^{-k_o} \frac{|\Gamma_m|^2 d\bar{k}_s}{\sqrt{\frac{k_s^2}{k_o^2} - 1}} + \int_{k_o}^{\infty} \frac{|\Gamma_m|^2 d\bar{k}_s}{\sqrt{\frac{k_s^2}{k_o^2} - 1}} \right] \quad \text{(D31)}$$

The first term in the right member represents the radiation damping whereas the second and third terms represent the fluid loading or added mass terms $= i\omega M_{loading}$. *We will consider the fluid loading problem only.* (Note that each integral in Equation (D31) represents a double integral since $d\bar{k}_s = dk_1 dk_2$.) Since the integrands are even functions, the terms within the brackets may be combined so that the fluid loading term may be written:

$$M_{loading} = \frac{\rho_o c}{4\pi^2 \omega} \int_{k_o}^{\infty} \frac{|\Gamma_m(\bar{k}_s)|^2}{\sqrt{\frac{k_s^2}{k_o^2} - 1}} d\bar{k}_s \quad \text{(D32)}$$

$$= \frac{1}{4\pi^2} \frac{\rho_o}{k_o} \int_{k_o}^{\infty} \frac{|\Gamma_m|^2}{\sqrt{\frac{k_s^2}{k_o^2} - 1}} d\bar{k}_s \quad \text{(D33)}$$

The product of the left and right members, respectively, of Equations (D23) and (D24) yields

$$|\Gamma_m|^2 = 4 \int_A \Psi_m(\bar{r}) e^{i\bar{k}_s \cdot \bar{r}} d\bar{r} \int_A \Psi_m(\bar{r}) e^{-i\bar{k}_s \cdot r} d\bar{r} \quad \text{(D34)}$$

93

The modal shape functions for the normal modes of a simply supported panel are:[*]

$$\Psi_m(\bar{r}) = 2 \sin \frac{m\pi x_1}{\ell_1} \sin \frac{n\pi x_2}{\ell_2} = 2 \sin k_m x_1 \sin k_n x_2 \qquad (D35)$$

Hence

$$|\Gamma_m|^2 = 16 \int_0^{\ell_1} e^{ik_{x_1} x_1} \sin k_m x_1 dx_1 \quad \int_0^{\ell_2} e^{ik_{x_2} x_2} \sin k_n x_2 dx_2 \cdot$$

$$\int_0^{\ell_1} e^{-ik_{x_1} x_1} \sin k_m x_1 dx_1 \quad \int_0^{\ell_2} e^{-ik_{x_2} x_2} \sin k_n x_2 dx_2 \qquad (D36)$$

Defining $I_1 = \frac{1}{\ell_1} \int_0^{\ell_1} e^{ik_{x_1} x_1} \sin k_m x_1 dx_1$, $I_2 = \frac{1}{\ell_2} \int_0^{\ell_2} e^{ik_{x_2} x_2} \sin k_n x_2 dx_2$

then

$$|\Gamma_m|^2 = 16A^2 \, I_1 I_2 I_1^* I_2^* = 16A^2 |I_1|^2 |I_2|^2 \qquad (D37)$$

Substituting Equation (D37) in Equation (D33), we obtain

$$M_{loading} = \frac{4\rho_o A^2}{\pi^2} \int_{k_o}^{\infty} \cdot \frac{|I_1|^2 |I_2|^2}{\sqrt{k_s^2 - k_o^2}} \, d\bar{k}_s \qquad (D38)$$

where $d\bar{k}_s = dk_1 dk_2$, $k_s^2 = k_1^2 + k_2^2$.

---

[*]Later in this Appendix it is shown that this normal mode representation includes the representation used in Appendix A as a special case; see Equation (A1).

94

We consider $k_s \gg k_o$ and for this region the quantity $1 / \sqrt{k_s^2 - k_o^2}$ $= K(k_s)$ is a smooth well-behaved function. We can then use the analytical approximation (presented in Appendix II of Reference 8) for the weighted integral given in Equation (D38).[*] For the range of k_s including k_m and k_n (see Equation AII.10 of Reference 8),[*] the added mass per unit area for radiation into the half space $x_3 > 0$ is (see Figures 9 and 10):

$$m_{mn} = \frac{M_{loading}}{A} = \frac{4\rho_o A}{\pi^2}\left[\frac{\pi}{2\ell_1} \cdot \frac{\pi}{2\ell_2} \cdot \frac{1}{\sqrt{k_{mn}^2 - k_o^2}}\right] \qquad (D39)$$

or

$$m_{mn} = \frac{\rho_o}{\sqrt{k_{mn}^2 - k_o^2}} \approx \frac{\rho_o}{k_{mn}} \text{ if } k_{mn} \gg k_o \qquad (D40)$$

The results given by Equation (D40) are in agreement with results presented by Equations (A27a), (B47), and (C28).

Finally, it is shown that the normal mode representation for a simply supported plate, Equation (D35), is more general than the corresponding representation used by Feit-Junger, Equation (A1). To see that Equation (D35) includes Equation (A1) as a special case, consider the sin $k_m x$ factor in Equation (D35); similar results are obtainable for the sin $k_n y$ factor (let $k_m \rightarrow k_n$, $x \rightarrow y$). We translate the origin of the abscissas from 0 to 0' (the midpoint along the plate length) as shown in Figure 11, by use of the equation:

$$x' = x - \frac{\ell}{2} \qquad (D41)$$

---

[*] $k_1 > k_m$

$$\int_{-k_m < k_1 < k_m} K(k_m)|I|^2 dk_1 \approx \frac{\pi}{2\ell_1} K(k_m) \text{ and similarly for the integral for}$$

k_2.

95
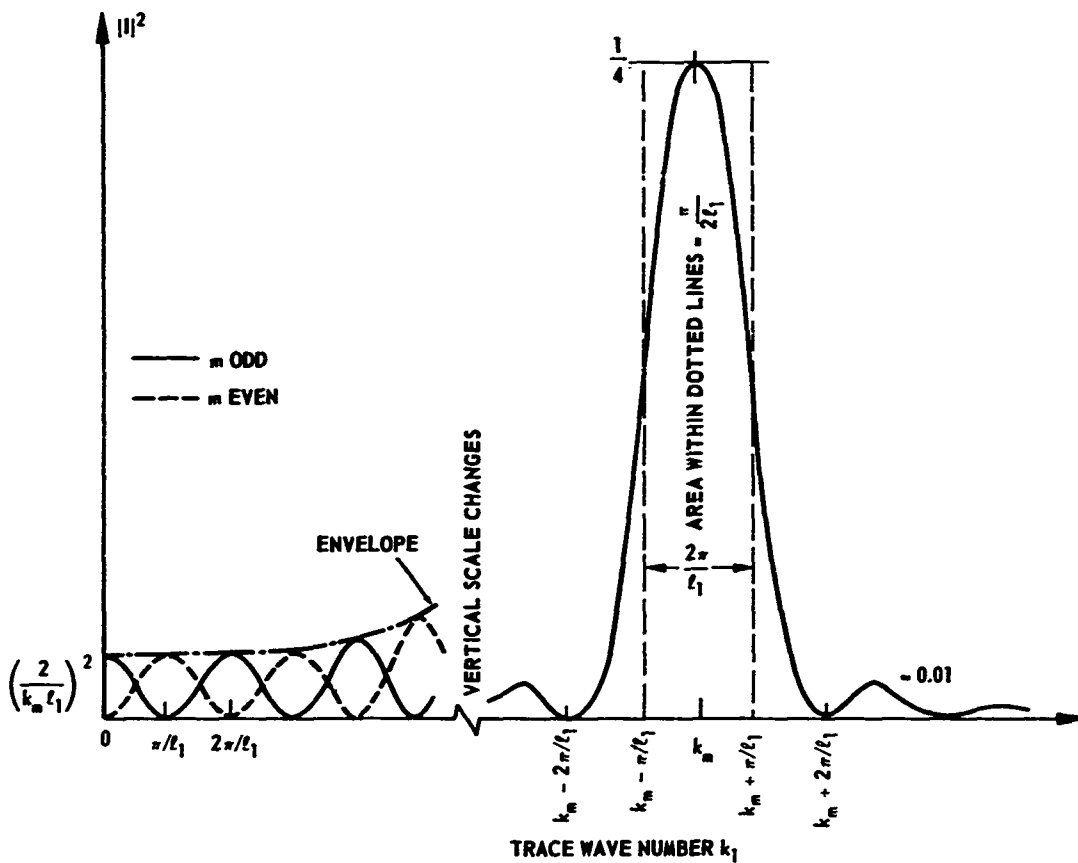
Figure 9 - Sketch of $|I|^2$ for Large Mode Numbers m (Applicable to small mode numbers if lower limit of integration of Equation AII-10 of Reference 8 is set to zero. See Figure 10 and page 216 of Reference 8).

96
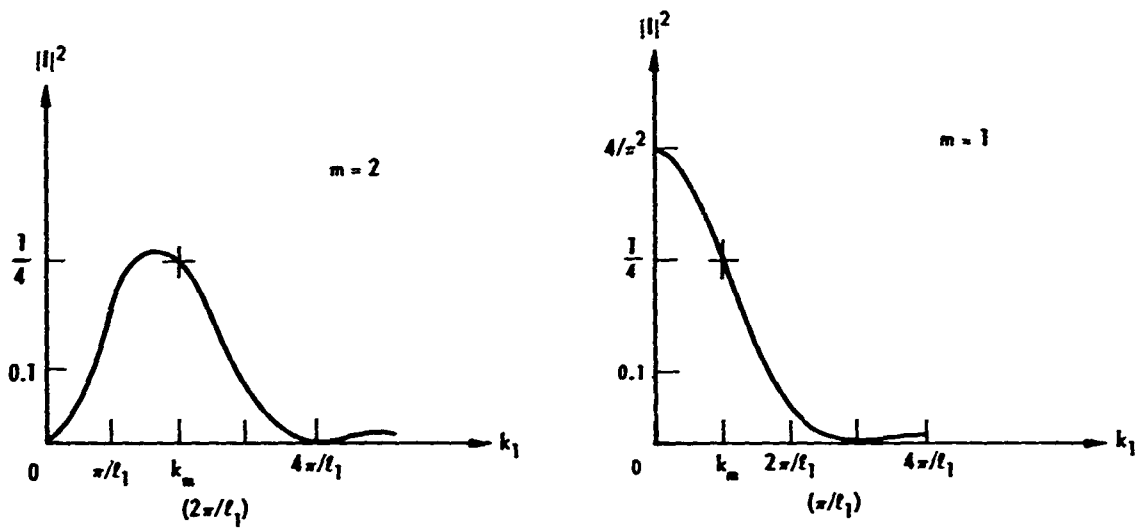
Figure 10 - Sketches of $|I|^2$ for m = 1, 2
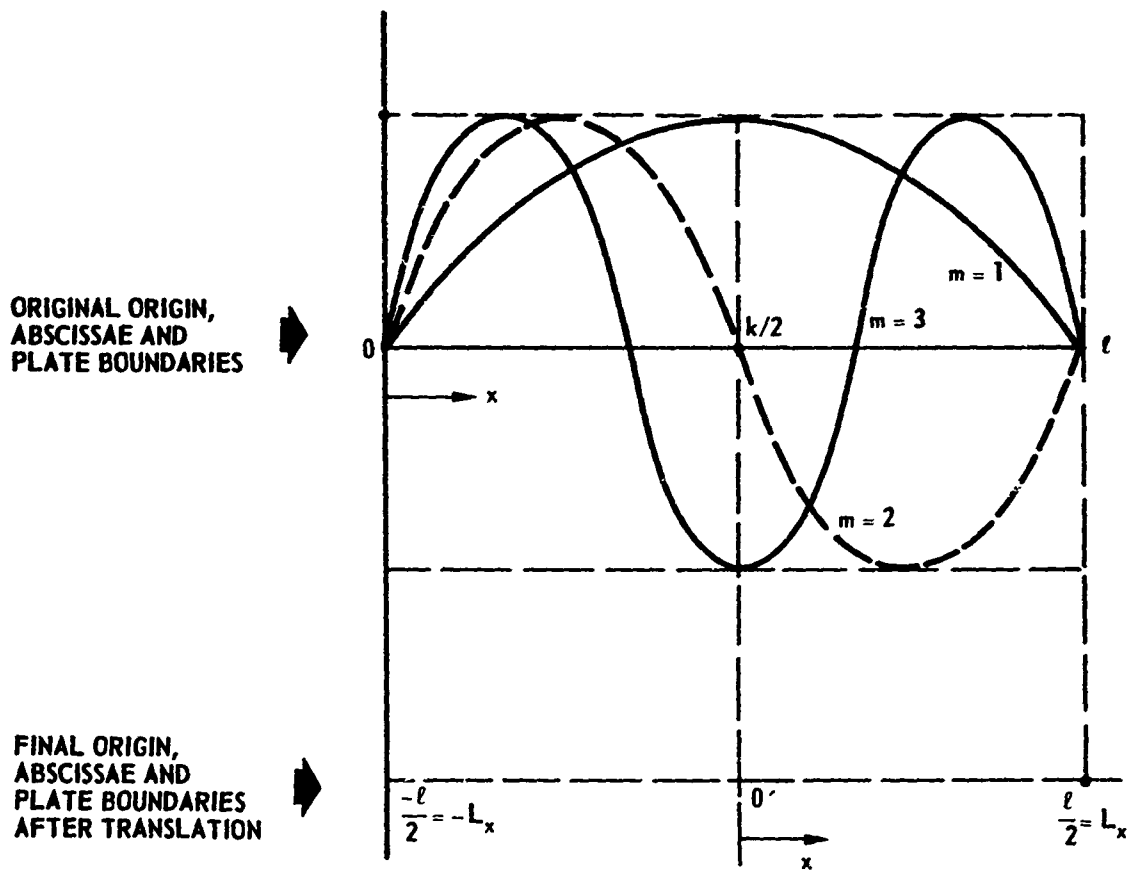
Figure 11 - Axial Systems for Normal Mode Representation

97

The new boundaries are:

$$x=0, \quad x' = -\frac{\ell}{2} = -L_x$$

$$x=\ell, \quad x' = +\frac{\ell}{2} = +L_x$$

where the notation $\mp L_x$ for the new plate boundaries has been introduced for compatibility with the Feit-Junger notation. Thus:

$$\sin k_m x = \sin k_m \left(x' + \frac{\ell}{2}\right) = \sin k_m (x' + L_x) = \sin \frac{m\pi x'}{2L_x} \cos \frac{m\pi}{2} + \cos \frac{m\pi x'}{2L_x} \sin \frac{m\pi}{2} \quad \text{(D42)}$$

where $k_m = \frac{m\pi}{\ell} \to \frac{m\pi}{2L_x} \qquad m = 0,1,2,3\cdots$

It is clear from Figure 11 that $m = 1,2,3\cdots$ represents odd modes with respect to the origin at $x=0$. However $m = 1,3\cdots$ odd and $m = 2,4\cdots$ even represent even and odd modes, respectively, with respect to the origin at 0'. In accordance with the Feit-Junger postulation, Equation (A1), we wish to retain the even modes only, i.e., $m = 1,3\cdots$ odd.

Equation (D42) shows that for the even modes, $m = 1,3\cdots$ odd, the first term in the right member is zero so that as a *special case*

$$\sin k_m x \to \cos \frac{m\pi x'}{2L_x} \sin \frac{m\pi}{2} \qquad m \text{ odd} \tag{D43}$$

$$\to \cos \frac{(2m'+1)\pi x'}{2L_x} (-1)^{m'} = (-1)^{m'} \cos k'_m x' \qquad m' = 0,1,2\cdots \tag{D44}$$

where $m = 2m' + 1$, an odd number and $k'_m = \frac{(2m'+1)\pi}{2L_x}$.

Thus Equation (D44), which contains even modes only in the axial system with origin 0', represents only half of the modes of $\sin k_m x$ in the axial system with origin 0. Moreover in the axial system with origin 0', if we take the mirror image of (i.e., reflect) the even modes $m=3, 7$, 11, etc. about the x' axis, then all even modes will have a positive value at $x' = 0$. Mathematically this is accomplished by letting $(-1)^{m'} \to 1$. Thus for even modes with respect to the origin 0' and positive values of $\sin k_m x$ at 0', $\sin k_m x \to \cos \frac{(2m'+1)\pi x'}{2L_x} = \cos k'_m x'$ which is identical to the corresponding factor in Equation (A1).

APPENDIX E

BOLT, BERANEK AND NEWMAN METHOD

NOTATION

A	Area of plate
c_L	Longitudinal wave speed
h	Plate thickness
k_f	Wave number in fluid, i.e., acoustic wave number
k_p, k_h	Plate wave number; $k_p^2 = (m\pi/\ell_1)^2 + (n\pi/\ell_2)^2 = k_h^2$
ℓ_1, ℓ_2	Length and width of plate, respectively
M_{added}	Added mass
M_{mn}	Total mass equal to $M_o + M_{added}$
M_o	Structural mass
m, n	Mode numbers for ℓ_1- and ℓ_2-directions, respectively
κ	Radius of gyration
ρ_f	Mass density of fluid
ρ_p, ρ_s	Mass density of plate
ω_{mn}	Resonance frequency for mn mode of vibration of plate *in vacu*.
$\bar{\omega}_{mn}$	Resonance frequency for mn mode of vibration of submerged plate

99

DERIVATION

Several researchers for Bolt Beranek and Newman have presented mathematical relationships for the added mass and submerged natural frequency of a vibrating finite rectangular plate radiating into half-space. The formulations are briefly considered.

Reference 10 gives the following relationship between the frequency and wavelength of a vibrating submerged structural panel[*]

$$\bar{\omega}_{mn}^2 \left(1 + \frac{\rho_f}{\rho_p k_p h}\right) = k_p^4 \kappa^2 c_\ell^2 \ ; \ k_p > k_f \tag{E1}$$

From Equation (iv.5.16) of Reference 8, $k_p^4 \kappa^2 c_\ell^2 = \omega_{mn}^2$, so that

$$\bar{\omega}_{mn} = \omega_{mn} \left[1 + \frac{\rho_f}{\rho_p k_p h}\right]^{-1/2} \ ; \ k_p > k_f \tag{E2}$$

Equation (E2) is identical in form to Equation (A34).

References 11 and 12 give the following relationships as precise for waves on a large flat submerged plate.

$$\bar{\omega}_{mn} = \omega \left(1 + \frac{\rho_f \, A/M_o}{k_h}\right)^{-1/2} = \omega \left(1 + \frac{\rho_f}{\frac{M_o}{Ah} k_h h}\right)^{-1/2} \tag{E3}$$

where $M_o = A\rho_s h$ and $M_{added} = \frac{A\rho_f}{k_h}$ so that $M_{mn} = A\rho_s h \left(1 + \frac{\rho_f}{\rho_s k_h h}\right)$

Hence

$$\bar{\omega}_{mn} = \omega \left[1 + \frac{\rho_f}{\rho_s k_h h}\right]^{-1/2} \ ; \ k_h > k_f \tag{E4}$$

Equation (E4) is identical in form to Equation (A34).

---

[*] In Equation (11) of Reference 10, let $\omega \to \omega_{mn}$ and in Equation (iv.5.16) of Reference 8, let $\omega_m \to \omega_{mn}$.

APPENDIX F

GREENSPON METHOD

NOTATION

A_{ij}, B_{ij}	Quantities which depend on the beam functions used to represent the mode shapes (see Table 4)
A_γ, A_δ	γ^{th} and δ^{th} elemental area of plate
a	Width of plate (shorter side)
b	Length of plate (longer side)
c_o	Sound velocity in water
F_{11}	Natural frequency in vacuo
$f(\frac{a}{b})$	Function of the aspect ratio
h	Thickness of plate
i, j	Mode numbers equal to m,n
i'	Equal to 1 if plate has water on one side and equal to 2 if plate has water on both sides
k	Wave number equal to ω_m/c_o
M_a	Apparent mass per unit area
m_p	Mass per unit area of plate
m, n	Mode numbers
$\bar{P}_m$	Water pressure due to vibrating plate in the mth mode of vibration
$\left[\bar{P}_m(x,y)\right]_{\gamma\delta}$	Average pressure on the γth elemental area A_γ due to modal vibration of the δth elemental area A_δ
t	Time
$[w(x,y,t)]_m$	Lateral deflection of plate in m^{th} mode
$[\dot{w}_\delta]_m$	Velocity in the mth mode of the δth elemental area
x, y	Rectangular coordinate axes
$[Z_{\gamma\delta}]_m$	Mutual radiation impedance between the γth and δ^{th} elemental areas on the plate for the mth mode of vibration
$[\theta_{\gamma\delta}]_m$	Resistive (radiation damping) component of impedance for the mth mode of vibration

101

λ	Wavelength
ρ_o	Mass density of water
ρ_t	Density (mass per unit volume) of plate
χ	Coefficient (reactance) depending on aspect ratio a/b
$[\chi_{\gamma\delta}]_m$	Reactive (added mass) component of impedance for the mth mode of vibration
$[\chi]_p$	Reactive (added mass) component of impedance of a rectangular piston
ω_{mn}	Circular frequency for the mn^{th} mode of vibration

Note: In Equations (F5), (F6), (F7), and (F8) the subscript $m \rightarrow mn$ for consistency with notation in the previous appendixes.

DERIVATION

References 13 and 14 present the following methods to account for the added mass of a rectangular plate vibrating in water.

Method 1 (see Reference 13)

Reference 13 quotes Reference 15 as the source of the following equation for the natural frequency of the first mode of a *simply supported* rectangular plate vibrating in water.[*]

$$(F_{11})_{water} = \frac{(F_{11})_{vacuum}}{\sqrt{1+i'\chi\,(\frac{a}{b})\frac{b}{7.85h}}} \qquad (F1)$$

The function $\chi(a/b)$ shown in Figure 12 has been derived in Reference 16 for a plate which is *clamped* on the edges $y = o, b$ and *simply supported* on the edges $x = 0, a$. This equation can be used to obtain the order of magnitude of the correction due to the added mass for both *simply supported* and *clamped plates*. However the reader is referred to Reference 15 for a more accurate analysis of added mass.

Method 2 (see References 13 and 14)

References 13 and 14 present the following analysis for the determination of the added mass per unit area.

Divide the plate into equal elemental areas and let $[\bar{P}_m(x,y)]_{\gamma\delta}$ be the average pressure on the γth elemental area A_γ due to modal vibration of the δth area A_δ (see Figure 13). Then

---

[*]Since $(F_{11})_{water} = \dfrac{(F_{11})_{vacuum}}{\sqrt{1+(M_a/M_p)}}$ (see Appendix A or Reference 15), then the present author deduces that the added mass per unit area $M_a = \left[i'\chi(\frac{a}{b})\,\frac{b}{7.85h}\right] m_p$ where m_p is the structural mass per unit area.
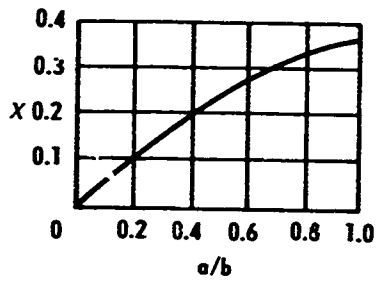
Figure 12 - Plot of Function
χ versus a/b
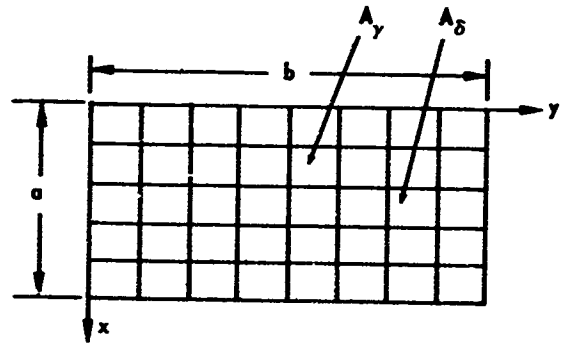
Figure 13 - Rectangular Plate Divided into
Finite Elements
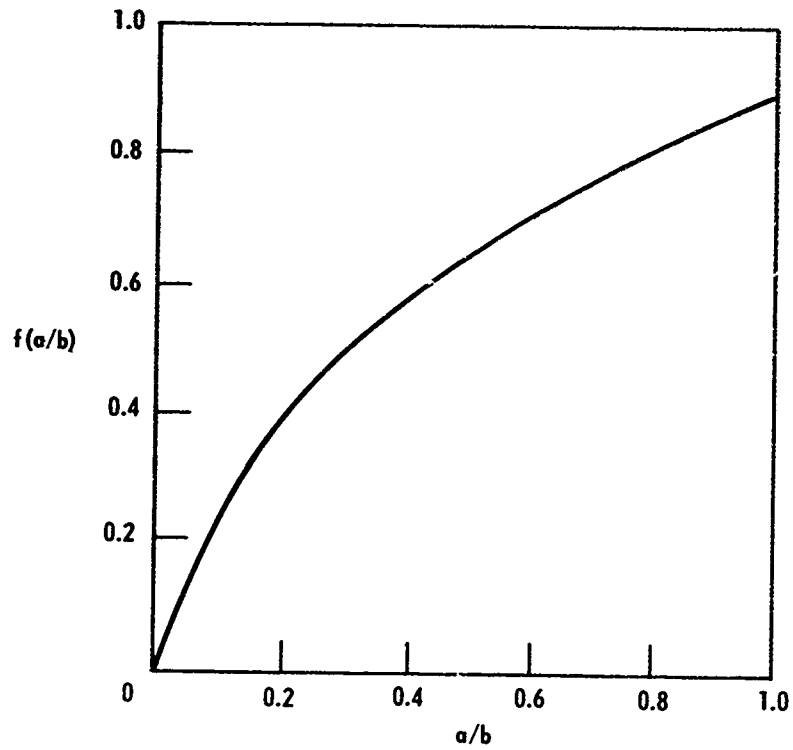
Figure 14 - Virtual Mass Function

104

$$[\bar{P}_m(x,y)]_{\gamma\delta} = \frac{(Z_{\gamma\delta})_m \, [\dot{w}(x,y,t)]_m}{A_\gamma} \qquad (F2)$$

The total pressure on the γth area due to the vibration of all other elements will be

$$\bar{P}_m = \sum_\delta \frac{(Z_{\gamma\delta})_m}{A_\gamma} \, [\dot{w}_\delta]_m \qquad (F3)$$

In these equations, the mutual radiation impedance $Z_{\gamma\delta}$ which is a function of the frequency and the distance between the elements may be written

$$(Z_{\gamma\delta})_m = \rho_o c_o A_{\gamma\delta} [(\theta_{\gamma\delta})_m + i(\chi_{\gamma\delta})_m] \qquad (F4)$$

The reactive or added mass component $(\chi_{\gamma\delta})_m$ is a function of the aspect ratio a/b and the nondimensional parameter $\pi b/\lambda = \omega_m b/2c_o$ (note ω_{mn} is denoted by P_m in References 13 and 14). The impedance of a rectangular piston is computed in Reference 17.[*] For relatively low frequencies $\pi b/\lambda < 1$, the reactance (added mass component) of the piston can be written (for consistency with previous results in Appendixes A-F exclusively, we let $\omega_m \rightarrow \omega_{mn}$):

$$\chi_p = f(\tfrac{a}{b}) \, \frac{\pi b}{\lambda} = f(\tfrac{a}{b}) \, \frac{\omega_{mn} b}{2c_o} \qquad (F5)$$

---

[*] In the analysis presented in References 13 and 14, leading to the computation of the plate natural frequencies, the sums involving $\theta_{\gamma\delta}$ and $\chi_{\gamma\delta}$ (Equation (F3)) are quite complex and require considerable computation. Therefore, it was assumed that the average pressure on the γth area can be computed by considering the entire plate to act as a rectangular piston with a deflection equal to the average of w_m over the plate (see Reference 13 for additional details). This simplified the mathematical analysis.

where $f(a/b)$ is a function of the aspect ratio and can be obtained directly from Figure 14. The circular natural frequency of the plate in water is then[13*]

$$(\omega_{mn})_{\text{water on one side}} = \frac{(\omega_{mn})_{\text{vacuum}}}{\sqrt{1 + \frac{\rho_o b}{2 m_p} f(\frac{a}{b}) \frac{A_{ij}^2}{B_{ij}}}} \; ; \; i,j=m,n \qquad (F6)$$

The A_{ij} and B_{ij} depend on the beam functions used to represent the mode shapes and therefore *depend on the boundary conditions* of the plate. The values of A_{ij} and B_{ij} for several modes of plates which are *clamped* or *simply supported* on all edges are shown in Table 2.

Plates with combinations of boundary conditions can also be solved so long as the mode shape can be approximated by a product of beam functions. For example, consider a uniform plate which is clamped at the longer edges $(0,b)$ and simply supported at the shorter edges $(0,a)$. (This is the case given in Reference 16.) Then for the first mode[13]

$$A_{ij}^2 = (0.8309 \times 0.6366)^2 = 0.2798$$

$$B_{ij} = 1 \times 0.5 = 0.5$$

$$(\omega_{mn})_{\text{water on one side}} = \frac{(\omega_{mn})_{\text{vac}}}{\sqrt{1 + \left[\frac{\rho_o b}{\rho_t h}\right] 0.2798 \, f(\frac{a}{b})}} \qquad (F7)$$

---

*In accordance with the previous footnote, we deduce that the added mass per unit area $M_a = \left[\frac{\rho_o b}{2 m_p} f(\frac{a}{b}) \frac{A_{ij}^2}{B_{ij}}\right] m_p$ for water on one side. For water on both sides, we double this value in Equations (F6) and (F7) and (F8). The symbol μ used in Reference 13 to denote the plate mass per unit area has been replaced here by the symbol m_p.

For a steel plate vibrating in water

$$(\omega_{mn})_{\substack{\text{water on} \\ \text{one side}}} = \frac{(\omega_{mn})_{vac}}{\sqrt{1 + \left[\frac{b}{7.85h}\right] 0.28 \ f(\frac{a}{b})}} \tag{F8}$$

Equation (F8) is of the same form as Equation (F1) originally found in Reference 16. For most of the practical cases, the correction of the frequency due to added mass given by Equations (D8) and (D1) will be of the same order of magnitude.

APPENDIX G

LEIBOWITZ METHOD III

NOTATION

The notation included for Appendix F also applies to this appendix.

DESCRIPTION

The approximate expression presented is convenient for the computation of the added mass and (low) natural frequencies of a vibrating rectangular plate. The development of this expression is based on the work of Reference 14 discussed in Appendix F.

DERIVATION

Ignoring plate damping and considering clamped or simply supported plates,[*] the natural frequency of a vibrating plate in water is given by Equation (F6). Following Reference 14, we take as a low frequency approximation

$$\chi_p = 0.48k[ab]^{1/2} = 0.48 \frac{\omega_{mn}}{c_o} [ab]^{1/2} \text{ for } \frac{\omega_{mn} \sqrt{\frac{ab}{\pi}}}{c_o} < 1 \qquad (G1)$$

Substituting Equation (G1) in Equation (F5), we get

$$f(\frac{a}{b}) = 0.96 (\frac{a}{b})^{1/2} \qquad (G2)$$

which is an approximate fit to Figure 14.

---

[*] Reference 14 also permits a solution of the frequencies for the more general case of a rotationally constrained beam including plate radiation and structural damping in the frequency equation.

Substituting Equation (G2) in Equation (F6), we get[*]

$$(\omega_{mn})_{\substack{\text{water on} \\ \text{one side}}} = \frac{(\omega_{mn})_{\text{vacuum}}}{\sqrt{1 + \frac{0.48 \, \rho_o (ab)^{1/2}}{m_p} \frac{A_{ij}^2}{B_{ij}}}} \quad ; \quad i,j = m,n \qquad (G3)$$

where A_{ij} and B_{ij} are values given in Table 4 for clamped and simply supported plates.

---

[*]The added mass per unit area $M_a = \dfrac{0.48 \, \rho_o (ab)^{1/2}}{m_p} \dfrac{A_{ij}^2}{B_{ij}} m_p$ for water on one side. For water on both sides, this quantity is doubled in Equation (G3).

110

PROCEDURE FOR MODIFYING THE MAESTRELLO PROGRAM TO INCLUDE EFFECTS OF FLUID LOADING (OPTION 3)

NOTATION

A_i	Constants
A_{ij}, B_{ij}	Quantities which depend on the beam functions used to represent the mode shapes (see Table 4)
a, b	Dimensions of plate (see footnote to ω_{mn} of aluminum plate in this Appendix for more precise description)
a_{mn}, $\bar{a}_{mn}$	Plate modal damping in air and water, respectively
c	Speed of sound in fluid
c_ℓ	Compressional wave velocity of the plate equal to $$\left[\frac{E}{\rho_s(1-\nu^2)}\right]^{1/2}$$
D, D_d	Specific damping energy at any stress σ and at peak stress σ_d respectively in a part under nonuniform stress $(0 < D < D_d)$
E	Young's modulus
e	Equal to 2.718; base for natural or Naperian system of logarithms
F	Equals $\frac{\delta^*}{U} \equiv \frac{\delta^*}{U_\infty}$
f	Frequency
f_{mn}	Plate natural frequency
$f(\frac{a}{b})$	Function of aspect ratio
h	Panel thickness
i,j	Mode numbers
K_i	Constants
k	Acoustic wave number equal to ω/c
k_s	Surface wave number equal to $[(m\pi/a)^2 + (n\pi/b)^2]$ for Method I; for Method II, a and b may or may not be interchanged (see footnote to ω_{mn} of aluminum plate in this Appendix)

111

M, m_p	Plate mass per unit area in air
M'	Total mass per unit area of plate in water; equal to sum of plate and added masses per unit area
M_a, m_{mn}	Added mass (or apparent mass or virtual mass) per unit area
m, n	Mode numbers
W_p, W_{mn}	Plate weight per unit area in air and added weight per unit area, respectively
W'	Total weight per unit area of plate in water; equal to sum of plate and added weight per unit area
$P(\omega)$	Power spectrum
$\overline{p^2}$	Mean square turbulence pressure
q	Equal to k/k_s (see footnote to q of aluminum plate in this Appendix)
U, U_∞	Free-stream velocity
U_c	Convection velocity
(x,y), (x',y')	Points on the panel at which displacements are measured
α	Equal to 1 for fluid loading on one side of plate only; equal to 2 for fluid loading on both sides of plate; dimensionless damping energy integral (see section on steel plate parameters in this Appendix)
β	Total damping coefficient of plate in a fluid; dimensionless strain energy integral (see section on steel plate parameters in this Appendix)
β_c	Critical damping
δ^*	Boundary layer displacement thickness
δ_{mn}, $\bar{\delta}_{mn}$	Total damping ratio of plate in air and water, respectively
η	Material loss factor; equals $y - y'$, lateral partial separation
η_s	Loss factor of a specimen or part
θ	Eddy lifetime for steady convection, i.e., time in which value of correlation coefficient obtained from envelope of correlation maxima (maxima-maximorum) drops to $1/e$
ν	Kinematic viscosity of fluid near wall
ξ	Equals $x - x'$, longitudinal partial separation

112

κ	Radius of gyration
ρ, ρ_o	Mass density of fluid medium
ρ_s	Mass density of plate
σ, σ_D	Amplitude of reversed stress and maximum value of stress in a part $(0 < \sigma < \sigma_D)$
τ	Equals $t - t'$, time delay
τ_w	Local wall shear stress
$\phi_{mn}(x,y)$, $\phi_{mn}(x',y')$	Plate eigenfunctions
ω	Circular frequency equal to $2\pi f$
ω_{mn}, $\bar{\omega}_{mn}$	Plate modal frequency in air and water, respectively

The Maestrello program[1] for determining the turbulence-induced vi-
bration and radiation of plates is modified and then extended to include
the effects of fluid loading. The modified program is used to obtain the
vibratory response for a fluid-loaded simply supported rectangular
aluminum isotropic plate and for a fluid-loaded simply supported rectangular
steel isotropic plate. The effects of hydrophone size* and boundary layer
thickness are excluded for simplicity and other plate boundary conditions
on the response are not considered. However, the user can correct for
these effects and treat various plate boundaries as well as plate curvature
by including Option 1 (Reference 2) and Option 2 (Reference 3) in the com-
putations (see DISCUSSION AND EVALUATION). The methods for determining the
input data used in the computations are also described.

MATHEMATICAL ANALYSIS

The results of the analytical study for the fluid loading of
rectangular plates presented in Appendixes A-G are summarized in Table 1.
Of these results, only the *uncoupled (dominant) modes* (see DISCUSSION AND
EVALUATION) are considered here for the modification of the original
Maestrello program which excludes fluid loading. With this practical
restriction, Table 1 shows that there are then two basic methods for compu-
ting the virtual or added mass and the associated natural frequencies of a
fluid loaded plate. The equations corresponding to the methods designated
as Methods 1 and 2 below are now summarized and modified for purposes of
practical computation.

Method I: Based on Analyses in Appendixes A-E

$$m_{mn} \text{(added mass per unit area)} = \frac{\alpha\rho}{(k_s^2 - k^2)^{1/2}} = \frac{\alpha\rho}{k_s[1-(\frac{k}{k_s})^2]^{1/2}} - \frac{\alpha\rho}{k_s[1-q^2]^{1/2}} \quad (H1)$$

where $0 \leq \frac{k}{k_s} = q < 1$.

---

*That is, the excitation function which represents *measured* turbulence
data is not corrected for hydrophone size in the present computations.

114

Hence in the original Maestrello program when fluid loading is included,

$$M \rightarrow M' = m_p + m_{mn} = m_p \left[1 + \frac{\alpha\rho}{k_s m_p (1 - q^2)^{1/2}} \right] \qquad (H2)$$

also

$$\bar{\omega}_{mn} = \omega_{mn} \left[1 + \frac{\alpha\rho}{\rho_s (k_s^2 - k^2)^{1/2} h} \right]^{-1/2} = \omega_{mn} \left[1 + \frac{\alpha\rho}{\rho_s k_s h \left[1 - \left(\frac{k}{k_s}\right)^2 \right]^{1/2}} \right]^{-1/2} \qquad (H3)$$

$$= \omega_{mn} \left[1 + \frac{\alpha\rho}{\rho_s k_s h [1 - q^2]^{1/2}} \right]^{-1/2}$$

In summary, when fluid loading is included, the original Maestrello program[1] is modified in accordance with Method I by letting $M \rightarrow M'$ and $\omega_{mn} \rightarrow \bar{\omega}_{mn}$ where M' and $\bar{\omega}_{mn}$ are given by Equations (H2) and (H3), respectively.

Method 2: Based on Analyses in Appendixes F and G

$$M_a (\text{added mass per unit area}) = \left[\frac{\alpha\rho_o b}{2m_p} f \left(\frac{a}{b}\right) \frac{A_{ij}^2}{B_{ij}} \right] m_p \quad ; \quad i,j=m,n \qquad (H4)$$

Values for $f(a/b)$ are obtained from Figure 14. For practical computation a finite number of values of $f(a/b)$ versus a/b can be tabulated and stored in the computer.[*] The numbers of such values should be sufficient to allow the computer to calculate required intermediate values with an acceptable accuracy by means of linear interpolation of the stored values. For the

---

[*]In this method of computation, b always represents the longest side of the plate. Thus b may lie along either x or y and in the direction of or orthogonal to the flow.

115

lower modes, A_{ij}, B_{ij} are obtained from Table 4. For the higher modes, A_{ij}, B_{ij} are obtained from tables found in References 18 and 19.

Hence in the original Maestrello program when fluid loading is included,

$$M \rightarrow M' = m_p + M_a = m_p \left[1 + \frac{\alpha \rho_o b}{2 m_p} f(\frac{a}{b}) \frac{A_{ij}^2}{B_{ij}} \right] \tag{H5}$$

and

$$\bar{\omega}_{mn} = \frac{(\omega_{mn})_{vacuum}}{\sqrt{1 + \frac{\alpha \rho_o b}{2 m_p} f(\frac{a}{b}) \frac{A_{ij}^2}{B_{ij}}}} \tag{H6}$$

For the *low frequencies*, these equations are approximated by

$$M_a = \frac{0.48 \ \alpha \rho_o (ab)^{1/2} \ A_{ij}^2}{m_p} \frac{A_{ij}^2}{B_{ij}} m_p \ ; \ i,j=m,n \tag{H7}$$

$$M \rightarrow M' = m_p + M_a = m_p \left[1 + \frac{0.48 \ \alpha \rho_o (ab)^{1/2}}{m_p} \frac{A_{ij}^2}{B_{ij}} \right] \tag{H8}$$

$$\bar{\omega}_{mn} = \frac{(\omega_{mn})_{vacuum}}{\sqrt{1 + \frac{0.48 \ \alpha \rho_o (ab)^{1/2}}{m_p} \frac{A_{ij}^2}{B_{ij}}}} \tag{H9}$$

In summary, when fluid loading is included, the original Maestrello program[1] is modified in accordance with Method 2 by letting $M \rightarrow M'$ and $\omega_{mn} \rightarrow \bar{\omega}_{mn}$ where M' and $\bar{\omega}_{mn}$ are given respectively by Equations (H5) and (H6) in general and by Equations (H8) and (H9) for low frequencies.

116

METHOD FOR DETERMINING INPUT DATA

The methods for determining the input data required for computer calculations are now described. Generally the methods are similar to those given in Appendix B2 of Reference 1. Eitner the data are arbitrarily prescribed by the user, i.e., the values are chosen to represent the range of interest, or the selections may correspond to experimental or analytically determined values for a parameter. However, the form and types of basic (raw) data available for use in computing some of the input data as well as some of the features of the response computations for the aluminum and steel plates differ somewhat. In consequence, different methods are used to evaluate certain of the input data for these plates. The logical presentation is then to furnish for each plate a description of the particular methods used for determining the data. Tabulations of the actual computed input data used in response calculations are also given for each plate.

The following input data are furnished to the computer.

Flow data: U_c, τ_w, $\delta^* = FU \equiv FU_\infty$, ω, $\overline{p^2}$, θ, A_i, K_i where $i = 1,2,3$ and α, q

Panel data: a, b, h, δ_{mn}, $\tilde{\delta}_{mn}$, E, M, M', ϕ_{mn}, ω_{mn}, $\bar{\omega}_{mn}$, ξ, η, τ, m, n, x, y, x', y'

Aluminum Plate

The values for the input data are tabulated in Tables 2a and 2b. The methods used in determining these values are:

Parameter	Description
A_i, K_i	Prescribed constants used in Equation (B7) of Reference 1
a, b, h	Prescribed quantities
E	A prescribed quantity
$M \equiv m_p$	A prescribed quantity
M'	Using Method 1 only for the aluminum plate, M' is computed by means of Equation (H2)
m, n	Prescribed data
$\overline{p^2}$	Equals $\int_0^\infty P(\omega)\,d\omega$ where $P(\omega)$ is obtained from Equation (B7) of Reference 1. This quantity can also be

117

measured directly. For the present calculation it is convenient to set $\overline{p^2} = 1$ so that the autocorrelation function for the turbulence pressures and the cross correlation function for the panel displacements given by Equations (B8) and (B52) respectively of Reference 1 can be regarded as normalized to this value (We can also compute $\overline{p^2}$. Thus for subsonic speeds Jacobs[1] shows that $\overline{p^2} \approx 3.1 \ \tau_w$ and from Reference 20, for a smooth plate $\tau_w/q \approx 0.060 \ (R_x)^{-1/5} = 0.060 \ (U_\infty x/\nu)^{-1/5}$ where $q = 1/2 \ \rho \ U_\infty^2$ is the free stream dynamic pressure.)

U_c A parameter whose values are prescribed by the user, $U_c = 0.8 \ U_\infty$; for the present problem, $U_c = 8, 16, 32, 64$ ft/sec

x,y,x',y' Prescribed points; the cross correlation of the displacements are computed for these points

$\delta^*=(FU)\equiv(FU_\infty)$ Equals* $0.37x/8 \ (U_\infty x/\nu)^{-1/5}$ (see Equations 21.6 and 21.8 of Reference 20), Tables 1.1 and 2.1 of that reference give values of ν in air and water. Using this equation, values of δ^* for a given fluid can be prescribed over a Range of U_∞. For an isolated plate, the equation shows that for a given value of x, δ^*_{max} occurs for U_∞ equal to the minimum prescribed value, i.e., $U_\infty = (U_\infty)_{min}$, and for $\nu = \nu_{air}$. For all $U_\infty > (U_\infty)_{min}$ the corresponding values of $\delta^* < \delta^*_{max}$ for both $\nu = \nu_{air}$ and $\nu = \nu_{water}$. However, we can also treat the displacement thickness of a plate in a structure, acting as a baffle. The plate can then be moved sufficiently rearward of the edge of the structure at zero incidence so that for a given position along the plate and all $U_\infty > (U_\infty)_{min}$, $\delta^* = $ constant $\geq \delta^*_{max}$ for both ν_{air} and ν_{water}. In effect we are considering series of plates of identical geometry so located in a structure that for all $U_\infty > (U_\infty)_{min}$ the displacement thickness at a fixed position on one of the plates in the series is always equal to $\delta^* = $ constant

---

*Due to a typographic error, this equation was incorrectly written as $0.37/8 \ (U_\infty x/\nu)^{-1/5}$ in Appendix B2 of Reference 1.

118

for $\nu = \nu_{air}$ and $\nu = \nu_{water}$. To reduce the amount of computation for the *aluminum plate only* (i.e., to eliminate δ^* as a parameter) we select for any of the prescribed values of $U = U_c/0.8$ and for $\nu = \nu_{air}$ and $\nu = \nu_{water}$ the plate whose position is such as to yield a displacement thickness $\delta^* = 0.033 > \delta^*_{max}$. It is assumed that on a given plate δ^* is sensibly constant in the direction of flow along the plate length

δ_{mn} Total damping ratio in air including the damping in the plate as well as radiation damping. In the present problem the radiation damping in air is considered to be much smaller than the material damping.[*] According to Jacobs the damping used for the aluminum plate in air was *experimentally* determined from an analysis of bandwidths between half-power points on response resonances from segmented, unpublished, high-resolution deflection power spectral density measurements (see page 5 of Reference 21, pages 24-25 and 34 of Reference 22, and page 273 of Reference 1)

A plot of the measured results given in References 21 and 22 indicates that $\delta_{mn} = 15/f_{mn}$ approximately. Hence

$$a_{mn} = \delta_{mn}\,\omega_{mn}/2 = 15\pi$$

$\bar{\delta}_{mn}$ Total damping ratio of panel in water including the damping in the plate, the damping associated with fluid loading and the radiation damping. *However, in the present problem the contribution of the radiation damping to $\bar{\delta}_{mn}$ is excluded.*[**] From page 41 of Reference 1 we deduce that

$$a_{mn} = \frac{\beta}{2M} = \frac{\delta_{mn}\,\omega_{mn}}{2}\ \text{in air}$$

$$\bar{a}_{mn} = \frac{\beta}{2M'} = \frac{\bar{\delta}_{mn}\,\bar{\omega}_{mn}}{2}\ \text{in water}$$

---

[*] In any event the experimentally measured damping will include the contributions of all damping mechanisms influencing the measurement results. The mathematical representation of damping in the equations of plate motion include these results as a viscous damping term.

[**] We are interested here in the radiation damping of a mode in the range $k_p > k$. For heavy fluid loading the corner mode contribution to radiation damping is applicable at all frequencies whereas the edge mode contribution is significantly applicable at high frequencies.[7] Simple equations for determining these contributions are given in Reference 7 and will appear in a companion report.

119

The first equation represents the viscous damping of the plate in air and agrees with Equations (A7) and (B18) of Reference 1 if we ignore the hysterestic[*] and acoustic radiation terms respectively in these equations. The second equation which includes the contribution of both viscous damping and fluid loading (also called added or virtual mass or liquid coupling) agrees with Equation (A51) of Reference 1 if the hysteretic[*] and radiation damping term in this equation is excluded. It is of interest to note that when radiation damping is not considered the increased mass associated with fluid loading reduces the modal damping term in water (see Equation (A51) of Reference 1) so that $\bar{a}_{mn} < a_{mn}$. As shown in Tables 3a and 3b, $W_p = 0.6$ lb/ft^2 for the aluminum plate. From the ratio of the above equation we get

$$\bar{a}_{mn} = a_{mn}\frac{M}{M'} = a_{mn}\frac{W_p}{W'} = 15\pi\left(\frac{0.6}{0.6 + W_{mn}}\right)$$

and

$$\bar{\delta}_{mn} = \frac{2\bar{a}_{mn}}{\bar{\omega}_{mn}} = \frac{30\pi}{\bar{\omega}_{mn}}\left(\frac{0.6}{0.6 + W_{mn}}\right) = \frac{15}{\bar{f}_{mn}}\left(\frac{0.6}{0.6 + W_{mn}}\right)$$

θ Corresponds to the time in which the value of the measured correlation coefficient of the fluctuating pressures at the wall, obtained from the envelope of the correlation maxima, drops to $1/e$. Plots of θ versus Mach number for broad- and narrow-band frequencies are given by Maestrello in Reference 23, Figure 5. The Maestrello narrow band measurements of eddy lifetime for frequencies centered at 1200 Hz were extrapolated to zero

---

[*]The user interested in including a hysteretic damping term as a separate contribution to a_{mn} and $\bar{a}_{mn}$ can easily determine this term by use of Equations (A7) and (A8) and the relevant term in Equation (A51) of Reference 1, substituting M' for M and $\bar{\omega}_{mn}$ for ω_{mn} when fluid loading is considered; see also Equations (13) through (15) of Reference 13 for similar results in terms of both a_{mn} and δ_{mn}. However to simplify the present computations and in accordance with the Maestrello procedure discussed in Appendix B of Reference 1, explicit division of the damping into its hysteretic and viscous components is not made here.

120

Mach number at which $\theta = 2.25 \times 10^{-3}$ sec. For all U_c under consideration, (Mach number)$_{water}$ < (Mach number)$_{air}$ = $U_\infty/c_{air} \leq 64/(0.8)(1129) < 0.08$. Since the extrapolated curve shows that θ(Mach numbers < 0.08) $\approx$ θ(Mach number equal zero) then approximately

$\theta = 2.25 \times 10^{-3}$ sec for all U_c considered.

ξ, η, τ Prescribed data

τ_w Determination of this quantity is based on the law of the wall which is further discussed on page 62 of Reference 1. The Maestrello measurements presented in Figure 1 of Reference 23 indicate that $\sqrt{\overline{p^2}}/\tau_w$ = 2.9 to 3.5 for M = 0.35 to M = 0.75. In reasonable agreement Jacobs finds that the results of various investigators yield $\sqrt{\overline{p^2}}/\tau_w$ = 3.1 as an average value for all subsonic Mach numbers (see pages 301 and 302 of Reference 1). Using the latter for the present calculations we have $\tau_w = \sqrt{\overline{p^2}}/3.1 = 1/3.1 \approx$ 0.323 lb/ft^2; see also description of computation for $\overline{p^2}$.

$\phi_{mn}(x,y)$, $\phi_{mn}(x',y')$ Data required for the computer program are calculated by the digital computer for a range of prescribed values of m, n, x, y, x', y'.

ω Prescribed in Equation (B7) of Reference 1 to obtain $P(\omega)$

ω_{mn} For a plate of given geometry, boundary conditions, and structural properties, this quantity can be computed by the methods of Option 2 (Reference 3). In the present problem values for ω_{mn} were computed by use of the Warburton program[3] for a simply supported plate and substantiated by means of the simple frequency expression*

$$\omega_{mn} = \kappa c_\ell \left[\left(\frac{m\pi}{a}\right)^2 + \left(\frac{n\pi}{b}\right)^2\right]$$

---

*In Method I, a and b lie along x and y respectively and are therefore identified with m and n respectively. In Method II, b is always the longer side so that in general a and b may lie along either x and y or y and x respectively and are correspondingly identified with either m and n or n and m respectively. If, in particular, a and b are identified with n and m, then for Method II (only) the equation $\omega_{mn} = \kappa c_\ell \left[(m\pi/b)^2 + (n\pi/a)^2\right]$ should be used.

121

$\bar{\omega}_{mn}$ Using Method I only for the aluminum plate $\bar{\omega}_{mn}$ is computed by means of Equation (H3)

α Equal to 1 for fluid loading on one side of the plate only; equal to 2 for fluid loading on both sides of the plate

q Equal* to $\dfrac{k}{k_s} = \dfrac{\dfrac{\omega}{c}}{\sqrt{\left(\dfrac{m\pi}{a}\right)^2 + \left(\dfrac{n\pi}{b}\right)^2}}$ where $0 \leq \dfrac{k}{k_s} = q < 1$.

---

*See footnote on previous page.

Steel Plate

The values for the input data are tabulated in Tables 3a-3f. The methods used in determining these values are:

Parameter	Description
A_i, K_i	Prescribed constants used in Equation (B7) of Reference 1
a, b, h	Prescribed quantities
E	A prescribed quantity
$M \equiv m_p$	A prescribed quantity
M'	Using Method I, M' is computed by means of Equation (H2); Using Method II, M' is computed by means of Equations (H5) and/or (H8)
m, n	Prescribed data
$\overline{p^2}$	Equal to $\displaystyle\int_0^\infty P(\omega)d\omega$ where $P(\omega)$ is obtained from Equation (B7) of Reference 1. This quantity can also be measured directly. For the present calculation it is convenient to set $\overline{p^2} = 1$ so that the autocorrelation function for the turbulence pressures and the cross correlation function for the panel displacements given by Equations (B8) and (B52) respectively of Reference 1 can be regarded as normalized to this value (We can also compute $\overline{p^2}$. Thus for subsonic speeds Jacobs[1] shows that $\overline{p^2} \approx 3.1\ \tau_w$ and from Reference 23 for a smooth plate, $\tau_w/q \approx 0.06\ (R_x)^{-1/5} = 0.060\ (U_\infty x/\nu)^{-1/5}$ where $q = 1/2\ \rho\ U_\infty^2$ is the free-stream dynamic pressure.)
U_c	A parameter whose values are prescribed by the user; $U_c = 0.8\ U$. For the present problem $U_c = 8, 16, 32, 64$ ft/sec
x, y, x', y'	Prescribed points; the cross correlation of the displacements are computed for these points

$\delta^* = (FU) \equiv (FU_\infty)$

The displacement thickness is determined by use of a computer program available at the Center entitled XG 75, Fortran IV by R.W. Brown. The program uses a relation developed by Mangler, i.e., the Mangler integral transformation, which permits reduction of the calculation of axially symmetrical boundary layers on arbitrary bodies of revolution[*] to that in two-dimensional flow. The Mangler method relates the distance along the axis of a body of revolution to the distance along a flat plate at which the boundary layer thickness is identical. The boundary layer displacement thickness is then calculated using an expression which is a function of the flat plate distance and flat plate Reynolds number (using kinematic viscosity of air at 90 deg F and of water at 39 deg F), developed by Granville.[24] The derivation of the expression is based on similarity arguments. The undetermined coefficients in the expression are evaluated by use of experimental data. The required input data for the program are the axial distance (in feet) and the radius of the body (in feet) at that position as well as the free stream velocity (in knots). The limitations of the program are those due to the assumptions required for the Mangler transformation and to the fit of the available data which Granville used in his theory. The assumptions involved are considered to have a greater bearing than the data fit on the accuracy of computation. In particular, we observe that Mangler assumes a two-dimensional flow which does not explicitly account for the local pressure gradient. The saving feature, with regard to this omission, is the fact that the boundary layer growth is sufficiently slow so that the imprecision in the calculation is considered to be approximately 10 percent. Figure 15 gives the results of the computation for δ^* of the actual structure[*] in water and in air obtained by use of the Brown computer program.

δ_{mn}

Total damping ratio in air including the damping of the plate as well as radiation damping. In the present problem the radiation damping in air is considered to be much smaller than the material damping.[**]

---

[*] The actual structure under consideration is a cylinder which is part of a cigar-shaped body of revolution. Our computations are made above the ring frequency which allows the cylinder to be treated approximately as a plate. The supports at the cylinder or equivalent plate are essentially simple.

[**] See second footnote for δ_{mn} of aluminum plate.

124
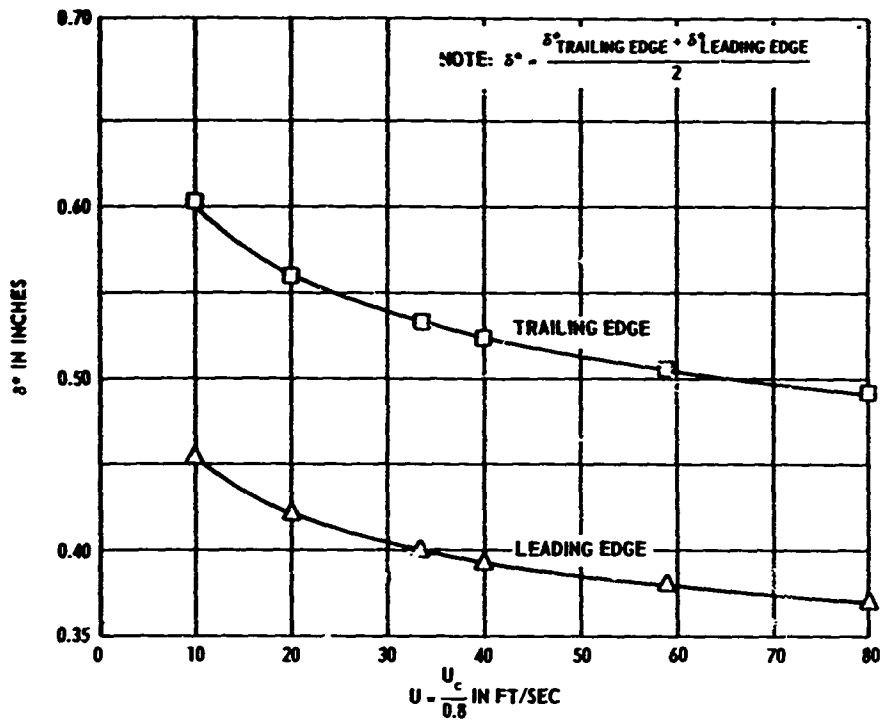
Figure 15a - Using ν for *Water* at 39° F
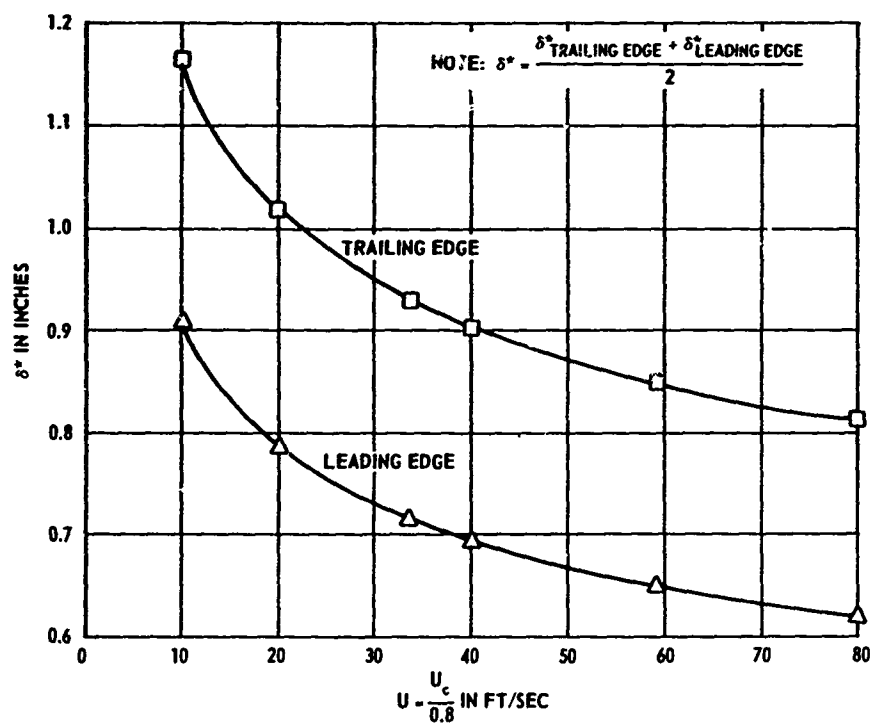
Figure 15b - Using ν for *Air* at 50° F

Figure 15 - Calculated Turbulent Boundary Layer Displacement
Thickness δ*

125

In Reference 25, Figure 36.9 used in conjunction with Figure 36.15 shows that the loss factor η of various steels at low and intermediate reversed stress values and with cyclic stress values well below the fatigue limit range approximately from a maximum of about 0.005 to a minimum of 0.001. Analytically, we can also obtain a value of this order of magnitude by use of Equation (36.13) of this reference, namely,

$$\eta_s = \frac{E}{\pi} \frac{D_d}{\sigma_d^2} \frac{\alpha}{\beta}$$ In this equation, E for

steel is known and D_d the specific damping energy associated with the peak stress level reached anywhere during the vibration (i.e., the value of D corresponding to $\sigma = \sigma_D$) can be obtained from published curves

such as Figure 36.15 and Figure 36.17 of Reference 25 or tabulated data. For materials with uniform stress distribution $\alpha/\beta = 1$ whereas for various specimens with variable stress distribution α/β is given by Figure 36.9 of Reference 25. For a rectangular beam with either a constant, linear, or quadratic moment distribution, at low and intermediate stress, $\alpha/\beta \approx 0.66$. Additional details on this procedure as well as a sample calculation are given in Reference 26.

Experimental data[27-34] for the loss factors of isotropic flat plates of steel and other materials, without substantial stress concentration,* over the range of frequencies 100 to 1000 Hz, also vary approximately from about 0.005 to 0.001. Considering the scatter of these data, a reasonably approximate empirical expression for the loss factor (over this range of frequencies) is $\eta = 0.5/f_{mn}$. Hence, $\beta/\beta_c = \eta/2 = 0.25/f_{mn}$

$= \delta_{mn}/2 = a_{mn}/\omega_{mn}$. Therefore, $\delta_{mn} = 0.5/f_{mn}$ and

$a_{mn} = 0.5\pi$.

The damping of the panel modes is a combination of viscous and structural damping where the viscous damping force is proportional to velocity and the

---

*
Thus the data refer to the loss factor for the bare (free) plate or to a simple supported plate if the corresponding stress concentration associated with the support is not large. The value of η for the particular boundary condition under consideration should be used in computations. For example, from data on clamped plates, Bies[35] determined that $\eta = 77/f$. This result is close to that used by Jacobs[1,21-22] for a clamped aluminum plate. Davies,[7] in his investigation of plate response and radiation, also assumed that $\eta = \beta/f$ where β is a constant.

$\bar{\delta}_{mn}$

hysteretic damping force is proportional to displacement. Measurements have shown that the damping of panels is small so that the damping can be represented adequately in most cases by considering it to be entirely viscous.

Total damping ratio of panel in water including the damping associated with fluid loading and the radiation damping. *However, in the present problem the contribution of the radiation damping to $\bar{\delta}_{mn}$ is excluded.*[*] Following the analysis and argument made for the aluminum plate and noting that $W_p = 20.4$ lb/ft^2 for the steel plate as shown in Table 3, then

$$\bar{a}_{mn} = a_{mn}\frac{M}{M'} = a_{mn}\frac{W_p}{W'} = 0.5\pi\left(\frac{20.4}{20.4 + W_{mn}}\right)$$

and

$$\bar{\delta}_{mn} = \frac{2\,\bar{a}_{mn}}{\bar{\omega}_{mn}} = \frac{\pi}{\bar{\omega}_{mn}}\left(\frac{20.4}{20.4 + W_{mn}}\right) = \frac{1}{2\,\bar{f}_{mn}}\left(\frac{20.4}{20.4 + W_{mn}}\right)$$

θ

Corresponds to the time in which the value of the measured correlation coefficient of the fluctuating pressures at the wall, obtained from the envelope of correlation maxima, drops to $1/e$. Plots of θ versus Mach number for broad- and narrow-band frequencies are given by Maestrello in Reference 23, Figure 5. The Maestrello narrow-band measurements of eddy life-time for frequencies centered at 1200 Hz were extrapolated to zero Mach number at which $\theta = 2.25 \times 10^{-3}$ sec. For all U_c under consideration, (Mach number)$_{water}$ < (Mach number)$_{air}$ = U_∞/c_{air} = $U_c/0.8c_{air}$ ≤ $64/(0.8)(1129)$ < 0.08. Since the extrapolated curve shows that θ(Mach numbers < 0.08) ≈ θ(Mach number equals zero), then approximately $\theta = 2.25 \times 10^{-3}$ sec for all U_c considered.

ξ, η, τ Prescribed data

τ_w Determination of this quantity is based on the law of the wall which is further discussed on page 62 of Reference 1. The Maestrello measurements presented in

---

[*]See first footnote for $\bar{\delta}_{mn}$ of aluminum plate.

Figure 1 of Reference 23 indicate that $\sqrt{\overline{p^2}}/\tau_w = 2.9$ to 3.5 for Mach number = 0.35 to Mach number = 0.75. In reasonable agreement, Jacobs finds that the results of various investigators yield $\sqrt{\overline{p^2}}/\tau_w = 3.1$ as an average value for all subsonic Mach numbers (see pages 301 and 302 of Reference 1). Using the latter for the present calculations we have $\tau_w = \sqrt{\overline{p^2}}/3.1 = 1/3.1 \approx 0.323$ lb/ft;^{2} see also description of $\overline{p^2}$

$\phi_{mn}(x,y)$, $\phi_{mn}(x',y')$ — Data required for the computer program are calculated by the digital computer for a range of prescribed values of m, n, x, y, x', y'

ω — Prescribed in Equation (B7) of Reference 1 to obtain $P(\omega)$

ω_{mn} — For a plate of given geometry, boundary conditions and structural properties, this quantity can be computed by the methods of Option 2 (Reference 3). In the present problem values for ω_{mn} were computed by use of the Warburton program[3] for a simply supported plate and substantiated by means of the simple frequency expression[*]

$$\omega_{mn} = \kappa c_\ell \left[\left(\frac{m\pi}{a}\right)^2 + \left(\frac{n\pi}{b}\right)^2 \right]$$

$\bar{\omega}_{mn}$ — Using Method I, $\bar{\omega}_{mn}$ is computed by means of Equation (H3); Using Method II, $\bar{\omega}_{mn}$ is computed by means of Equations (H6) and/or (H9)

α — Equal to 1 for fluid loading on one side of the plate only; equal to 2 for fluid loading on both sides of the plate

q — Equal to[*] $k/k_s = \dfrac{\dfrac{\omega}{c}}{\sqrt{\left(\dfrac{m\pi}{a}\right)^2 + \left(\dfrac{n\pi}{b}\right)^2}}$

---

[*] See footnote for ω_{mn} defined for the aluminum plate.

128

COMPUTER PROGRAMS

Four computer programs associated with the mean square displacement computations performed in this report for a simply supported fluid-loaded plate subject to turbulence excitation are described below.*

Program A': Modification of the Maestrello subprogram A (designated TURAD), described in Reference 1, for computation of the mean square displacement. The modification which incorporates certain corrections, additions, deletions, and improvements in efficiency in conjunction with its running on the CDC 6700 supersedes subprogram A and should be used henceforth. Details of the modification are discussed below.

Program B': Computes the fluid-loaded natural (or modal) frequencies $\bar{\omega}_{mn}$ as well as k_s, k_s^2, added weight $w_{mn} = m_{mn}g$, and total weight $w' = M'g = (m_p + m_{mn})g$. In the program $w_p = m_p g \to WP$, $W_{mn} = m_{mn}g \to W(M,N)$, $W' = M'g \to FW$, and $\bar{\omega}_{mn} \to BOMEGA$. *This program is designated as Option 3.*

Program C': Warburton program[3] for computing the plate natural frequencies f_{mn} and ω_{mn} in air for both simply supported and clamped-clamped boundary conditions.

Program D': Computes the displacement thickness for an arbitrary body of revolution. The displacement thickness is used to calculate the variable FUCSQ in Program A'. Program D' was developed by Mr. R.W. Brown (see previous section of this Appendix).

Computes turbulent boundary layer thickness.
Symbol is $\delta*$

Computes $\bar{\omega}_{mn}$.
Fluid loading routine

Computes ω_{mn} by the Warburton Method.
Air loading routine

---
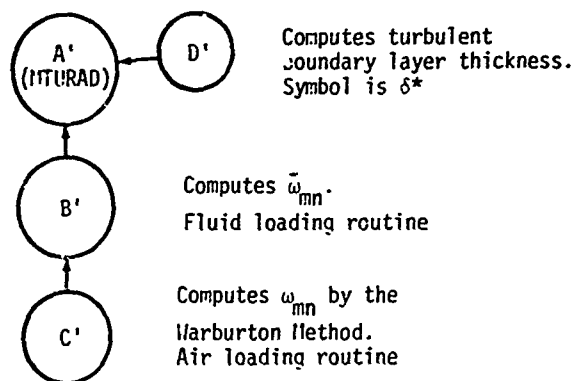
*As previously discussed, computations for clamped-clamped boundaries can also be performed with the same program. The program can also compute the modal acoustic-power radiation of a plate in a reverberant field. These computations are not made here.

129

As shown in the preceding chart, when fluid loading is omitted Programs C' and D' generate data for use in Program A'. The methods for determining additional imput data have been described in the previous section.

When fluid loading is included, Program C' generates data for Program B' and then Programs B' and D' generate data for use in Program A'. Determination of additional data inputs have previously been described.

The computer and running times of a calculation associated with each program are given in the following chart.

Program	Computer (at NSRDC)	Time	Cost for Total Computation
A'	CDC 6700	Using the Simpson rule of integration the computer running time is approximately 5 min for obtaining a curve of $Y^2(\omega)$ versus U_c for each set of mode numbers (m,n) and four convection velocities U_c	$75.00
B'	IBM 7090	1.0 min for (m,n) ranging from 1,1 to 10,10, i.e., 100 values of $\bar{\omega}_{mn}$	4.00
C'	IBM 7090	1.3 min for (m,n) ranging from 1,1 to 10,10, i.e., 100 values of ω_{mn}	5.50
D'	IBM 7090	1.1 min for 198 values of axial distance, flat plate distance, local flat plate Reynolds number, and $\delta = 8\ \delta*$	4.60

Program A'

To make the original Maestrello subprogram A, designated TURAD, a more efficient program and to enable it to run on the CDC 6700, the following changes have been made in the coding of the original program (the modified program A' is designated MTURAD):

1. Reduction of the four-dimensional array IXYZ to a three-dimensional array

    *IXYZ (M,N,IT,L2) ────────► IXYZ (N,1,L2)

2. Increase in the dimension of the following variables:

    *IXYZ (10,1,50,3) ────────► IXYZ (10,1,3)

    IYZ (20,1) ────────────► IYZ (20,10)

130

IY (1) ──────────────────▶ IY (10)

G3 (11,1) ──────────────▶ G3 (101,10)

YY (11) ─────────────────▶ YY (101)

TEMP1 (11) ──────────────▶ TEMP1 (101)

3. Rearrangement of certain data cards

   *FUCSQ

   FM2

4. Deletion of some original data

   *NP - no longer needed

   PARAM - no longer needed (see below)

   THETA - no longer a dimensional variable

5. Correction in coding of Simpson's rule. Original coding is:

   *525 G2 (J,M) = G2 (M,M)*2

   should read

   *525 G2 (J,M) = G2 (J,M)*2

6. Elimination of double precision functions due to no declaration of such at the beginning of the program. Such occurrences were on cards numbered 2310 and 2330.

7. Introduction of a tolerance as an option for $\overline{Y^2}(\omega)$ for any plate material. An exceeded tolerance produces an error message to be printed in the output. If use of the option is not desired, the user reads in the value 0 for the variable IOPT. If the option is used then any number other than 0 is read in for the variable IOPT.

8. Rearrangement of lines of coding due to rearrangement of data. The lines are on cards numbered 0620-0670, 0750 and 0760 in the original listing.

For completeness we include an explanation of the procedure by which θ and a_{mn} were obtained by the computer program in Reference 1. For the present program, the method given in Section 2 of this Appendix for the determination of θ and a_{mn} has superseded this procedure. However, if the user finds the earlier procedure useful in computation, it can be reintroduced into the present program.

From page 7 of Reference 44 and from Section 3 of DISCUSSION AND EVALUATION (Equation 7b), the following condition obtains at hydrodynamic coincidence

$$\omega_{mn} \; \theta = k_{mn} \; U_c \; \theta = \frac{2\pi}{\lambda_{mn}} \; U_c \; \theta$$

We define PARAM = $2U\theta/\lambda_{mn}$. Hence $\omega_{mn} \; \theta = \pi \cdot$ PARAM and

$$\theta = \frac{\pi \cdot \text{PARAM}}{\omega_{mn}} = \frac{\pi \cdot \text{PARAM}}{\kappa \; c_\ell \; \pi^2 \left[\left(\frac{m}{a}\right)^2 + \left(\frac{n}{b}\right)^2\right]} = \frac{\text{PARAM}}{\kappa \; c_\ell \; \pi \left[\left(\frac{m}{a}\right)^2 + \left(\frac{n}{b}\right)^2\right]}$$

Now U_c is the convection velocity along x (i.e., flow) direction only. Therefore at hydrodynamic coincidence, the trace wave speed of the free plate bending wave is matched to the convection speed in the flow direction, yielding a greatly increased response. Thus,

$$U_c = \frac{\omega_{mn}}{k_{mn}} = \kappa \; c_\ell \; \pi \left[\left(\frac{m}{a}\right)^2 + \left(\frac{n}{b}\right)^2\right]^{1/2} \rightarrow \kappa \; c_\ell \; \pi \; \frac{m}{a}$$

so that (neglecting the quantity $(n/b)^2$ in the expression for θ)

$$\theta = \frac{\text{PARAM}}{U_c \; \frac{m}{a}} = \frac{\text{PARAM} \cdot a}{m \; U_c}$$

Maestrello (Figure 21 of Reference 45 or Figure 18 of Reference 46) has shown experimentally that the maximum vibratory response (i.e. maximum mean square displacement) occurs at hydrodynamic coincidence where the turbulence and plate modal wave numbers are matched for a constant frequency.

132

Maestrello has also performed computations which show that the condition $\pi \cdot PARAM = \omega_{mn}\theta = 1$ represents the aerodynamic coincidence condition for which maximum excitation of the panel occurs; see Figure 7 of Reference 1. This figure also gives results for $\omega_{mn}\theta < 1$ and $\omega_{mn}\theta > 1$ corresponding to the conditions below and above coincidence, respectively.[*]

Thus, selection of the value PARAM for a given plate, value of U_c and mode number m will yield the corresponding value of θ. For PARAM = $1/\pi$, the value of θ corresponds to the coincidence condition. For PARAM $\lessgtr 1/\pi$, the value of θ corresponds to the condition below and above coincidence, respectively.

In subprogram A, Maestrello chooses the magnitude of a_{mn} according to the $\omega\theta$ region of the curve that interests him. For example, Figure 7 of Reference 1 plots $\overline{Y^2}(\omega)$ against $\omega\theta$. In the region $\omega\theta = 10^{-1}$ to 1.0, he uses $a_{mn}/10$; however for $\omega\theta = 1.0$ to 40, he uses a_{mn}. The Maestrello methods for determining a_{mn} are given in Reference 1.

---

[*] For $\omega_{mn}\theta \ll 1$ the modal mean square displacement is inversely proportional to the total damping and at the peak is inversely proportional to the square of the damping. In this region the effect of damping on $\overline{Y^2}(\omega)$ is greatest. For $\omega_{mn}\theta > 1$ coincidence is not possible. In this region the effect of damping on $\overline{Y^2}(\omega)$ is much smaller, see References 45 and 46.

TABLE 6

Input Data, Computer Listing, Flow Chart, and Column Headings
for Input Forms on Data Cards for Updated Maestrello Pro-
gram A' Used to Compute Mean Square Displacement of Plate
with and without Fluid Loading

TABLE 6a

Input Required for Program A' (MTURAD)

(Units are given in foot-pound-seconds)

Data	Description	Format	Symbol Used in Program	Unit
Flow Characteristics (Program A'-an updated version of Subprogram A given in Reference 1)				
U_c	Broadband convection velocity	F10.0	UC(I)	ft/sec
$\overline{p^2}$	Mean-square wall-pressure fluctuations, which vary with U_c*	F10.0	PB2*DPB2(I)	$(lb/ft^2)^2$
$(FU_c)^2$	Quantity $\left(\dfrac{\delta^* U_c}{U}\right)$ squared where: $\delta^* \equiv$ boundary layer displacement thickness $U \equiv$ free stream velocity	F10.0	FUCSQ	ft^2
K_1, K_2, K_3	Universal constants: $K_1 = 0.470$ $K_2 = 3.0$ $K_3 = 14.0$	F10.0	AK	
A_1, A_2, A_2	Universal constants: $A_1 = 1.6$ $A_2 = 7.2$ $A_3 = 12.0$	F10.0	AN	

(*PB2 would represent a unique value of $\overline{p^2}$ if $\overline{p^2}$ were independent of U_c. It enters the program (i.e., data cards) once only. Since $\overline{p^2}$ actually varies with U_c, a correction factor DPB2(I) is entered with every value of U_c. Thus $\overline{p^2}$ as a function of U_c is accounted for by the quantity PB2* DPB2(I).

Data	Description	Format	Symbol Used in Program	Unit
Plate Characteristics				
h	Panel thickness	F10.0	11	ft
* $(W')^2$	Square of total weight per unit area	F10.0	FW2	lb/ft
a,b	Lengths of panel sides	F10.0	ZUP,YUP	ft
** δ_{mn}, $\bar{\delta}_{mn}$	Total damping ratio	F10.0	DAMP	
** ω_{mn}, $\bar{\omega}_{mn}$	Modal frequencies of the plate	F10.0	OMEGA	rad/sec
Additional Quantities				
Range of plate mode numbers for which calculations are desired	First m mode number, last m mode number, interval between m mode number, total number of m's $m \leq 20$, MSTEPS ≤ 20. Same information as previously described, with respect to n mode numbers $n \leq 10$, NSTEPS ≤ 10. To run program A' for $m > 20$, $n > 10$ the size of the dimensioned variables IXYZ,IYZ,IY,G2,G3,YY, TEMP,OMEGA,DAMP,FA, FC,EIGEN and FUDGE must be examined and increased accordingly	I10 I10 I10 I10 I10 I10 I10 I10	MLOW MUP DM MSTEPS NLOW NUP DN NSTEPS	
τ	Time delay	F10.0	TAU	sec
Number of values of U_c to be calculated		I10	KUC	
x_0, y_0	Coordinates of a point on plate at which mean square displacement and acoustic power are calculated	F10.0	XO,YO	ft

* Total weight area = $W' = M' \cdot g$ where M' = total mass per unit area. We stress that the user submits inertial data in terms of *weight* per unit area and the computer program converts these data to mass per unit area.

** $\bar{\delta}_{mn}$ = Total damping ratio of plate in water; δ_{mn} = total damping ratio of plate in air, $\bar{\omega}_{mn}$ = modal frequencies of plate in water; ω_{mn} = modal frequencies of plate in air.

Table 6a (Continued)

Data	Description	Format	Symbol Used in Program	Unit
x_0', y_0'	Any point on plate different from x_0, y_0	F10.0	XOP, YOP	ft
Calculated Output				
$\phi_{m,n}$	Value of eigen-functions of mean square displacement. A value of EIGEN is computed for each mode (m,n) with three values of total damping; $1/10\ a_{m,n}$; $a_{m,n}$; $10a_{m,n}$	E16.8	EIGEN	
$*a_{m,n}, \bar{a}_{m,n}$	Values of total damping associated with each mode (m,n)	E16.8	FA(m,n,1) for computation; A(m,n,DAMP) in output	1/sec
$\dfrac{Vol_{m,n}}{\sqrt{2}\ \gamma}$	Volume under each eigenfunction	E16.8	VOL	in.^{2}
$I(m,n)$	Triple integral of Equation (B52) of Reference 1; integral of cross correlation	E16.8	IXYZ I(m,n)	
$\overline{\gamma^2(\omega)}$	Mean square displacement for values of $1/10\ a_{m,n}$; $a_{m,n}$; $10a_{m,n}$	E16.8	ANS	in.^{2}
* $\bar{a}_{m,n}$ = Total damping for each mode of fluid loaded plate. $a_{m,n}$ = Total damping for each mode of plate in air.				

136

TABLE 6b

Computer Listing for Updated Maestrello Program A'

```
FTN(T)
LGO.
.
      PROGRAM MTURAD(INPUT,OUTPUT,TAPE5=INPUT,TAPE6=OUTPUT)
C     REORGANISED PROGRAM FOR COMPUTING TRIPLE                          0 10
C     INTEGRAL                                                           20
C     USING SIMPSONS RULE                                                30
COMMENT    TRANS = 0.0 MEANS NO TRANSDUCER EFFECTS INCLUDED
COMMENT      THIS RUN OF MTURAD HAS SIMPLY-SUPPORTED        *******
C*********FREQUENCIES W//UT TRANSDUCER    *)*********************************
      DIMENSION VOL(20,10)                                               40
      DIMENSION F3(3),ANS(3)                                             50
      DIMENSION IXYZ(10,1,3),IYZ(20,10),IY(10),G2(401,20),G3(101,10),
     1YY(101),TEMP1(101),G5(4000)
      DIMENSION AK(3),AN(3),TITLE(7)
      DIMENSION OMEGA(20,10),DAMP(20,10)                               0100
      DIMENSION FA(20,10,3),FC(20,10,3),EIGEN(20,10,3),FUDGE(20,10,3)  0110
      DIMENSION UC(20),DPB2(20)                                        0120
      REAL IXYZ,IYZ,IY                                                 0130
      INTEGER DM,DN                                                    0140
      READ(5,13)  TAU,TRANS                                           0140
   13 FORMAT(2F10.0)
      WRITE(6,801)  TAU                                               0170
  801 FORMAT(1H1,/5H TAU=E15.6)                                       0180
      READ(5,1212) IOPT
 1212 FORMAT(I5)
      WRITE(6,1213) IOPT
 1213 FORMAT(1H0,5HIOPT=I5)
      READ(5,103)H,XO,YO,XOP,YOP,PB2,AK,AN,(TITLE(I),I=1,7)
  103 FORMAT(12(F10.0/),(7A10))
      WRITE(6,201) (TITLE(I),I=1,7)
  201 FORMAT(7A10)
      WRITE(6,203)PB2,AK,AN,XO,YO,
     1XOP,YOP,                                                         250
  203 FORMAT(1X,8H RHO-BAR 9H SQUARED=E16.8,
     24H0K1=E16.8,4H K2=E16.8,4H K3=E16.8/                             0290
     34H A1=E16.8,4H A2=E16.8,4H A3=E16.8/                            0300
     44H XO=E16.8,4H YO=E16.8,5H XOP=E16.8,5H YOP=E16.8)              0310
      READ(5,102) KUC,(UC(I),DPB2(I),I = 1,KUC)                       0320
  102 FORMAT(I10/(2F10.0))                                            0330
      WRITE(6,204) (UC(I),DPB2(I),I = 1,KUC)                          0340
  204 FORMAT(1H07X2HUC13X4HDPB2/(1H 2E16.8))                          0350
   99 READ(5,1) ZUP,YUP,H,MLOW,MUP,DM,MSTEPS,NLOW,NUP,DN,NSTEPS       0360
    1 FORMAT(3(F10.0/),(4I10))                                        0370
      WRITE(6,2)MLOW,MUP,DM,MSTEPS,NLOW,NUP,DN,NSTEPS                 0380
    2 FORMAT(9H0M  FROM I5,4H  TOI5,7H    DM=I5,                      0390
     112H A TOTAL OF I5,7H  STEPS/9H N  FROM I5,                      0400
     24H  TOI5,7H    DN=I5,12H A TOTAL OFI5,7H  STEPS)                0410
      WRITE(6,202) ZUP,YUP,H                                          0420
  202 FORMAT(3H A=E16.8,5H   B=E16.8,5H   H=E16.8)                    0430
      READ(5,101) ((OMEGA(M,N),M=MLOW,MUP,DM),N=NLOW,NUP,DN)
  101 FORMAT(F10.0)                                                    450
      IF(NUP .GT. 10) WRITE(6,888)
  888 FORMAT(1H0,78HDIMENSIONS FOR G3,IYY,TEMP1 ARE EXCEEDED. CHECK EQUA
     1TION FOR KUP ON CARD 1360.)
      WRITE(6,205)((OMEGA(M,N),M=MLOW,MUP,DM),                        0460
     1N=NLOW,NUP,DN)                                                   470
  205 FORMAT(7H0OMEGA=/(8E16.8))                                      0480
      IF(TRANS.EQ.0.0) GO TO 17
      READ(5,1477) R,DEL
```

137

```
1477 FORMAT(2F10.0)
     DO 1453  J = 1,3
1453 AK(J) = AK(J) * SQRT(R/DEL)
  17   DO 7 N=1,NUP,DN                                              490
       DO 7 M=1,MUP,DM                                              500
   7   DAMP(M,N)=.01                                                510
       READ (5,104) ((DAMP(M,N),M=MLOW,MUP,DM),N=NLOW,NUP,DN)
 104 FORMAT(F10.0)                                                  530
       WRITE(6,206) ((DAMP(M,N),M=MLOW,MUP,DM),                    0540
      1N=NLOW,NUP,DN)                                               550
 206   FORMAT(6HODAMP=/(8F16.8))                                   0560
       N1=8                                                         570
       READ(5,207)THETA
 207 FORMAT(F10.5)
       A=ZUP                                                        600
       B=YUP                                                        610
   8   B7 = AN(1) / AK(1)
       B8=AN(2)/AK(2)                                               690
       B9=AN(3)/AK(3)                                               700
       C1=4.0/(A*B)
       C2=3.14159265                                                720
       C3=1./C2                                                     730
       C4=C2*C2                                                     740
       C6=C4/(A*B)                                                  770
       DO 10 M=MLOW,MUP,DM                                          780
       DO 10 N=NLOW,NUP,DN                                          790
       XM=M                                                         800
       XN=N                                                         810
       XO=A/2.                                                      820
       YO=B/2.                                                      830
       IF(M-M/2*2.NE.0)GO TO 43                                    0840
       XO=A/2.-A/(XM*2.)                                            850
  43   IF(N-N/2*2.NE.0)GO TO 44                                    0860
       YO=B/2.-B/(XN*2.)                                            870
  44   XOP=XO                                                       880
       YOP=YO                                                       890
       DAMP(M,N)=DAMP(M,N)/10.                                     0900
       DO 45 L=1,3                                                  910
       FA(M,N,L)=DAMP(M,N)/2.*OMEGA(M,N)                           0920
       FA(M,N,L)=FA(M,N,L)*0.5                                     0930
       FC(M,N,L)=OMEGA(M,N)/FA(M,N,L)                              0940
       FUDGE(M,N,L)=XM*XN*OMEGA(M,N)*(FA(M,N,L)**2  +OMEGA(M,N)**2  )  0950
       EIGEN(M,N,L)=C1/FUDGE(M,N,L)*SIN(XM*C2*XO/A)*SIN(XN*C2*YO/B)*   0960
      1SIN(XM*C2*XOP/A)*SIN(XN*C2*YOP/B)                           0970
  45   DAMP(M,N)=DAMP(M,N)*10.                                     0980
  10   CONTINUE                                                     990
       WRITE(6,1003)                                               1000
1003 FORMAT(33HOXO=XOP,YO=YOP,AND THEY VARY WITH                   1010
      117H THE MODE NUMBERS)                                        1020
       DO 46 L=1,3                                                 1030
       WRITE(6,3)((EIGEN(M,N,L),M=MLOW,MUP,DM),N=NLOW,NUP,DN)      1040
   3   FORMAT(7HOEIGEN=/(8E16.8))                                  1050
  46   CONTINUE                                                    1060
       DO 47 L=1,3                                                 1070
       WRITE(6,48)((FA(M,N,L),M=MLOW,MUP,DM),N=NLOW,NUP,DN)        1080
  48   FORMAT(13HOA(M,N,DAMP)=/(8E16.8))                           1090
  47   CONTINUE                                                    1100
       CALL VOLUM(A,B,MLOW,MUP,DM,NLOW,NUP,DN,VOL)                 1110
       ICOUNT=1
       READ(5,225) FUCSQ
```

138

```
225     FORMAT(F10.0)
3       DO 777 KU=1,KUC
        WRITE(6,303)UC(KU)
303     FORMAT(4H UC=,E16.8)
        B1=AK(1)**2*FUCSQ                                          620
        B2=AK(2)**2*FUCSQ                                          630
        B3=AK(3)**2*FUCSQ                                          640
        B4=AN(1)*AK(1)*FUCSQ                                       650
        B5=AN(2)*AK(2)*FUCSQ                                       660
        B6=AN(3)*AK(3)*FUCSQ                                       670
        DO 778 M=MLOW,MUP,DM                                      1170
5       KCOUNT=1
        READ(5,222)FW2
666     FORMAT(F10.2)
        C5=(A*B*PB2)/(2.*C4*FW2*(B7+B8+B9))
        C5=C5*32.2*32.2*12.*12.                                   0760
        CONST=C5*DPB2(KU)                                         1140
        WRITE(6,304)CONST
304     FORMAT (12X,7H CONST=,E16.8)
        XM=M                                                      1180
        WRITE(6,780)THETA
780     FORMAT(1H0,6HTHETA=,E12.5)
        IF(THETA .GT. 100) GO TO 999
        XLOW=0.                                                   1240
        DX=1./(20.*OMEGA(M,NUP )/2./3.14159265)
        IUP=5./DX*THETA+1.
        IF(IUP .GT. 3599) IUP=3599
        IF(IUP-IUP/2*2) 501,500,501                              1270
500     IUP=IUP+1                                                1280
501     IUP = IUP +400                                           1290
502     DX=THETA/40.
        ZLOW=-A                                                  1310
        JUP=20*M+1                                               1320
        ZJUP=JUP-1                                               1330
        DZ=2.*A/ZJUP                                             1340
        YLOW=0.                                                  1350
        KUP=10*NUP+1                                             1360
        YKUP=KUP-1                                               1370
        DY=B/YKUP                                                1380
        DO 11 I=1,IUP                                            1390
        G5(I)=1.                                                 1400
        IF(I.EQ.401)GO TO 11                                     1410
        IF(I.NE.1.AND.I.NE.IUP) GO TO 510                        1420
        GO TO 511                                                1430
510     G5(I)=G5(I)*2.                                           1440
511     IF(I-I/2*2.EQ.0) GO TO 513                               1450
        GO TO 11                                                 1460
513     G5(I)=G5(I)*2.                                           1470
11      CONTINUE                                                 1480
        Z=ZLOW                                                   1490
        DO 21 J=1,JUP                                            1500
        XM=M                                                     1510
        D1=XM*C2*Z/A                                             1520
        D2=COS(D1)                                               1530
        G2(J,M)=D2+1./(XM*C2)*(SIN(ABS(D1))-ABS(D1)              1540
       1*D2)                                                     1550
        IF(J.NE.1.AND.J.NE.JUP) GO TO 520                        1560
        GO TO 521                                                1570
520     G2(J,M)=G2(J,M)*2.                                       1580
521     IF(J-J/2*2.EQ.0)GO TO 525                                1590
```

```
      GO TO 21                                                          1600
525   G2(J,M)=G2(J,M)*2.
21    Z=Z+DZ                                                           1620
      Y=YLOW                                                           1630
      DO 31 K=1,KUP                                                    1640
      DO 30 N=NLOW,NUP,DN                                              1650
      XN=N                                                             1660
      D3=XN*C2*Y/5                                                     1670
      D4=COS(D3)                                                       1680
      G3(K,N)=D4+1./(XN*C2)*(SIN(D3)-D3*D4)                            1690
      IF(K.NE.1.AND.K.NE.KUP)  GO TO 530                              1700
      GO TO 531                                                        1710
530   G3(K,N)=G3(K,N)*2.                                              1720
531   IF(K-K/2*2.EQ.0) GO TO 533                                      1730
      GO TO 30                                                         1740
533   G3(K,N)=G3(K,N)*2.                                              1750
30    CONTINUE                                                         176'
31    Y=Y+DY                                                           1770
      Y=YLOW                                                           1780
      DO 39 K=1,KUP                                                    1790
      YY(K)=Y*Y                                                        1800
39    Y=Y+DY                                                           1810
      DO 40 L1=1,3                                                     1820
      DO 40 N=NLOW,NUP,DN                                              1830
40    IXYZ(N,1,L1)=0.
      KAPPA=0                                                          1860
      X=XLOW                                                           1870
      DO 160 I=1,IUP                                                   1880
      IF(TAU .EQ.0.0)  GO TO 630                                      1890
      E1 = UC(KU)*(TAU-X)                                             1900
      GO TO 632                                                        1910
630   E1 = UC(KU)*X                                                   1920
632   CONTINUE                                                         1930
      DO 50 N=NLOW,NUP,DN                                              1940
50    IYZ(M,N)=0.                                                     1950
      Z=ZLOW                                                           1960
      DO 120 J=1,JUP                                                   1970
      E2=(Z-E1)*(Z-E1)                                                1980
      E4=B1+E2                                                         1990
      E5=B2+E2                                                         2000
      E6=B3+E2                                                        ·2010
      DO 60 K=1,KUP                                                    2020
60    TEMP1(K)=B4/(E4+YY(K))+B5/(E5+YY(K))+B6/(E6+YY(K))              2030
      DO 70 N=NLOW,NUP,DN                                              2040
70    IY(N)=0.                                                        2050
      DO 90 K=1,KUP                                                    2060
      DO 90 N=NLOW,NUP,DN                                              2070
90    IY(N)=IY(N)+G3(K,N)*TEMP1(K)                                    2080
      DO 100 N=NLOW,NUP,DN                                             2090
100   IY(N)=IY(N)*DY/3.                                               2100
      DO 110 N=NLOW,NUP,DN                                             2110
      TEMP=IY(N)                                                       2120
110   IYZ(M,N)=IYZ(M,N)+G2(J,M)*TEMP                                  2130
120   Z=Z+DZ                                                           2140
      DO 130 N=NLOW,NUP,DN                                             2150
130   IYZ(M,N)=IYZ(M,N)*DZ/3.                                         2160
1001  CONTINUE                                                         2170
      DO 140 N=NLOW,NUP,DN                                             2180
      TEMP=IYZ(M,N)                                                    2190
      XM=M                                                             2200
```

140

```
      XN=N                                                          2210
      F1=XM*XN*C6                                                   2220
      F2=OMEGA(M,N)*ABS(X)                                          2230
      DO 140 L1=1,3                                                 2240
      F3(L1)=FA(M,N,L1)*ABS(X)                                      2250
      IF(F3(L1).GT.5.)GO TO 140                                     2260
      F6=F1*EXP(-F3(L1))*(SIN(F2)+FC(M,N,L1)*COS(F2))               2270
      IF(X .GT. 5.*THETA) GO TO 137
      IF(TAU.EQ.0.0) GO TO 634                                      2300
      G6=EXP(-ABS((TAU-X)/THETA))
      GO TO 636                                                     2320
634   G6=EXP(-ABS(X/THETA))
636   CONTINUE                                                      2340
      G1=2.*F6*G6*G5(I)                                             2350
       IXYZ(N,1 ,L1) = IXYZ(N,1 ,L1) + G1*TEMP*DX/3.
137   CONTINUE                                                      2370
140   CONTINUE                                                      2380
      IF(KAPPA.NE.0)GO TO 160                                       2390
      IF(I.NE.401)GO TO 160                                         2400
      KAPPA=1                                                       2410
      DX=1./(20.*OMEGA(M,NUP )/2./3.14159265)
      GO TO 1001                                                    2430
160   X=X+DX                                                        2440
      DO 601 N=NLOW,NUP,DN                                          2450
      IF(THETA .GT. .100) GO TO 999
      WRITE(6,141) M,N                                              2470
141   FORMAT(3H1M=I5,3H N=I5//45X6HI(M,N)38X,18HI(M,N)*EIGEN*CONST// 2480
     12X5HTHETA4X11HOMEGA*THETA6X11HDAMP=1./10.5X7HDAMP=1.9X8HDAMP=10.  2490
     28X11HDAMP=1./10.5X7HDAMP=1.9X8HDAMP=10.)
      DO 602 L2=1,3                                                 2520
602   ANS(L2)=IXYZ(  N,1      ,L2)*EIGEN(M,N,L2)*CONST
      T=THETA*OMEGA(M,N)
      WRITE(6,142)THETA      ,T,(IXYZ(  N,1 ,L2),L2=1,3),(ANS(L2),L2=1,3) 2550
 142  FORMAT(1X,F9.6,E14.6,6E16.8)                                 2570
      IF(IOPT .EQ. 0) GO TO 600
      IF(N .EQ. NLOW) THOLD=ANS(2)
      IF(N .EQ. NLOW) GO TO 600
      IF(ANS(2) .EQ. THOLD/10. .OR. ANS(2) .GT. THOLD/10.) GO TO 600
      WRITE(6,998)
998   FORMAT(1H0,72HMODE IS MORE THAN 1/10 BELOW VALUE OF Y**2 OF OMEGA
     1AT CORRESPONDING UC.)
      GO TO 778
600   KCOUNT=KCOUNT+1
      IF(KCOUNT .GT. NSTEPS) GO TO 778
      READ(5,222)FW2
      C5=(A*B*DPP2)/(2.*C4*FW2*(B7+B8+B9))
      C5=C5*32.2**2*12.**2
      CONST=C5*DPB2(KU)
 601  CONTINUE
778   CONTINUE
779   ICOUNT=ICOUNT+1
      IF(ICOUNT .GT. KUC) GO TO 777
      READ(5,225) FUCSQ
777   CONTINUE                                                     2600
 999  STOP                                                         2610
      END                                                          2620
      SUBROUTINE VOLUM(A,B,MLOW,MUP,DM,NLOW,NUP,DN,VOL)            2640
      INTEGER DM,DN                                                2650
      DIMENSION VOL(20,10)                                         2660
      PI=3.14159265                                                2670
```

141

```
      DO 10 N=NLOW,NUP,DN                                         2680
      XN=N                                                        2690
      DO 10 M=MLOW,MUP,DM                                         2700
      XM=M                                                        2710
      VOL(M,N)=0.                                                 2720
      IF(N-N/2*2.EQ.0)GO TO 10                                    2730
      IF(M-M/2*2.EQ.0)GO TO 10                                    2740
      GAMMAN=(2.*XN+1.)*PI/2.                                     2750
      GAMMAM=(2.*XM+1.)*PI/2.                                     2760
      XKN=SIN(GAMMAN/2.)/SINH(GAMMAN/2.)                          2770
      XKM=SIN(GAMMAM/2.)/SINH(GAMMAM/2.)                          2780
      VOL(M,N)=16.*A*B/GAMMAM/GAMMAN/(1.+XKM)*144.                2790
     1/(1.+XKN)*SIN(GAMMAM/2.)*SIN(GAMMAN/2.)                     2800
   10 CONTINUE                                                    2810
      WRITE(6,20)((VOL(M,N),M=MLOW,MUP,DM),N=NLOW,NUP,DN)         2820
   20 FORMAT(28HOVOLUME UNDER EIGENFUNCTION=//                    2830
     1(8E16.8))                                                   2840
      RETURN                                                      2850
      END                                                         2860
      FUNCTION SINH (X)
      SINH=0.5*(EXP(X)-EXP(-X))
      RETURN
      END
```

323

TABLE 6c

Flow Chart for Updated Maestrello Program A'

① **READ AND WRITE INPUT DATA**

② **CALCULATE VARIABLES USED INSIDE LOOPS**

③ **CALCULATE**
$$\frac{nbp^{\overline{2}}}{2\pi^2 N^2 \sum\limits_{\nu=1}^{3} \dfrac{A_\nu}{K_\nu}}$$

④ **DOUBLE DO LOOP ON 10**

m and n Vary
$$X0 = A/2, \; Y0 = B/2$$

m IS EVEN — Yes → $Y0 = A/2 - A/(2m)$

No

n IS EVEN — Yes → $Y0 = B/2 - B/2n$

DO on 45
Set up for 3 damps
$\frac{1}{10}, 1, 10$

CALCULATE for each damp
$$\sum \frac{\phi_{mn}(x,y)\,\phi_{mn}(x'y')}{mn\,\omega_{mn}\left[a_{mn}^2 + \omega_{mn}^2\right]}$$

45 CONTINUE

10 CONTINUE

⑤ **WRITE** Values just Calculated

⑥ **CALL SUBR VOLUM**

⑦

SUBROUTINE VOLUM

Calculates 1 per m,n

$$Vol_{mn} = \frac{16\, ab\, 144 \sin\!\left(\frac{2m+1}{2}\right)\frac{\pi}{2}\sin\!\left(\frac{2n+1}{2}\right)\frac{\pi}{2}}{(2n+1)\frac{\pi}{2}(2n+1)\frac{\pi}{2}\left[1 + \dfrac{\sin(2m+1)\frac{\pi}{2}}{\sinh(2m+1)\frac{\pi}{2}}\right]\left[1 + \dfrac{\sin(2n+1)\frac{\pi}{2}}{\sinh(2n+1)\frac{\pi}{2}}\right]}$$

WRITE answers
RETURN

For convenience, fluid-loaded parameters (represented by barred quantities) are not distinguished from corresponding parameters for the plate in air. Thus, for the fluid-loaded plate we must *think* of certain parameter symbols being converted as follows: $\omega_{mn} \to \bar{\omega}_{mn}$, $a_{mn} \to \bar{a}_{mn}$, $\delta_{mn} \to \bar{\delta}_{mn}$, i.e. ω_{mn} is really $\bar{\omega}_{mn}$ in the water case, etc.

143

Table 6c (Continued)

7

ICOUNT=1 — Set counter for reading FUSCQ

READ
FUCSC

DO 777
(VARY U_c)

WRITE
U_c

DO 778
(Vary m)

KCOUNT=1 — Set counter for reading FW2

READ FW2

CALCULATE
C5, CONST

Set upper and lower limits for x,y,z
integrals; Determine number of steps
for each integral and the step size
for each

8

144

Table 6c (Continued)

$\boxed{8}$

```
CALCULATE

Coefficients
for Simpson's
rule
```

z Set variable of integration = lower limit on z
   Calculate function of z values

$$f_{(z)} = \int_{-a}^{a} \left(\cos \frac{m\pi z}{a} + \frac{1}{m\pi} \left[\sin \left| \frac{m\pi z}{a} \right| - \left| \frac{m\pi z}{a} \right| \cos \left(\frac{m\pi z}{a} \right) \right] \right) dz$$

y Set variable of integration = lower limit on y
   Calculate function of y values

$$f_{(y)} = \int_{0}^{b} f_{(z)} \left[\cos \frac{n\pi y}{b} + \frac{1}{n\pi} \left[\sin \left(\frac{n\pi y}{b} \right) - \frac{n\pi y}{b} \cos \left(\frac{n\pi y}{b} \right) \right] \right] dy$$

```
Set up and initialize to zero the
array for summing on outside
integral
```

$\boxed{9}$

145

Table 6c (Continued)

$$f_{(x)} = \int_0^\infty f_{(y)} \left[mn \frac{4}{ab} e^{-a_{mn}x} \left[\sin\left(\omega_{mn}|x|\right) + \frac{\omega_{mn}}{a_{mn}} \cos\left(\omega_{mn} |x|\right)\right] e^{-|x/\theta|} + \sum_{\nu=1}^{3} \frac{A_\nu K_\nu}{k_\nu^2 + \left(\frac{1}{FU_c}\right)^2 \left(\left(z - U_c (\tau - x)\right)^2 + y^2\right)} \right] dx$$

x   Set variable of integration = lower limit on x

Calculate function of x varying y and z and sum up parts previously calculated.

DO 601
(n varies)

WRITE
Answers of
triple integral
IXYZ

COMPUTE AND
WRITE
ANS=IXYZ *
EIGEN * CONST

146

Table 6c (Continued)

```
                    ( 10 )
                      │
                      ▼
              ╱───────────────╲
             ╱       IS         ╲      YES
            ╱      IOPT=0        ╲──────────────────────┐
            ╲         ?          ╱                      │
             ╲                  ╱                       │
              ╲───────────────╱                        │
                      │ NO                              │
                      ▼                                 │
          ┌─────────────────────┐                      │
          │    Set tolerance     │                      │
          │     for ANS(2)       │                      │
          └─────────────────────┘                      │
                      │                                 │
                      ▼                                 │
┌──────────────┐  ╱───────────╲                        │
│ WRITE error  │ ╱     IS       ╲   YES                 │
│ message for  │◄─  tolerance   ─                       │
│ exceeding    │ ╲  exceeded    ╱                       │
│ tolerance    │  ╲     ?      ╱                        │
└──────────────┘   ╲─────────╱                          │
        │               │ NO                            │
        │               ▼                               │
        │      ┌─────────────────┐                      │
        │      │     KCOUNT=      │◄─────────────────────┘
        │      │    KCOUNT + 1    │
        │      └─────────────────┘
        │               │
        │               ▼
        │        ╱───────────╲
        │       ╱     IS       ╲   YES
        │      ╱  KCOUNT.GT.    ╲──────────────────┐
        │      ╲    NSTEPS      ╱                  │
        │       ╲              ╱                   │
        │        ╲───────────╱                     │
        │             │ NO                         │
        │             ▼                            │
        │      ┌─────────────────┐                 │
        │      │   READ FW2       │                 │
        │      │     AND          │                 │
        │      │  CALCULATE       │                 │
        │      │  C5, CONST       │                 │
        │      └─────────────────┘                 │
        │             │                            │
        │       601   CONTINUE                     │
        └──────►778   CONTINUE◄────────────────────┘
                      │
                      ▼
                    ( 11 )
```

147
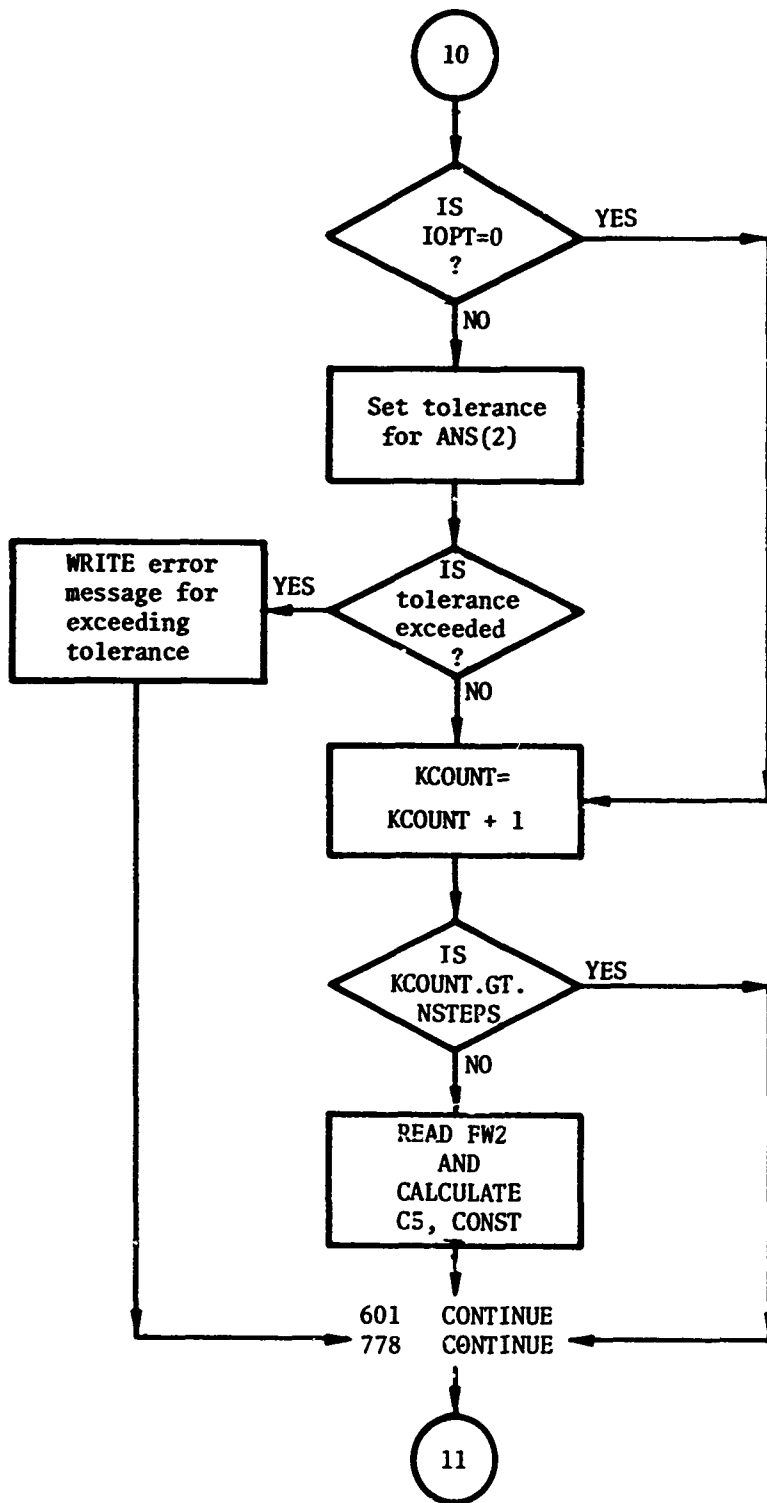
Table 6c (Continued)
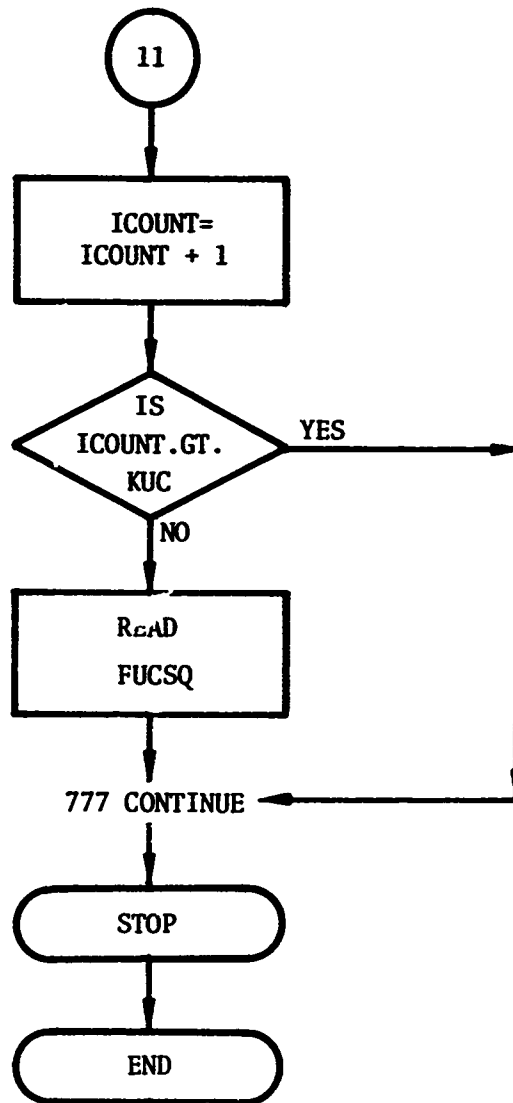
TABLE 6d

Column Headings for Input Forms on Data Cards

TAU	10 TRANS 20		80

PLATE 10		
H		80

X0		80

Y0		80

X0P		80

Y0P		80

PB2		80

AK(1)		80

AK(2)		80

AK(3)		80

AN(1) 10 80

AN(2) 10 80

AN(3) 10 80

TITLE 60 80

KUC 10 80

UC(1) 10 DPB2(1) 20 80

ZUP 10 NUMBER OF CARDS NEEDED FOR U_c, DPB2 ARRAYS IS EQUAL TO KUC 80

YUP 10 80

H 10 80

MLOW 10 MUP 20 DM 30 MSTEPS 40 80

NLOW 10   NUP 20   DN 30 NSTEPS40   80

OMEGA(1,1)10   80
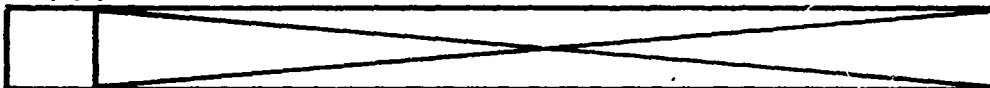
OMEGA(2,1)10   80

WITH THE ORDER OF CARDS (1,1),(2,1),...(M,1),(1,2),...(M,2)...,(1,N),..(M,N) TO COMPLETE
THE OMEGA(M,N) ARRAY

   R 10   DEL   20   80

DAMP(1,1) 10   80

WITH THE ORDER OF CARDS (1,1),(2,1),...(M,1),(1,2),..(M,2)...,(1,N),..(M,N) TO COMPLETE
DAMP(M,N) ARRAY

   THETA 10   80

FUCSQ(1)10   80
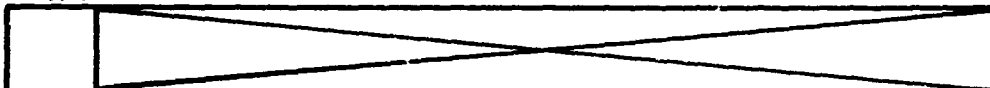
FW2(1) 10   80
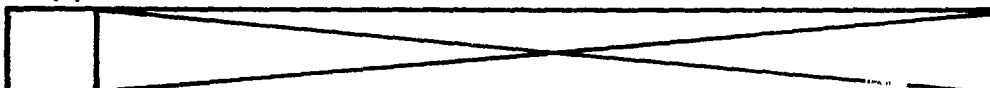
FW2(2)10   80
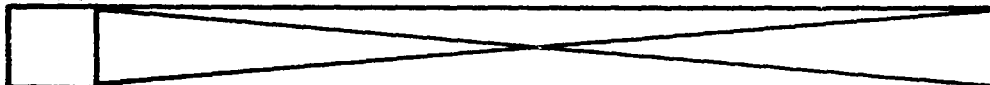
THE NUMBERING OF FW2 IS DETERMINED BY THE NUMBER OF (M,N) MODES

   FUCSQ(2)10   80
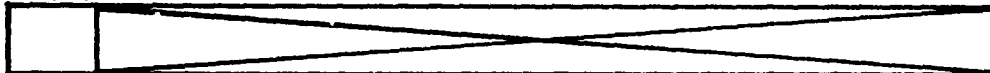
THE NUMBER OF FUCSQ IS DETERMINED BY USER.

Program B'

A description of Program B' (Option 3) is given in Tables 7a-7d.

TABLE 7

Input Data, Computer Listing, Flow Chart, and Column Headings
for Input Forms on Data Cards for Program B' (Option 3)
Used to Compute Added and Total Weight per Unit Area and
Modal Frequencies of Fluid-Loaded Plate

TABLE 7a

Input Required for Program B'

Variable Name	Format	Description	Unit
WP	F10.8	Weight per unit area of plate	lb/ft^2
RHOF	F10.4	Weight density of fluid	lb/ft^3
RHOW	F10.4	Weight density of plate	lb/ft^3
H	F10.4	Panel thickness	ft
RL1	F10.4	Length of panel side, x-direction	ft
RL2	F10.4	Length of panel side, y-direction	ft
ALPHA	F10.4	For α = 1, fluid loading is on one side of plate α = 2, fluid loading is on both sides of plate	-
MLOW	I10	Lower limit of M mode $\quad m \leq 20$	
MUP	I10	Upper limit of M mode	
NLOW	I10	Lower limit of N mode $\quad n \leq 10$	-
NUP	I10	Upper limit of N mode	
OMEGA(m,n)	F10.2	Array for modal frequencies of plate in air	rad/sec

TABLE 7b

Computer Listing for Program B'

```
$IBJOB         MAP,FIOCS
$EXECUTE       IBJOB
$IBFTC OMEGA
       DIMENSION OMEGA(20,10),POMEGA(20,10),BOMEGA(20,10),W(20,10)
       READ(5,15)WP
 15    FORMAT(F10.2)
       READ(5,20) RHOF,RHOW,H,RL1,RL2,ALPHA
 20    FORMAT(6F10.4)
       READ(5,1)MLOW,MUP,NLOW,NUP
     1 FORMAT(4I10)
       READ(5,10)((OMEGA(M,N),M=MLOW,MUP),N=NLOW,NUP)
 10    FORMAT(F10.4)
C
C METHOD 1
C
       WRITE(6,40)
 40    FORMAT(1H1,10X,8HMETHOD 1)
       Q=0.
       DO 244 L=1,4
       DO 25 M=MLOW,MUP
       DO 25 N=NLOW,NUP
       FKS2=((FLOAT(M)*3.1416)/RL1)**2+((FLOAT(N)*3.1416)/RL2)**2
       FKS=SQRT(FKS2)
       W(M,N)=(ALPHA*RHOF)/(FKS*SQRT(1.-Q**2)
       FW=WP*(1.+((ALPHA*RHOF)/(FKS*WP*SQRT(1.-Q**2))))
       POMEGA(M,N)=OMEGA(M,N)
       BOMEGA(M,N)=POMEGA(M,N)*SQRT(1./(1.+((ALPHA*RHOF)/(RHOW*FKS*H*SQRT
      1(1.-Q**2)))))
       WRITE(6,30)M,N,Q
  30 FORMAT(1H0,2HM=,I2,2X,2HN=,I2,2X,2HQ=,F5.3)
       WRITE(6,35)FKS2,FKS,FW,BOMEGA(M,N),W(M,N)
 35    FORMAT(1H0,5HFKS2=,F12.4,2X,4HFKS=,F12.4,2X,3HFW=,F12.4,2X,7HBOMEG
      1A=,F12.4,2X,2HW=,F12.4)
  25 CONTINUE
       Q=Q+.3
 244 CONTINUE
       STOP
       END
```

153

TABLE 7c

Flow Chart for Program B'

```
                    ( START )
                        |
                        v
                 +--------------+
                 |    READ      |
                 |   INPUT      |
                 |    DATA      |
                 +--------------+
                        |
                        v
                 +---------------\
                 |    DO 244      >
                 |   L = 1,4     /
                 +--------------/
                        |
                        v
                 +---------------\
                 |    DO 25       >
                 | M = MLOW, MUP /
                 +--------------/
                        |
                        v
                 +---------------\
                 |    DO 25       >
                 |  N = NLOW     /
                 |    NUP       /
                 +-------------/
                        |
                        v
                 +--------------+
                 |  CALCULATE   |
                 | WEIGHT PER   |
                 |  UNIT AREA   |
                 +--------------+
                        |
                        v
                 +--------------+
                 |  CALCULATE   |
                 |    TOTAL     |
                 |   WEIGHT     |
                 +--------------+
                        |
                        v
                 +--------------+
                 |  CALCULATE   |
                 | PLATE MODAL  |
                 | FREQUENCY IN |
                 |    WATER     |
                 +--------------+
                        |
                        v
                 25 CONTINUE
                 244 CONTINUE
                        |
                        v
                    ( STOP )
```

154
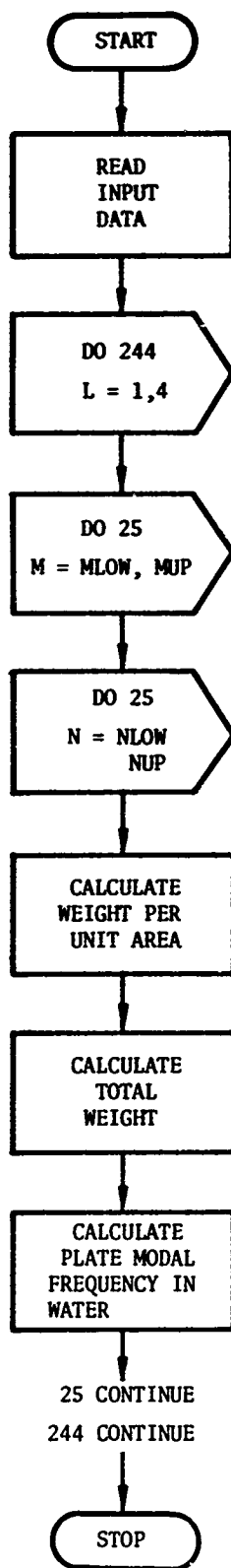
TABLE 7d

Column Headings for Input Forms on Data Cards

WP	10						80

RHOF	10	RHOW	20	H	30	RL1	40	RL2	50	ALPHA	60		80

MLOW	10	MUP	20	NLOW	30	NUP	40		80

OMEGA(1,1) 10
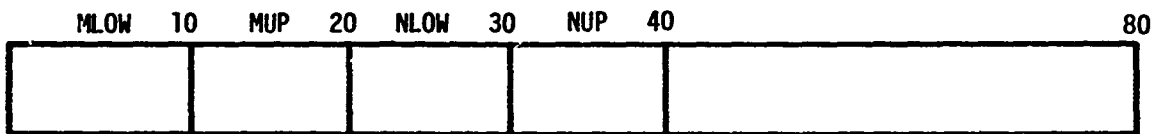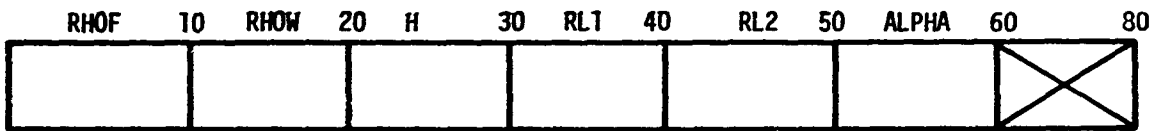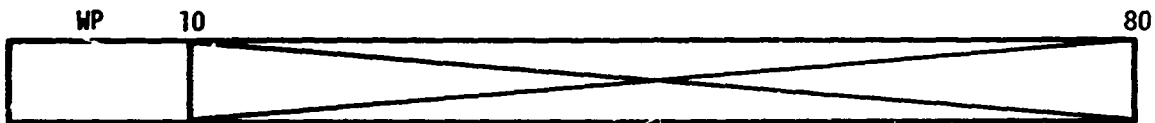
With the order of cards (1,1), (2,1) .....(m,1), (1,2) ..... (m,2) ....
(1,n) .... (m,n) to complete OMEGA (m,n) array.

155

Program C'

This program yields a solution for clamped and simply supported plates corresponding to the Warburton Method as described in Appendix 1 of Reference 3. Warburton treats the frequency parameter subscripts m,n as the number of *nodal points* along the plate length and width respectively. However, most other authors treat m,n as the *mode numbers* along these dimensions (or define it for the opposite dimensions). Thus (m = 2, n = 3)$_{Warburton}$ means the 1, 2 mode containing 2 nodes along x and 3 along y whereas (m = 2, n = 3)$_{others}$ means the 2, 3 mode containing either 3 nodes along x and 4 along y or 4 nodes along x and 3 along y depending on the definition of m,n with respect to the x,y coordinates. To avoid confusion and for compatibility with most investigators, the program assigns the *modal (not nodal) meaning* to m,n for all computations.

In computing the simply-supported plate frequencies by the Warburton Method the value of SPEC must be 1.0. In computing the clamped-clamped plate frequencies by this method any value of SPEC other than 1.0 is used.

In all computations, the frequency f (Hertz) is obtained as the product of the frequency parameter $\lambda_{m,n}$ (or $\alpha_{m,n}$) and a factor. For the Warburton computations the factors are expressed as

$$\frac{h\pi}{a^2} \sqrt{\frac{E}{48\ \rho_m (1-\sigma^2)}}$$

where the mass density σ_m = RHOW/G

156

TABLE 8

Input Data, Computer Listing, Flow Chart, and Column
Headings for Input Forms on Data Cards for Program C'
(Warburton Program) Used to Compute Natural Frequencies
of Simply Supported and Clamped-Clamped Plate *in Vacuo*

TABLE 8a

Input Required for Program C'

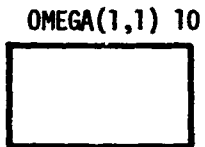| Variable Name	Format	Description	Unit
NCASE	I5	Number of cases	--
M	I5	Modes in x-direction $m \leq 20$	--
N	I5	Modes in y-direction $n \leq 10$	--
A	F12.6	Plate dimensions, length in x direction	in.
B	F12.6	Plate dimensions, length in y direction	in.
H	F12.6	Plate thickness	in.
E	E16.8	Young's modulus	$lb/in.^2$
SIGMA	F12.6	Poisson's ratio	--
RHOW	F12.6	Weight density of plate	$lb/in.^3$
G	F12.6	Acceleration due to gravity	$in./sec^2$
SPEC	F10.0	Option for obtaining frequencies of either simply supported or clamped-clamped plate	

Computer Listing for Program C'

```
$EXECUTE          IBJOB
$IBJOB            MAP,FIOCS
$IBFTC WARB
C      ***************************************************************
       COMMON M,N,A,B,H,E,SIGMA,RHOM,PI,G
C      N - MODES IN X DIRECTION
C      N - MODES IN Y DIRECTION
C      A - LENGTH IN X DIRECTION
C      B - LENGTH IN Y DIRECTION
C      H - PLATE THICKNESS
C      E - YOUNGS MODULUS
C      SIGMA - POISSONS RATIO
C      RHOW - PLATE DENSITY
C      G - ACCELERATION DUE TO GRAVITY
C      ***************************************************************
       PI=3.1415927
       READ(5,2)NCASE
       DO 500 L=1,NCASE
       READ(5,2) M ,N
       READ(5,3) A,B,H
       READ(5,4)E,SIGMA,RHOW,G
     2 FORMAT(2I5)
     3 FORMAT(3F12.6)
     4 FORMAT(E16.8,3F12.6)
       RHOM=RHOW/G
    10 CALL WARB
   500 CONTINUE
       STOP
       END
$IBFTC WARBER
       SUBROUTINE WARB
       REAL LAMBDA,JX,JY,K,KP
       DIMENSION  OMEGA(20,10)
       DIMENSION FREQ(25,10), GX(100),HX(100),JX(100),GY(100),HY(100),
      1 JY(100)
       COMMON M,N,A,B,H,E,SIGMA,RHOM,PI,G
       READ(5,111)SPEC
   111 FORMAT(F10.0)
       A2=A*A
       B2=B*B
       A4=A2*A2
       B4=B2*B2
       MP1=M+1
       NP1=N+1
       IF(SPEC.EQ. 1.0)  GO TO 510
       GX(1)=1.
       HX(1)=1.
       JX(1)=1.
       GY(1)=1.
       HY(1)=1.
       JY(1)=1.
       GX(2)=1.506
       HX(2)=1.248
       JX(2)=1.248
       GY(2)=1.506
       HY(2)=1.248
       JY(2)=1.248
       DO 100 M1=3,MP1
       GX(M1)=FLOAT(M1)-.5
       HX(M1)=((FLOAT(M1)-.5)**2)*(1.-2./((FLOAT(M1)-.5)*PI))
```

```
      JX(M1)=HX(M1)
  100 CONTINUE
      DO 150 N1=3,NP1
      GY(N1)=FLOAT(N1)-.5
      HY(N1)=((FLOAT(N1)-.5)**2)*(1.-2./((FLOAT(N1)-.5)*PI))
      JY(N1)=HY(N1)
  150 CONTINUE
      GO TO 590
  510 DO 500   M1 = 1,MP1
      GX(M1) = FLOAT(M1) - 1.0
      HX(M1) = GX(M1) **2
  500 JX(M1) = HX(M1)
      DO 550   N1 = 1,MP1
      GY(N1) = FLOAT(N1)-1.0
      HY(N1) = GY(N1)**2
  550 JY(N1) = HY(N1)
  590    WRITE(6,20)A,B,H,E,SIGMA,RHOM
   20 FORMAT(1H1,3H A=,F7.2,3H B=,F7.2,3H H=,F7.4,3H E=,E11.4,7H SIGMA=,
     1 F7.2,6H RHOM=,E11.4)
      WRITE(6,19)
   19 FORMAT(//23X, 22H WARBURTON FREQUENCIES)
      IW = 1
      DO 400 N2=2,NP1
      N21=N2-1
      WRITE(6,21)N21
   21 FORMAT(3H N=,I2)
      WRITE(6,22)
   22 FORMAT(9X,1HM,15X,6HLAMBDA,16X,5H FREQ)
      DO 300 M2=2,MP1
      M21=M2-1
      XLAMSQ=(GX(M2)*GX(M2)*GX(M2)*GX(M2)+(GY(N2)*GY(N2)*GY(N2)*GY(N2)
     1 *A4)/B4+(2.*A2/B2)*(SIGMA*HX(M2)*HY(N2)+(1.-SIGMA)*JX(M2)*JY(N2))
      LAMBDA=SQRT(XLAMSQ)
      FREQ(M2,N2)=((LAMBDA*H*PI)/A2)*SQRT(E      /(48.*RHOM*(1.-SIGMA**2)))
      WRITE(6,23)M21,LAMBDA,FREQ(M2,N2)
      OMEGA(M2,N2) = 2. * PI * FREQ(M2,N2)
      WRITE(6,30)   OMEGA(M2,N2),      IW
   23 FORMAT(5X,I5,5X,E15.8,5X,E15.8)
      WRITE(3,30)   OMEGA(M2,N2),      IW
   30 FORMAT(1X,F15.4,65X,I5)
      IW = IW + 1
  300 CONTINUE
  400 CONTINUE
      RETURN
      END
```

159

TABLE 8c

Flow Chart of Program C'

EXECUTIVE ROUTINE

Table 8c (Continued)

SUBROUTINE WARB

```
        ┌─────────────┐
        │    START    │
        └─────────────┘
               │
               ▼
       ┌───────────────┐
       │    READ IN     │
       │   Value for    │
       │     SPEC       │
       └───────────────┘
               │
               ▼
           ◇ IS          NO      ┌──────────────────────────┐
        SPEC=1  ──────────────▶  │ Setup coefficients for    │
           ?                     │ boundary condition        │
           │ YES                 │ expression of clamped plate│
           ▼                     └──────────────────────────┘
  ┌────────────────────┐                      │
  │ Setup coefficients  │                      │
  │ for boundary         │                      │
  │ condition            │                      │
  │ expression of simply │                      │
  │ supported plate      │                      │
  │ functions            │                      │
  └────────────────────┘                      │
           │                                   │
           ▼                                   │
  ┌────────────────────┐◀────────────────────┘
  │ WRITE               │
  │  A,B,H,E, SIGMA,     │
  │  RHO                 │
  └────────────────────┘
           │
           ▼
  ┌────────────────────┐
  │   COMPUTE            │
  │  Frequencies         │
  │  without fluid       │
  │  loading             │
  └────────────────────┘
           │
           ▼
  ┌────────────────────┐
  │   WRITE             │
  │  Frequencies         │
  └────────────────────┘
           │
           ▼
      ┌─────────────┐
      │   RETURN     │
      └─────────────┘
```

161
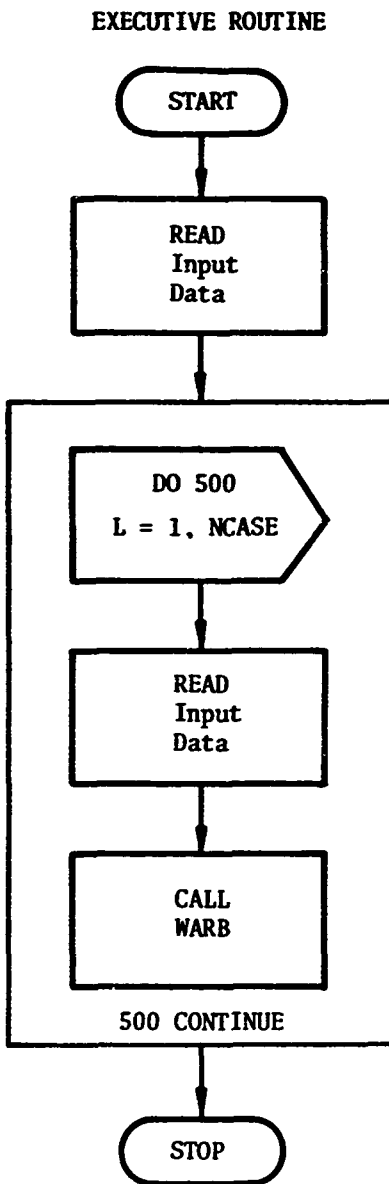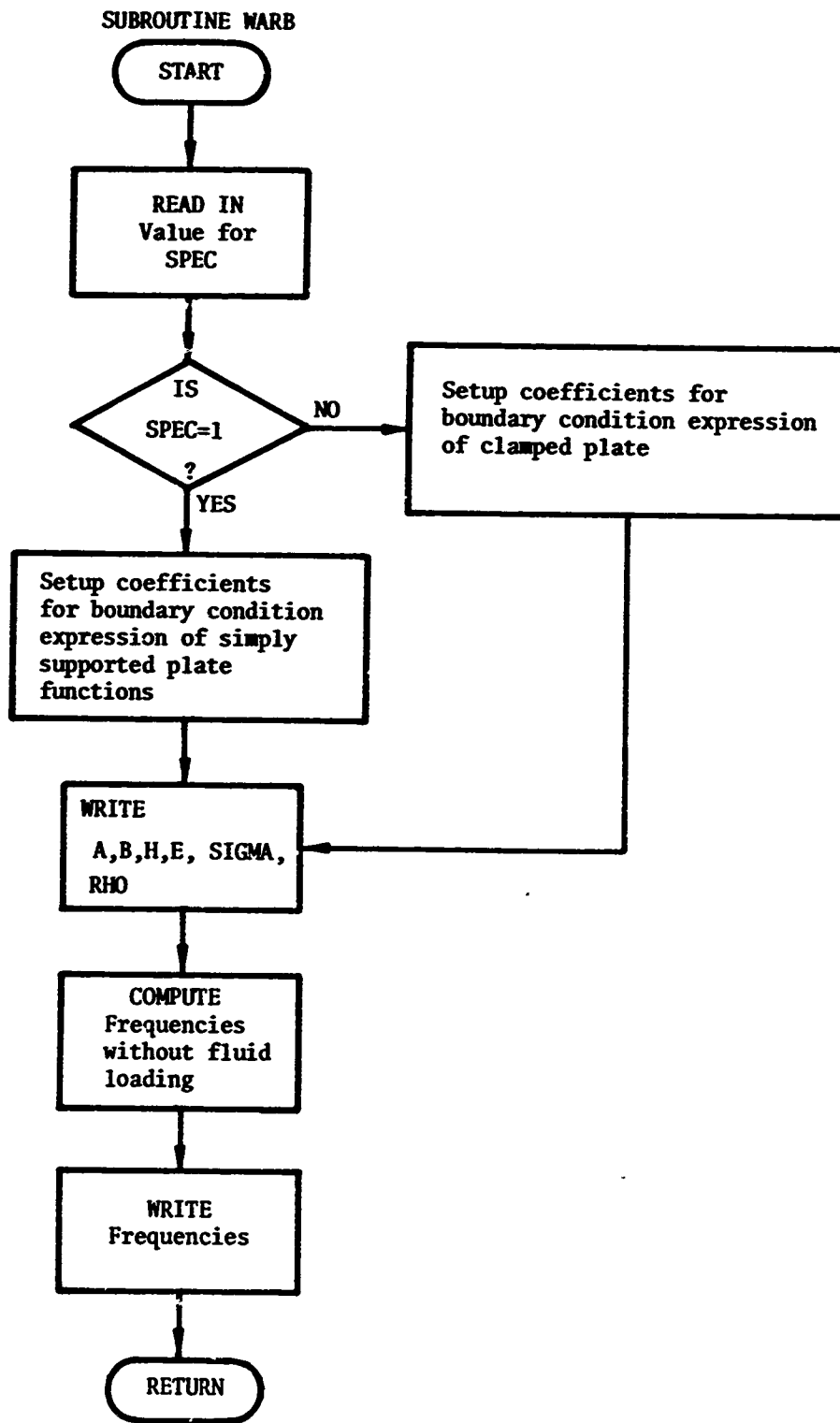
TABLE 8d

Column Headings for Input Forms on Data Cards for Program C'

NCASE	5	10		80

M	5	N	10		80

A	12	B	24	H	36		80

E	16	SIGMA	28	RHOW	40	G	52

SPEC	10		
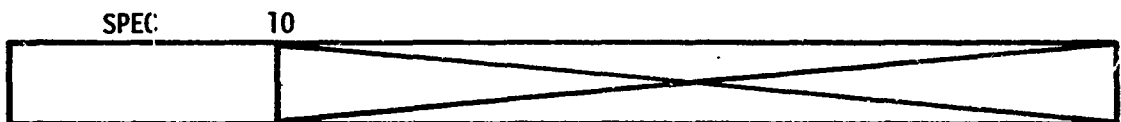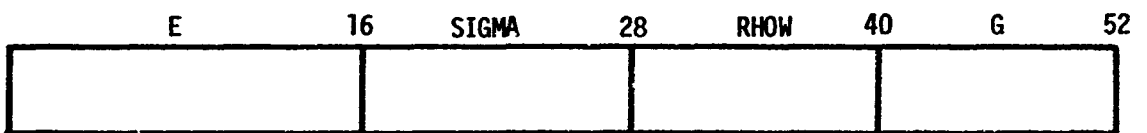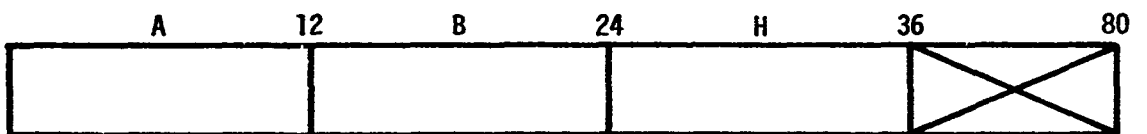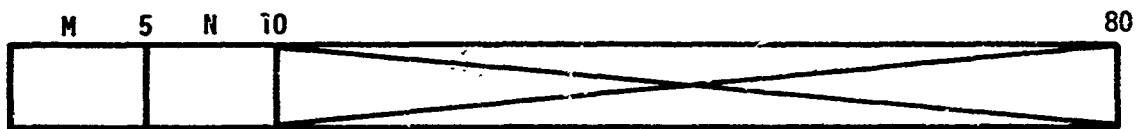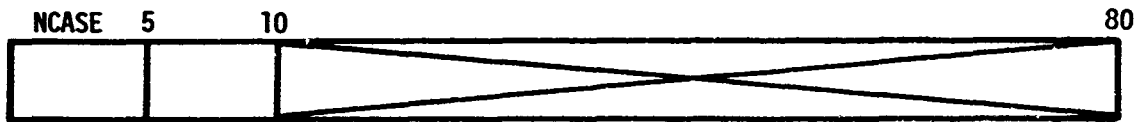
The input data and results are labeled and printed out for each value of NCASE. The mode numbers (m,n), nondimensional frequency λ, and final frequency f (Hertz) are given.

Program D'

This program calculates turbulent boundary layer thickness for an arbitrary body of revolution.

TABLE 9

Input Data, Computer Listing, Flow Chart, and Column
Headings for Input Forms on Data Cards for Program D'
(Brown Program) Used to Compute Turbulent Boundary Layer
Thickness for an Arbitrary Body of Revolution

TABLE 9a

Input Required for Program D'

Variable Name	Unit	Format	Description
N	-	I5	Number of pairs of data points describing the body of revolution
R	ft	F12.8	Length of the body of revolution
Z	-	F12.8	Constant to which all of the data points are normalized
X(I)	ft	6F10.5	Axial distance along the body
Y(I)	ft	6F10.5	Radial distance of the body from the axis
L	-	I5	Number of speeds
U(K)	ft/sec	6F12.8	Speed

163

Computer Listing for Program D'

```
C    MANGLER INTEGRALS
C    R. WILLIAM BROWN, INITIALS CWC, NSRDC CODE 942, PHONE 227-1252
C    THIS IS A PROGRAM FOR THE CALCULATION OF THE TURBULENT BOUNDARY
C    LAYER THICKNESS, DELTA.   IT USES A RELATION AFTER MANGLER WHICH
C    RELATES THE DISTANCE ALONG THE AXIS OF A BODY OF REVOLUTION TO
C    THE DISTANCE ALONG A FLAT PLATE AT WHICH THE BOUNDARY LAYER THICK-
C    NESS IS IDENTICAL.   THE BOUNDARY LAYER THICKNESS IS THEN CALCULAT-
C    ED,USING A RELATION DUE TO GRANVILLE (DTMB REPORT NO. 1340).  THIS
C    EXPRESSION IS BASED ON FLAT PLATE DISTANCE AND FLAT PLATE REYNOLDS
C    NUMBER.
C
C
C    688 COORDINATES (REFERENCE-GENERATING FUNCTION--BRIAN BOWERS)
C
C
     ODIMENSION X(500), Y(500), XZ(500), YZ(500), XZR(500), YZR(500), YZ
    1R2(500), XBAR(500), RXBAR(500,15), DELTA(500,15), U(15)
C    READ IN THE CONSTANTS N, R, AND Z.
C    N = THE NUMBER OF PAIRS OF DATA POINTS DESCRIBING THE BODY OF
C    REVOLUTION.
C    R = THE LENGTH OF THE BODY OF REVOLUTION.
C    Z = THE CONSTANT TO WHICH ALL OF THE DATA POINTS ARE NORMALIZED.
C    READ IN THE DATA POINTS DESCRIBING THE BODY OF REVOLUTION.   X(I)
C    = THE AXIAL DISTANCE ALONG THE BODY.  Y(I) = THE RADIAL DISTANCE
C    OF THE BODY FROM THE AXIS.
     READ(5,1) N, R, Z
   1 FORMAT (I5, 2F12.8)
     READ(5,2) (X(I), I = 1, N)
     READ(5,2) (Y(I), I = 1, N)
   2 FORMAT(6F10.5)
C    READING IN THE NUMBER OF SPEEDS, L.
     READ (5, 18) L
  18 FORMAT (I5)
C    READING IN THE SPEED, U(K), IN FEET PER SECOND.
     READ (5, 19) (U(K), K = 1, L)
  19 FORMAT (6F12.8)
C    SETTING X(1) AND Y(1) EQUAL TO ZERO, AND SHIFTING ALL OF THE DATA
C    POINTS, IF NECESSARY.
     IF (X(1)) 15, 8, 9
   9 M = N + 1
     TEMP1 = X(1)
     DO 10 J = 2, M
     TEMP2 = X(J)
     X(J) = TEMP1
     TEMP1 = TEMP2
  10 CONTINUE
   8 IF (Y(1)) 15,12, 11
  11 M = N + 1
     TEMP1 = Y(1)
     DO 13 J = 2, M
     TEMP2 = Y(J)
     Y(J) = TEMP1
     TEMP1 = TEMP2
  13 CONTINUE
     X(1) = 0.0
     Y(1) = 0.0
     N = N + 1
C    CONVERTING THE DATA POINTS WHICH WERE READ IN INTO ACTUAL BODY CO-
C    ORDINATES.
  12 DO 3 I = 1, N
```

Table 9b (Continued)

```
      XZ(I) = X(I)/Z
      YZ(I) = Y(I)/Z
      XZR(I) = R*XZ(I)
      YZR(I) = R*YZ(I)
      YZR2(I) = (YZR(I))**2
      IF(I-2) 6, 7, 7
    6 XBAR(I) = 0.
      GO TO 3
C     CALCULATING THE DISTANCE ALONG A FLAT PLATE, XBAR.
    7 XBAR(I) = (1./YZR2(I))*SIMPUN(XZR, YZR2, I)
    3 CONTINUE
      WRITE(6, 25)
  250FORMAT(99H1    INPUT X VALUES        INPUT Y VALUES        AXIAL DISTAN
     1CE          BODY RADIUS    FLAT PLATE DISTANCE//)
      WRITE(6,5) (X(I), Y(I), XZR(I), YZR(I), XBAR(I), I = 1, N)
    5 FORMAT(5F20.8)
      DO 26 K = 1, L
      RXBAR(1,K) = 0.0
      DELTA(1,K) = 0.0
   26 CONTINUE
      DO 17 K = 1, L
C     CALCULATING THE LOCAL FLAT PLATE REYNOLDS NUMBER, USING A KINEMA-
C     TIC VISCOUSITY OF WATER AT 39 DFGREES F.
      DO 16  I = 2, N
      RXBAR(I,K) = U(K)*XBAR(I)/0.00001684
C     CALCULATING THE TURBULENT BOUNDARY LAYER THICKNESS, DELTA.
      IF(RXBAR(I,K))16,30,31
   30 DELTA(I,K) = 0.0
      GO TO 16
   31 DELTA(I,K) = 0.0598*XBAR(I)/(ALOG10(RXBAR(I,K)) - 3.170)
   16 CONTINUE
   17 CONTINUE
      DO 20  K = 1, L
      WRITE(6, 24) U(K)
   24 FORMAT(12H1VELOCITY = ,F12.8, 14H FEET / SECOND///)
      WRITE(6, 21)
  210FORMAT(116H    AXIAL DISTANCE  FLAT PLATE DISTANCE       LOCAL FLAT
     1 PLATE REYNOLDS NUMBER        BOUNDARY LAYER THICKNESS, DELTA//)
      WRITE(6,22)(XZR(I), XBAR(I), RXBAR(I,K), DELTA(I,K), I = 1, N)
   22 FORMAT(F17.8, F20.8, 18XE15.8, 28XF12.8)
   20 CONTINUE
   15 STOP
      END
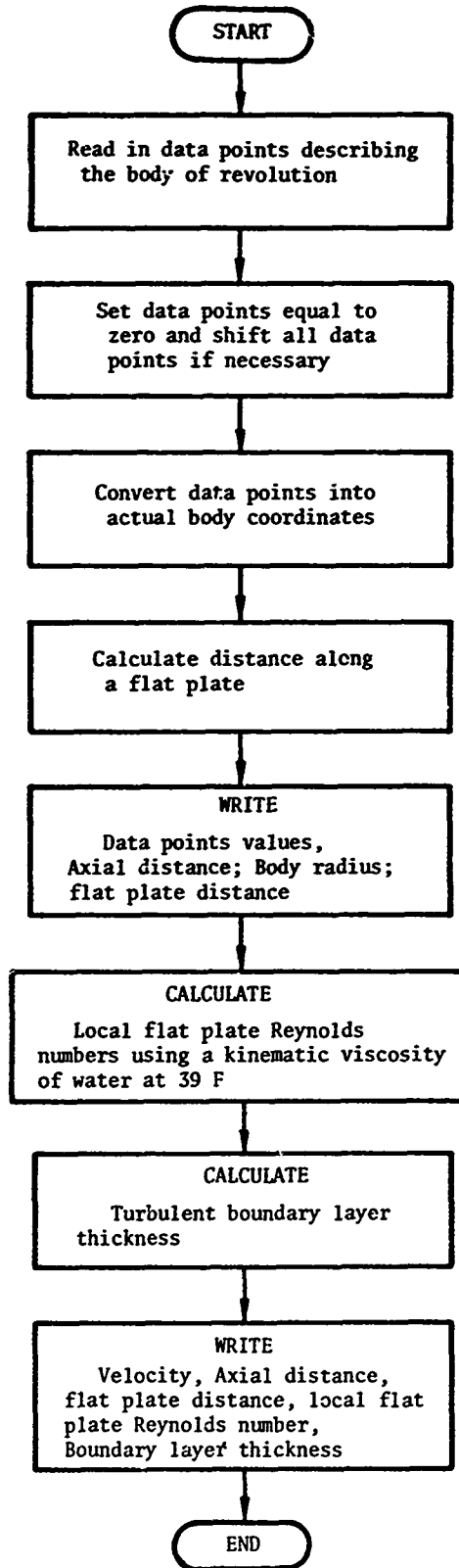```

165

TABLE 9c

Flow Chart for Program D'

```
                    ┌─────────────┐
                    │    START    │
                    └─────────────┘
                           │
                           ▼
        ┌───────────────────────────────────┐
        │  Read in data points describing   │
        │     the body of revolution        │
        └───────────────────────────────────┘
                           │
                           ▼
        ┌───────────────────────────────────┐
        │     Set data points equal to      │
        │     zero and shift all data       │
        │        points if necessary        │
        └───────────────────────────────────┘
                           │
                           ▼
        ┌───────────────────────────────────┐
        │       Convert data points into    │
        │       actual body coordinates     │
        └───────────────────────────────────┘
                           │
                           ▼
        ┌───────────────────────────────────┐
        │      Calculate distance along     │
        │            a flat plate           │
        └───────────────────────────────────┘
                           │
                           ▼
        ┌───────────────────────────────────┐
        │              WRITE                 │
        │        Data points values,        │
        │   Axial distance; Body radius;    │
        │         flat plate distance       │
        └───────────────────────────────────┘
                           │
                           ▼
        ┌───────────────────────────────────┐
        │            CALCULATE               │
        │      Local flat plate Reynolds     │
        │  numbers using a kinematic viscosity│
        │         of water at 39 F          │
        └───────────────────────────────────┘
                           │
                           ▼
        ┌───────────────────────────────────┐
        │            CALCULATE               │
        │      Turbulent boundary layer      │
        │            thickness               │
        └───────────────────────────────────┘
                           │
                           ▼
        ┌───────────────────────────────────┐
        │              WRITE                 │
        │     Velocity, Axial distance,      │
        │    flat plate distance, local flat │
        │       plate Reynolds number,       │
        │      Boundary layer thickness      │
        └───────────────────────────────────┘
                           │
                           ▼
                    ┌─────────────┐
                    │     END     │
                    └─────────────┘
```

166

TABLE 9d

Column Heads for Input Forms on Data Cards for Program D'

N	5	R	17	Z	29	

X(1)	10	X(2)	20	X(3)	30	X(4)	40	X(5)	50	X(6)	60

NUMBER OF VALUES ON CARD IS EQUAL TO N

Y(1)	10	Y(2)	20	Y(3)	30	Y(4)	40	Y(5)	50	Y(6)	60

NUMBER OF VALUES ON CARD IS EQUAL TO N

L	5	

U(1)	12	U(2)	24	U(3)	36	U(4)	48	U(5)	60	U(6)	72

NUMBER OF VALUES ON CARD IS EQUAL TO L

COMPUTER RUNS

Results obtained from the computer programs for the input data of
Tables 2 and 3 are presented in Figures 1 and 2 respectively. The figures
show computer runs for the normalized model mean square displacement of the
turbulence excited simply supported aluminum and steel plates with fluid
loading effects included.

168

APPENDIX I

HYDROSTATIC PRESSURE EFFECTS ON NATURAL FREQUENCIES

a	Plate length
b	Plate width
D	Equal to $\dfrac{Eh^3}{12(1 - \nu^2)}$
E	Young's modulus
G	Constant dependent on k_m/k_n (see Reference 37)
h	Plate thickness
K	Constant depending on aspect ratio of plate; for the panel dimensions cited in Appendix I, K = 0.0018 (see Reference 42)
K_1	Effective wavelength equivalencing factor, dependent on $\sigma h a^2/D$ (see References 36 and 37)
k_m, k_n	Mode numbers in the x- and y-directions respectively
M	Mass per unit area of plate
m,n	Mode numbers
P_H	Hydrostatic pressure
$\left.\begin{array}{l} R, R_a, \\ R_b, R_c \end{array}\right\}$	Radii of curvature
W(x)	Deflection shape of panel to loading by uniform pressure
W_o	Deflection at the center of the plate due to hydrostatic pressure P_H
x,y	Plate coordinates
γ	Equal to 1.5
λ	Wavelength
ν	Poisson's ratio, generally taken to be equal to 0.3
σ_x, σ_y	Stresses in directions associated with m and n respectively
ω_n	Circular natural frequency of vibration

169

DESCRIPTION

A clamped panel below the water surface is subject to essentially uniformly distributed pressure which deflects the panel and creates bending stresses. The natural frequencies of singly curved stressed plates are given approximately by[36-39]

$$\omega_n = \left(\frac{D}{M}\right)^{1/2} \left[(k_m^2 + k_n^2)^2 + \frac{\sigma_x h k_m^2}{D} + \frac{\sigma_y h k_n^2}{D} + \frac{12G}{h^2 R^2} \right]^{1/2} \tag{I1}$$

where $k_m = \dfrac{m}{K_1 a}$, $K_n = \dfrac{n}{K_1 b}$.

Equation (I1) is based upon wavelength equivalencing which effectively reduces the dimensions of the clamped plate to those of the equivalent simply supported plate in each mode. For an unstressed flat plate this equation yields values of natural frequencies which agree within ±10 percent of those calculated by the Warburton method.[3,40] In this equation, G and K_1 are considered to be determinable quantities (see Notation). Hence it remains to determine the stress and curvature produced by the hydrostatic pressure.

The deflected shape of the panel due to loading by a uniform pressure is the same as the fundamental mode shape. It is given by[40,41]

$$W(x) = \frac{W_o}{1.133} \left(\cos \frac{\gamma \pi x}{a} + 0.133 \cosh \frac{\gamma \pi x}{a} \right) \tag{I2}$$

where[42] $W_o = K P_H b^4 / D$

Since

$$R \approx \frac{1}{\dfrac{d^2 W}{dx^2}} = -\frac{\gamma^2 \pi^2 W_o}{1.133 \, a^2} \left| \cos \frac{\gamma \pi x}{a} - 0.133 \cosh \frac{\gamma \pi x}{a} \right| \tag{I3}$$

From Equation (I3) then we can find $R_c = R_{x=a/2}$, the radius of curvature at the center of the plate in the direction of a. Similarly we can find the radius of curvature of the center of the plate in the direction of b. For either case the effect of curvature, or the mean radii R_a and R_b, may be

170

estimated[39] by using $R = R_c \sqrt{2}$. The effect of the curvature upon ω_n is then found by substituting the estimated mean curvature in Equation (I1).

Similarly, the mean stresses σ_x and σ_y are estimated by letting $\sigma_x = \frac{(\sigma_{max})_x}{\sqrt{2}}$, $\sigma_y = \frac{(\sigma_{max})_y}{\sqrt{2}}$ where $(\sigma_{max})_i$ is a maximum bending stress along i derived from Reference 42. The effect of the stresses on ω_n is then found by substituting the estimated values of σ_x and σ_y in Equation (I1).

For a 30 in. x 24 in. x 3/16 in. clamped plate in a horizontal plane subject to a uniformly distributed hydrostatic pressure of 1.5 psi the effects of stress and curvature were found in Reference 39. The results show that the natural frequency is more affected by stress than curvature. Moreover, while stress and curvature due to hydrostatic loading caused the natural frequencies of the panel to increase, the virtual mass effect* (i.e., fluid loading) caused a more significant reduction.

---

*If hydrostatic loading is considered in computations then the plate (in an infinite baffle) cannot be considered to be submerged in an infinite water medium. The effect of the proximity of the water surface on the virtual mass must be treated. However, for a plate located more than $\lambda/6$ below the waterline the presence of the free surface will have no significant effect on the fluid loading. This is clearly a frequency-dependent criterion.[43] If the plate is not in a horizontal plane then the variation of pressure with depth necessitates an integral formulation for the hydrostatic pressure. The problem is then to determine the center of pressure.

REFERENCES

1. Leibowitz, R.C. and Wallace, D.R., "Engineering Guide and Computer Programs for Determining Turbulence-Induced Vibration and Radiation of Plates," NSRDC Report 2976 (Jan 1970). *AD- 878 619*

2. Leibowitz, R.C. and Wallace, D.R., "Computer Program for Correction of Boundary Layer Pressure Fluctuations for Hydrophone Size and Boundary Layer Thickness Effects - Option 1," NSRDC Report 2976A (Sep 1970). *AD- 718 815*

3. Leibowitz, R.C. and Wallace, D.R., "Computer Program for Plate Vibration Including the Effects of Clamped and Rotational Boundaries and Cylindrical Curvature - Option 2," NSRDC Report 2976B (Jan 1971). *AD- 724 642*

4. Junger, M.C. and Feit, D., "Sound, Structures, and Their Interaction," Massachusetts Institute of Technology Press (in preparation).

5. Robson, J.D., "An Introduction to Random Vibration," Elsevier Publishing Company (1964).

6. Hurty, W.C. and Rubinstein, M.F., "Dynamics of Structures," Prentice-Hall (1964).

7. Davies, H.G., "Acoustic Radiation from Fluid Loaded Rectangular Plates," Massachusetts Institute of Technology Report 71476-1 (Dec 1969); also "Low-Frequency Random Excitation of Water-Loaded Rectangular Plates," J. Sound Vibration, Vol. 15, No. 1, pp. 107-126 (1971).

8. Smith, P.W., Jr. and Lyon, R.H., "Sound and Structural Vibration," NASA CR-160 (Mar 1965).

9. Cremer, L. and Heckl, M., "Korperschall," Springer-Verlag, New York (1967).

10. Lyon, R.H., "Fluid-Loading Effects on Vibrating Structures," from "Fluid-Solid Interaction," presented at Winter Annual Meeting of A.S.M.E. Pittsburgh, Pa.; sponsored by Shock and Vibration Committee of the Applied Mechanics Division of the A.S.M.E., edited by Joshua E. Greenspon (Nov 1967).

11. Smith, P.W. Jr. and Kerwin, E.M. Jr., "Underwater Sound Radiation from a Finite Cylinder: General Analysis," Bolt Beranek and Newman Report 1229 (15 Mar 1965).

12. Smith, P.W., "Underwater Sound Radiation from a Finite Cylinder, Part II: Statistical Analysis," Bolt Beranek and Newman Report 1292 (30 Jan 1967).

13. Greenspon, J.E., "An Approximate Method for Obtaining the Frequencies, Deflections, and Stresses in Sandwich and Cross-Stiffened Rectangular Plates," J.G. Engineering Research Associates, David Taylor Model Basin Contract Nonr-3123 (00)X, Technical Report 1 (Jul 1960).

14. Leibowitz, R.C. and Greenspon, J.E., "A Method for Predicting the Plate-Hull Girder Response of a Ship Incident to Slam," David Taylor Model Basin Report 1706 (Oct 1964).

15. Babayev, N.N., "Investigation of the Free Vibrations of Rectangular Plates Surrounded by Water," Krylov Central Scientific Research Institute of the Ministry of the Shipbuilding Industry, Leningrad, Report 16 (1947).

16. Fedenko, G.I., "The Dynamic Analysis of Ships' Plates Supported by Ships' Framing," translated from the Russian Technical Periodical "Sudostroyeniye" (Shipbuilding) Official Organ of the Ministry of the Shipbuilding Industry and the Scientific-Technical Society of Shipbuilding, Leningrad, No. 10 (1965).

17. Stenzel, H., "Die Akustische Strahlung der Rechteckigen Kolbenmembran," Acustica, Vol. 2, No. 6, p. 263 (1952).

18. Young, D. and Felgar, R.P., "Table of Characteristic Functions Representing the Normal Modes of Vibration of a Beam," Engineering Research Series, No. 44, University of Texas, Austin, Texas (1 Jul 1949).

19. Felgar, R.P., "Formulas for Integrals Containing Characteristic Functions of a Vibrating Beam," Univ. of Texas, Circular 14 (1950).

20. Schlicting, H., "Boundary Layer Theory," McGraw-Hill (1960).

21. Jacobs, L.D. et al, "Response of Complex Structures to Turbulent Boundary Layers," American Inst. of Aeronautics and Astronautics Seventh Aerospace Sciences Mtg., New York (20 Jan 1969).

22. Jacobs, L.D. and Lagerquist, D.R., "A Finite Element Analysis of Simple Panel Response to Turbulent Boundary Layers," Technical Report AFFDL-TR-67-81, Boeing Company, Commercial Airplane Div., Renton, Washington (Jul and Dec 1967).

23. Maestrello, L., "Measurement and Analysis of the response Field of Turbulent Boundary Layer Excited Panels," J. of Sound and Vibration, Vol. 2, No. 3, pp. 270-292 (1965).

24. Granville, P., "The Determination of the Local Skin Friction and the Thickness of Turbulent Boundary Layers from the Velocity Similarity Laws," David Taylor Model Basin Report 1340 (Jul 1959).

25. Harris, C.M. and Crede, C.E., "Shock and Vibration Handbook," Vol. 2, Chapters 36 and 37, McGraw-Hill (1961).

26. Adams, R.D. and Mead, D.J., "Comparison of Different Materials in Vibrating Structures," Institute of Sound and Vibration Report 158 (Nov 1966).

27. "Damping of Flexural Vibrations in Plates by Free and Constrained Visco-Elastic Layers," Bolt Beranek and Newman Report 632 (28 May 1959).

28. Kerwin, E.M. Jr., "Acoustic Damping Mechanisms," Wright Air Force Development Center Technical Report 59-676 (15 Aug 1959).

29. Kerwin, E.M. Jr. and McQuillan, R.J., "Vibration Damping Studies," Bolt Beranek and Newman Report 852 (29 Sep 1961).

30. Lyon, R.H. and Maidanik, G., "Power Flow between Linearly Coupled Oscillators," Journal Acoustical Society of America, Vol. 34, No. 5 (May 1962).

31. Unger, E.E., "Energy Dissipation at Structural Joints, Mechanisms and Magnitudes," Bolt Beranek and Newman, FDL-TDR 64-98 (Jul 1964).

32. Ungar, E.E. and Kyung, S.L., "Considerations in the Design of Supports for Panels in Fatigue Tests," Technical Report Air Force Flight Dynamics Lab 67-86 (Sep 1967).

33. Wilby, John F., "The Response of Simple Panels to Turbulent Boundary Layer Excitation," Technical Report Air Force Flight Dynamics Lab 67-70 (Oct 1967).

34. Moore, James A., "Response of Flexible Panels to Turbulent Boundary Layer Excitation," Acoustics & Vibration Lab., Massachusetts Institute of Technology Report 70208-3 (Jul 1969).

35. Bies, D.A., "A Wind Tunnel Investigation of Panel Response to Boundary Layer Pressure Fluctuations at Mach 1.4 and Mach 3.5," NASA CR-501 (May 1966).

36. Szechenyi, E.A., "An Approximate Method for the Determination of the Natural Frequencies of Single and Stiffened Panel Structures," Institute of Sound and Vibration Research Technical Report 23 (1970).

37. Szechenyi, E.A., "An Approximate Solution for the Natural Frequencies of Cylindrically Curved Rectangular Shells with In-Plane Loads," Institute of Sound and Vibration Research Technical Report 29 (1970).

38. Mills, D., "Acoustically Propagated Cracks in Biaxially Tensioned Plates," Ph.D. Thesis, University of Southampton (1970).

39. White, R.G., "The Application of a Transient Test Technique to the Study of the Local Vibration Characteristics of Ship Structures," Institute of Sound and Vibration Research Technical Report 31 (May 1970).

40. Warburton, G.B., "The Vibration of Rectangular Plates," Proc. Inst. Mech. Engrs., London, Vol. 168, pp. 371-381 (1954).

41. Hendry, A.W. and Jaeger, L.G., "The Analysis of Grid Frameworks and Related Structures," Chatto and Windus (1958).

42. Timoshenko, S., "Theory of Plates and Shells," McGraw-Hill (1959).

43. Copley, T.G., et al. "Background Theory of Destroyer Machinery Radiated Noise," Cambridge Acoustical Association Report U-349-214 (May 1970).

175

44. Maestrello, L., "Design Criterion for Minimum Structural Response and Sound Radiation of a Panel Excited by a Turbulent Boundary Layer," AIAA Fifth Aerospace Sciences Meeting, New York, AIAA Paper 67-12, (23-26 Jan 1967).

45. Maestrello, L., "Use of Turbulent Model to Calculate the Vibration and Radiation Responses of a Panel, with Practical Suggestions for Reducing Sound Level," J. Sound Vib. Vol. 5, No. 3, pp. 407-448 (1967).

46. Maestrello, L., "Lectures on Boundary Layer Noise," NASA (Mar 1971).

BIBLIOGRAPHY

1. Leehey, P., "Trends in Boundary Layer Noise Research," AFOSR-UTIAS Symposium on Aerodynamic Noise, Toronto (20-21 May 1968).

2. White, P.H., "Flow Noise-Induced Sound Radiation," Presented at Symposium on Acoustics of Submerged Structures, Annapolis, Maryland (15-17 Feb 1967).

3. Leehey, P., "A Review of Flow Noise Research Related to the Sonar Self-Noise Problem," Bolt Beranek and Newman under subcontract to Arthur D. Little Inc. for Department of the Navy, Bureau of Ships, Report 4110366 (Mar 1966).

4. Strawderman, Wayne A., "Turbulence-Induced Plate Vibrations: an Evaluation of Finite- and Infinite-Plate Models," Journal Acoustical Society of America, Vol. 46, No. 5 (Part 2) (May 1962).

5. Franken, P.A. et al., "Energy-Method Estimates of Response to Inflight Dynamic Loads," Proceedings of Annual Technical Meeting of Institute of Environmental Sciences (1966).

6. Lyon, R.H. et al., "Aerodynamic Noise Simulation in Sonic Fatigue Facility," Bolt Beranek and Newman, AFFDL-TR-66-112 (Nov 1966); also, Bolt Beranek and Newman Report 1171 (24 Dec 1964).

7. Lyon, R.H., "Boundary Layer Noise Response Simulation with a Sound Field," Article in "Accustical Fatigue in Aerospace Structures," Syracuse University Press (Copyright 1965).

8. Williams, J.E.F. and Lyon, R.H., "The Sound Radiated from Turbulent Flows near Flexible Boundaries," Bolt Beranek and Newman Report 1054 prepared for ONR Code 438 (15 Aug 1963).

9. Obermeier, F., "On the Response of Elastic Plates Backed by Enclosed Cavities to Turbulent Flow Excitations," Mass. Inst. Technol. Technical Report 70208-6 (Apr 1971).

10. Blank, F.G., "Radiation Impedance of a Strip Executing Flexural Vibrations in an Infinite Baffle," Soviet Physics-Acoustics, Vol. 14, No. 2 (Oct-Dec 1968).

11. Tarnoczy, T., "Vibration of Metal Plates Covered with Vibration Damping Layers," J. Sound Vib. Vol. 11, No. 3, pp. 299-307 (1970).

12. Szechenyi, E., "Approximate Methods for the Determination of the Natural Frequencies of Stiffened and Curved Plates," J. Sound Vib., Vol. 14, No. 3, pp. 401-418 (8 Feb 1971).